FORSCHUNGSZENTRUM ROSSENDORF FZR

WISSENSCHAFTLICH-TECHNISCHE BERICHTE
FZR-290
März 2000
ISSN 1437-322X

Susanne Pompe, Marianne Bubner, Katja Schmeide, Karl Heinz Heise, Gert Bernhard, Heino Nitsche

Influence of humic acids on the migration behavior of radioactive and non-radioactive substances under conditions close to nature

Synthesis, radiometric determination of functional groups, complexation

Herausgeber:
FORSCHUNGSZENTRUM ROSSENDORF
Postfach 51 01 19
D-01314 Dresden
Telefon +49 351 26 00
Telefax +49 351 2 69 04 61
http://www.fz-rossendorf.de/

Als Manuskript gedruckt

FORSCHUNGSZENTRUM ROSSENDORF
WISSENSCHAFTLICH-TECHNISCHE BERICHTE
FZR-290
März 2000

Susanne Pompe, Marianne Bubner, Katja Schmeide,
Karl Heinz Heise, Gert Bernhard, Heino Nitsche

Influence of humic acids on the migration behavior of radioactive and non-radioactive substances under conditions close to nature

Synthesis, radiometric determination of functional groups, complexation

Das diesem Bericht zugrundeliegende Vorhaben wurde mit Mitteln des Bundesministeriums für Bildung, Wissenschaft, Forschung und Technologie unter dem Förderkennzeichen 02 E 8815 0 gefördert. Die Verantwortung für den Inhalt dieser Veröffentlichung liegt bei den Autoren.

Vorhaben:

EINFLUSS VON HUMINSTOFFEN AUF DAS MIGRATIONSVERHALTEN RADIOAKTIVER UND NICHTRADIOAKTIVER SCHADSTOFFE UNTER NATUR-NAHEN BEDINGUNGEN

- SYNTHESE, RADIOMETRISCHE BESTIMMUNG FUNKTIONELLER GRUPPEN, KOMPLEXIERUNG -

Abstract

The interaction behavior of humic acids with uranium(VI) and the influence of humic substances on the migration behavior of uranium was investigated. A main focus of this work was the synthesis of four different humic acid model substances and their characterization and comparison to the natural humic acid from Aldrich. A radiometric method for the determination of humic acid functional groups was applied in addition to conventional methods for the determination of the functionality of humic acids. The humic acid model substances show functional and structural properties comparable to natural humic acids. Modified humic acids with blocked phenolic OH were synthesized to determine the influence of phenolic OH groups on the complexation behavior of humic acids. A synthesis method for ^{14}C-labeled humic acids with high specific activity was developed.

The complexation behavior of synthetic and natural humic acids with uranium(VI) was investigated by X-ray absorption spectroscopy, laser-induced fluorescence spectroscopy and FTIR spectroscopy. The synthetic model substances show an interaction behavior with uranium(VI) that is comparable to natural humic acids. This points to the fact that the synthetic humic acids simulate the functionality of their natural analogues very well. For the first time the influence of phenolic OH groups on the complexation behavior of humic acids was investigated by applying a modified humic acid with blocked phenolic OH groups. The formation of a uranyl hydroxy humate complex was identified by laserspectroscopic investigations of the complexation of Aldrich humic acid with uranium(VI) at pH 7.

The migration behavior of uranium in a sandy aquifer system rich in humic substances was investigated in column experiments. A part of uranium migrates non-retarded through the sediment, bound to humic colloids. The uranium migration behavior is strongly influenced by the kinetically controlled interaction processes of uranium with the humic colloids.

The influence of humic acids on the sorption of uranium(VI) onto phyllite was investigated in batch experiments using two different humic acids. The uranium(VI) sorption onto the phyllite is influenced by the pH-dependent sorption behavior of the humic acids.

Zusammenfassung

Im Rahmen des Forschungsvorhabens wurde das Wechselwirkungsverhalten von Huminsäuren mit Uran(VI) sowie der Einfluß von Huminstoffen auf das Migrationsverhalten von Uran untersucht. Einen Schwerpunkt der Arbeiten bildete die Synthese von vier verschiedenartigen Huminsäuremodellsubstanzen sowie deren Charakterisierung im Vergleich zur natürlichen Huminsäure von Aldrich. Eine radiometrische Methode zur Bestimmung funktioneller Gruppen wurde neben herkömmlichen Methoden zur Bestimmung der Huminsäurefunktionalität eingesetzt. Die Modellhuminsäuren zeigen mit natürlichen Huminsäuren vergleichbare funktionelle und strukturelle Eigenschaften. Zur Bestimmung des Einflusses phenolischer OH-Gruppen auf das Komplexbildungsverhalten von Huminsäuren wurden modifizierte Huminsäuren mit blockierten phenolischen OH-Gruppen synthetisiert. Ein Syntheseverfahren für ^{14}C-markierte Huminsäuremodellsubstanzen mit hoher spezifischer Aktivität wurden entwickelt.

Das Komplexbildungsverhalten synthetischer und natürlicher Huminsäuren mit Uran(VI) wurde mittels Röntgenabsorptionsspektroskopie, laserinduzierter Fluoreszenzspektroskopie und FTIR-Spektroskopie untersucht. Es wurde nachgewiesen, daß die synthetischen Huminsäuremodellsubstanzen ein mit natürlichen Huminsäuren vergleichbares Wechselwirkungsverhalten gegenüber Uran(VI) zeigen und somit die Funktionalität der natürlichen Analoga gut simulieren. Erstmals wurde unter Verwendung einer modifizierten Huminsäure der Einfluß phenolischer OH-Gruppen auf das Komplexbildungsverhalten von Huminsäuren untersucht. Im Rahmen von laserspektroskopischen Untersuchungen zur Komplexierung von Aldrich Huminsäure mit Uran(VI) bei pH 7 wurde die Bildung eines Uranylhydroxyhumat-Komplexes nachgewiesen.

Das Migrationsverhalten von Uran in einem sandigen huminstoffreichen Grundwasserleiter wurde in Säulenexperimenten untersucht. Ein Teil des Urans wird ungehindert, huminstoffgebunden durch das Sediment transportiert. Das Migrationsverhalten von Uran wird stark durch kinetisch kontrollierte Wechselwirkungsprozesse mit den Huminstoffkolloiden beeinflußt.

Der Einfluß von Huminsäuren auf die Sorption von Uran an Phyllit wurde in Batchexperimenten mit zwei verschiedenen Huminsäuren untersucht. Die Sorption von Uran an Phyllit wird durch das vom pH-Wert abhängige Sorptionsverhalten der Huminsäuren beeinflußt.

Content

1 Introduction

The study of the migration behavior of radioactive and toxic metal ions in the environment is important for long-term risk assessment of potential nuclear waste repositories, of facilities of the former uranium mining and milling in Saxony and Thuringia, and of subsurface dumps and sites with radioactive and/or heavy metal-containing inventory. The behavior of such pollutants is strongly influenced by humic substances.

Humic substances are ubiquitous, polyelectrolytic organic macromolecules. They are formed by the decomposition of biomass. Because of the multitude on precursor substances the formation process of humic substances can not be described by simple chemical or biochemical reactions. Depending on their origin humic substances show different structural and functional properties. This leads to the fact that humic substances show a great structural and functional heterogeneity which causes difficulties in the description of their chemical properties. Humic substances can be divided by an operational definition into three fractions [1]. Humin represents the fraction of humic substances which is insoluble at all pH values, whereas the humic acid fraction is soluble at pH values greater than pH 3.5 and the fulvic acid fraction is soluble at all pH values.

Humic acids play a decisive role within natural interaction processes because of their good solubility in the pH range of natural waters and because of their high complexing capacity. For instance, due to their high complexing capacity, humic acids influence the speciation of metal ions, e.g., actinides, and therefore, the migration and/or immobilization of this pollutants in the environment. Due to their complicated and heterogeneous nature, a thermodynamically based description of the complex formation of humic acids with metal ions is difficult but nevertheless important. There are different thermodynamic models describing the complexation behavior of humic acids. However, these models differ from each other in the definition of the complexation reaction and of the humic acid ligand concentration. Moreover, the existing database for the interaction between metal ions and humic acids is incomplete, especially for actinides in the pH and concentration range of natural systems.

It was the scope of this project to improve the knowledge about the interaction of metal ions with humic acids under natural conditions. For this purpose model substances for humic acids were developed to investigate the humic acid complexation with well-defined substances. Applying natural and synthetic humic acids, studies concerning the interaction process metal ion - humic acid were performed and thermodynamic data were determined. In addition,

migration and sorption studies under conditions close to the nature were carried out. Such information are essential to allow more precise geochemical modeling for the migration of radioactive and toxic metal ions in the environment in the presence of humic acids.

Within the framework of this project the research program of the Institute of Radiochemistry of the Forschungszentrum Rossendorf included the following main topics:

1. The development of synthesis procedures for the preparation of humic acids with defined properties and their labelling with ^{13}C or ^{14}C. Synthetic humic acids were to be provided to the project partners.
2. The radiometric determination of functional groups of synthetic and natural humic acids and their selective blocking by methylation and/or acetylation. Functional groups should be blocked by selective chemical reactions to determine their contribution to the complexation behavior of humic acids with metal ions.
3. The investigation of the complexation behavior of uranium in humic acid-containing solutions above pH 4.
4. First studies regarding the sorption of uranium - humic acid - complexes onto relevant sediment materials.

This research project was performed in cooperation with a R&D-project of the Universities of Mainz and Saarbrücken funded by BMBF (contract number: 02 E 8795 8).

2 Model substances for humic acids

To gain a more basic knowledge about the influence of humic acids on the speciation of metal ions in the environment, especially about the interaction process between humic acid and radionuclides, it is necessary to perform model investigations with well-defined humic acid model substances [2]. Compared to natural humic acids such model substances should be characterized by comparable chemical and operational properties. However, they should show a higher homogeneity, a simpler overall structure and a well defined functionality compared to their natural analogues. The synthesis of such model substances should be easy and reproducible. Furthermore, the model substances should offer the possibility for well-defined variations in their functionality and for a defined isotopic labelling (^{13}C, ^{14}C). Model substances for the investigation of the interaction between humic acids and metal ions should be characterized by a functionality comparable to natural humic acids [3].

Low-molecular organic substances, e.g., salicylic acid and malonic acid, which were identified as structural elements of natural humic acids are potential functional models for humic acids. These substances are useful to investigate elementary processes of the humic acid behavior, e.g., the interaction of such structural elements with metal ions. However, these monomeric substances are not sufficient to precisely describe the overall behavior of the polymeric humic acids because they are highly ordered in contrast to natural humic acids.
Furthermore, synthetic humic acid-like polymers, e.g., humic acid-like melanoidin fractions [3] or condensation products of phenolic compounds [4] can be used as humic acid model substances. Within the scope of this project, we synthesized humic acid-like melanoidins, condensation products of reducing sugars and α-amino acids, as functional models for humic acids.

2.1 Melanoidins as humic acid model substances with defined properties

Melanoidins are formed by condensation of reducing sugars and amino acids, peptides or proteins [5-8]. They play a special role in many natural processes. Their formation is considered as one possible way for the formation of humic substances in the environment [9]. Melanoidins represent a mixture of different polymers that can be operational separated into a humin-like, humic acid- and fulvic acid-like fraction because of their different solubility at different pH values. It was shown [3,10] that humic acid-like melanoidin fractions, which were obtained from the whole melanoidin by alkaline dissolution and acid precipitation, show chemical properties comparable to natural humic acids.
Melanoidins are especially suitable as functionality models for humic acids because they show both structural and also functional similarities with natural humic acids. In contrast to the condensation products of phenolic compounds they contain aliphatic nitrogen and they offer many possibilities to vary their structural and functional properties by selective variations of their precursor substances [3]. For instance, it is possible to increase the number of carboxylic groups by using amino dicarboxylic acids as precursor substance or to change the amount of aromatic or aliphatic structural elements by using aromatic or aliphatic amino acids. In addition, it is possible to change the elemental composition of the synthetic humic acids [3]. All of that offer the possibility to investigate the influence of different functional groups or structural elements on the chemical behavior of humic acids, for instance the complexation behavior with metal ions. Furthermore, the synthesis of melanoidins starting

from isotopically labelled precursor substances enables us to synthesize stable isotopically labelled humic acids with high specific activity.

3 General description of the synthesis of humic acid-like melanoidins

The synthesis of humic acid model substances is based on the preparation of a "standard melanoidin" by Enders and Theis [6]. The synthesis of humic acid-like melanoidins is carried out starting from a mixture of α-amino acid, sugar and water. This mixture is heated temperature- and time-controlled under reflux in a nitrogen stream. During the reaction a solid, dark brown, polymeric substance is formed. This solid is separated from the solution by centrifugation. From the solid phase the humic acid-like fraction is extracted with NaOH and then precipitated with HCl (pH < 3). The humic acid precipitate is centrifuged, washed, dialyzed against purified water using dialysis tubes (Thomapor®, exclusion limit MWCO < 1000, Reichelt Chemietechnik, Heidelberg, Germany), and then lyophilized.

Within this project four different types of synthetic humic acid were developed. The precursor substances, i.e., α-amino acids and sugars, as well as their quantitative proportions were varied depending on the aspired humic acid functionality. The used precursors, their proportions and special requirements of the synthesis are summarized in the paragraphs which deal with the synthesis and characterization of the specific humic acid type.

4 Purification of natural humic acid reference materials

The commercially available natural humic acid from Aldrich (Aldrich, Steinheim, Germany) was used as reference material. It was purchased in its sodium humate form (charge H1, 675-2).

The natural humic acid was purified according to the purification method described by Kim and Buckau [11]. The sodium humate was dissolved in 0.1 M NaOH + 0.01 M NaF and stirred over night under nitrogen atmosphere. Then, the solution was centrifuged. The supernatant was acidified with HCl to pH 1. The humic acid precipitate was washed several times with 0.1 M HCl. The whole procedure was repeated three times. The precipitate was then lyophilized.

Furthermore, the commercially available natural humic acid from Fluka (Fluka, Neu-Ulm, Germany) was used as reference material for some investigations. The purification method of Fluka humic acid, based on alkaline dissolution and acid precipitation with HCl, is described in detail elsewhere [10].

5 Radiometric determination of functional groups by derivatization with [^{14}C]diazomethane

The radiometric determination of functional groups [12] is an alternative method for the characterization of humic acids regarding their functional group content. This method bases on the derivatization of carboxylic and phenolic OH groups with [^{14}C]diazomethane by esterification and etherification, respectively. The number of methylated functional groups of the humic acid can be determined precisely by measuring the specific activity of the reaction product and comparison with the specific activity of the [^{14}C]diazomethane. The differentiation between carboxylic and phenolic OH groups is accomplished by the alkaline saponification of methyl esters, whereby the phenolic ethers remain blocked as methyl ethers. The advantage of this method is the possibility to distinguish between phenolic OH groups and carboxylic groups because of the different behavior of ethers and esters in alkaline solutions. In contrast to potentiometric methods this method represents a procedure for the characterization of the humic acid functionality which is independent of the pKa values of the functional groups.

Fig. 5.1 shows the reaction scheme for the radiometric determination of carboxylic, phenolic OH and ester groups.

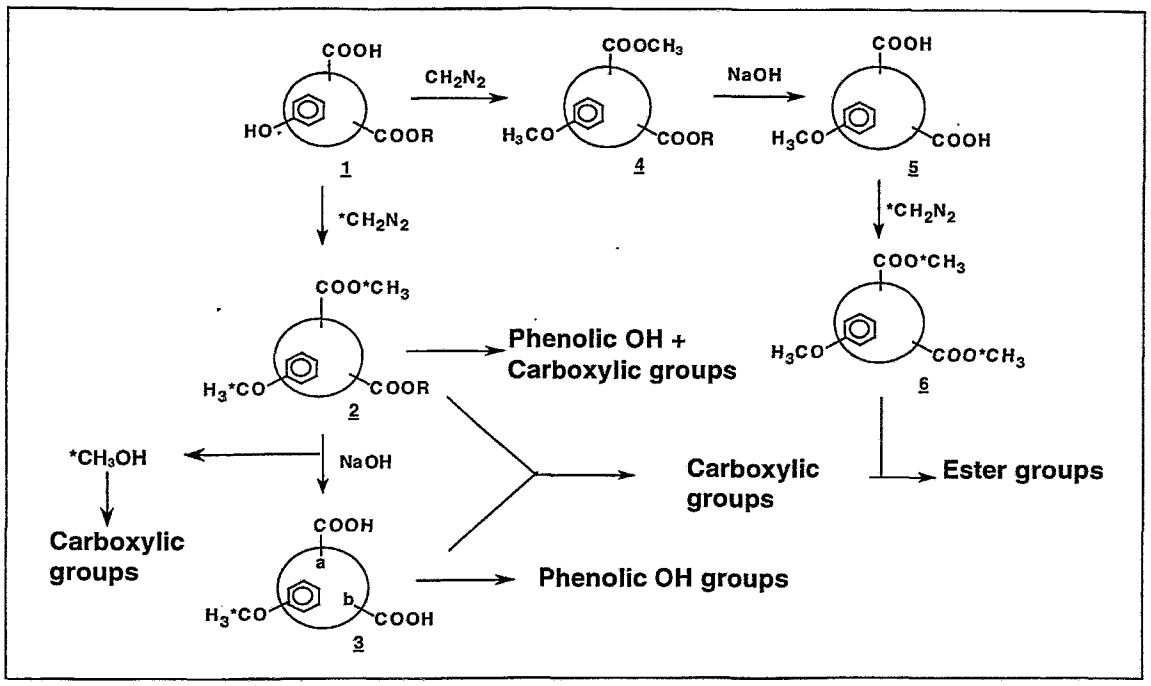

Figure 5.1: Radiometric determination of humic acid functional groups (*C = ^{14}C) [12].

During the first reaction step phenolic OH and carboxylic groups are methylated simultaneously with [^{14}C]diazomethane (cf. Fig. 5.1, (2)). The total number of methylated groups, i.e., carboxylic and phenolic OH groups, in the humic substance is derivable from the specific activity of the reaction product (2) in connection with the specific molar activity of the radioactive reagent. In the next reaction step the carbonic methyl esters of the carboxylic groups are hydrolyzed by alkaline saponification of the methylation product. The phenolic OH groups remain blocked as methyl ethers (3). The resulting specific activity of the humic acid (3) represents the amount of phenolic OH groups of the humic acid. The number of carboxylic groups can be calculated from the total activity of [^{14}C]methanol that is released during the saponification process ($^{14}CH_3OH$) and the specific activity of the used radioactive reagent ([^{14}C]diazomethane). The specific activity of the released methanol is equivalent to the number of hydrolyzed [^{14}C]methyl ester groups. In addition, the number of carboxylic groups can be determined by subtracting the number of phenolic OH groups (3) from the total number on methylated groups (2).

The original ester groups of the humic acid are hydrolyzed simultaneously during the saponification of the methyl esters. This effect can be used for the determination of the ester groups in the original humic acid. For this determination the humic acid is methylated with inactive diazomethane in the first derivatization step and than saponified with NaOH,

resulting in a blocking of the phenolic OH groups and a hydrolysis of the original ester groups of the humic acid (4,5). Following, the humic acid is methylated with [^{14}C]diazomethane. The specific activity of the reaction product (6) represents the sum of all carboxylic groups of the humic acid, i.e., the initial carboxylic groups as well as the hydrolyzed original ester groups. The difference between this amount and the number of carboxylic groups represents the number of ester groups in the original humic acid.

However, acidic hydroxyl groups which are substituted to five-membered heterocycles or other H-acidic hydroxyl groups, may also be methylated by [^{14}C]diazomethane beside phenolic OH groups. The resulting [^{14}C]methyl ether groups are also not hydrolyzable. Hence it follows, that these acid hydroxyl groups are determined together with phenolic OH groups, which leads to an overevaluation of the number of phenolic OH groups.

Disadvantages exist in the occurrence of secondary reactions which may occur during the methylation, e.g., the methylation of aldehyde, keto and amino groups. Such secondary reactions may cause an overestimation of the sum of carboxylic and phenolic OH groups. The determination of carboxylic groups is not influenced by such reactions, if the methanol which is released during the saponification is used for their quantification. Further sources of errors are secondary reactions caused by UV light and metal catalysts as well as the many required operations, especially weightings, during the analytical process. However, the extent of these errors can be minimized.

6 Synthesis and characterization of humic acids

The objective of the synthesis of humic acids was to prepare model substances which show operational properties comparable to natural humic acids, a defined functionality and a higher chemical homogeneity than natural humic acids.

The following paragraphs show the synthesis and characterization of four different humic acids:

- a humic acid with a low content of carboxylic groups and a high amount of aromatic structural elements (Type M1, [10]),
- a humic acid type M1 with an ultra high purity,
- a humic acid with a carboxylic group content comparable to most natural humic acids (Type M42), and
- a nitrogen-free humic acid.

The characterization of the synthetic humic acids was performed in comparison to Aldrich humic acid as reference material.

6.1 Synthesis of humic acid type M1 with a low content of carboxylic groups and a high amount of aromatic structural elements

6.1.1 Synthesis

Synthetic humic acid type M1 (charge R36/95) was synthesized from a mixture of 34 g xylose (Merck, Darmstadt, Germany), 10 g phenylalanine (Merck), 5 g glycine (Merck) and 80 mL water (Fig. 6.1). This mixture was refluxed in a nitrogen stream for 10 hours.

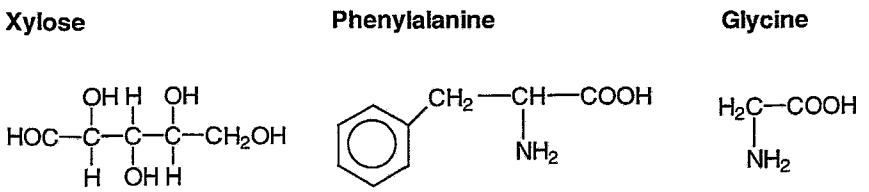

Figure 6.1: Precursor substances of humic acid type M1.

The reaction product was washed and then ground with ethanol (Merck) and ether (Merck). Subsequently, the product was shaken with 2 M NaOH (Merck) for 24 hours under inert gas. After centrifugation the supernatant was acidified with 2 M HCl (Merck) to pH < 3. The resulting humic acid precipitate was washed, dialyzed against purified water using dialysis tubes (Thomapor®, exclusion limit MWCO < 1000), and lyophilized. The synthesis was repeated five times. The total yield of synthetic humic acid amounts to 90 g.

This synthetic humic acid was handed out to all project partners for comparative studies and to establish similar experimental conditions for further investigations.

6.1.2 Characterization

Elemental analysis

The results of the elemental analysis for humic acid type M1 and Aldrich humic acid are summarized in Tab. 6.1. in comparison to literature values. The values were corrected considering the moisture and ash content of both humic acids.

Table 6.1: Elemental composition of synthetic humic acid type M1 in comparison to natural humic acids.

Element / (%)	Synthetic humic acid type M1 (charge R36/95)	Aldrich humic acid (charge A2)	Literature [13]
C	63.92 ± 0.72	54.47 ± 1.42	50 – 60
H[a]	4.75 ± 0.26	3.82 ± 0.14	4 – 6
N	5.34 ± 0.07	0.75 ± 0.04	2 - 6
S	-	3.80 ± 0.10	0 – 2
O[b]	22.51 ± 0.53	29.26 ± 1.53	30 – 35
Ash content / (%)	0.7	3.7	-
Moisture content / (%)	2.8	4.2	-

[a] Corrected for water content of the humic acid. [b] The oxygen content was calculated from the difference to 100 %.

The synthetic product exhibits an elemental composition that is close to literature values for natural humic acids of different origins. Contrary to Aldrich humic acid the synthetic product contains no sulfur due to the use of sulfur-free amino acids. The synthetic product has a higher amount of carbon and nitrogen and a slightly lower oxygen content than Aldrich humic acid.

The elemental composition of the synthetic humic acids, e.g., the nitrogen or sulfur content, could be modified by varying the precursor substances as well as their proportions.

Inorganic constituents

Tab. 6.2 summarizes the amount of inorganic constituents of synthetic humic acid type M1 in comparison to Aldrich humic acid.

Table 6.2: Inorganic main constituents of synthetic humic acid type M1 in comparison to the purified Aldrich humic acid.

Element / (ppm)	Synthetic humic acid type M1	Aldrich humic acid
Na	2451 ± 698	2465 ± 418
Mg	206 ± 104	10 ± 5
Al	204 ± 179	78 ± 9
Si	205 ± 128	372 ± 187
Ca	886 ± 604	126 ± 95
Fe	**< 250**	**3651 ± 224**

As expected, the synthetic humic acid has only a low amount of inorganic impurities. The inorganic impurities that are present in the synthetic product may be caused by the precursor materials applied and by the glassware used. The high sodium content is due to an incomplete sodium elimination by dialysis.

Contrary to the purified Aldrich humic acid and other natural humic acids, which always contain non-removable iron, the synthetic humic acid shows a smaller amount of iron. The iron which is non-removable bound to natural humic acids can compete to other metal ions, e.g., in experiments investigating the complexation behavior of humic acids with metal ions. This might lead to incorrect results. Thus the low iron content of synthetic humic acids represents a great advantage of these products compared to natural humic acids, when they are used for model investigations.

Functional groups

Tab. 6.3 shows the functional group content of synthetic humic acid type M1 and Aldrich humic acid in comparison to literature data [14]. The synthetic humic acid has fewer functional groups than Aldrich humic acid. Particularly the amount of carboxylic groups, which are the most important functional groups for the protolysis and complexation behavior of humic acids, is smaller than in Aldrich humic acid. However, other natural humic acids having low amounts of functional groups and comparable low amounts of carboxylic groups like humic acid type M1 have been reported in the literature [14].

Table 6.3: Functional groups of synthetic humic acid type M1 (charge R36/95) compared to the natural humic acid from Aldrich (charge A2) and to literature data of additional natural humic acids.

Functional groups /	Radiometric determination		Calcium acetate exchange		Barium hydroxide method		Direct titration		Literature [14]
(meq/g)	Type M1	Aldrich	Type M1	Aldrich	Type M1	Aldrich	Type M1	Aldrich	Natural
COOH + phenolic OH	3.6 ± 0.1	6.9 ± 0.7	-	-	3.04 ± 0.93	7.45 ± 0.29	-	-	5.6 – 8.9
COOH	1.3 ± 0.1	4.0 ± 0.4	1.02 ± 0.06	4.74 ± 0.05	-	-	-	-	1.5 – 5.7
phenolic OH	2.3 ± 0.1	3.2 ± 0.7	-	-	2.02 ± 0.99[b]	2.71 ± 0.34[b]	-	-	2.1 – 5.7
PEC [a]	-	-	-	-	-	-	1.36 ± 0.08	5.33 ± 0.12	-

[a] PEC = Proton exchange capacity.
[b] Calculated from the difference between the total acidity determined by the barium hydroxide method and the carboxylic group content determined by the calcium acetate exchange method.

Capillary electrophoresis

Fig. 6.2 depicts the electropherograms of synthetic humic acid type M1 and purified Aldrich humic acid. The electropherograms are different. Aldrich humic acid shows superimposed peaks that were also present in other natural humic acids [15]. We assume that this is due to the presence of several individual humic acid fractions with different charge-to-size-ratios. Synthetic humic acid type M1 shows only one peak in the electropherogram. From this, we conclude that our synthetic product is more homogeneous (smaller charge-to-size-ratio distribution) than the natural humic acid. Furthermore, the synthetic product shows a shorter migration time compared to Aldrich humic acid. This can be explained by a smaller charge-to-size-ratio of humic acid type M1 caused by a larger molecular size and a smaller number of dissociated functional groups, which are the charge carriers of the humic acid. Its relatively smaller number of dissociated functional groups corresponds to its lower total amount of functional groups. The larger molecular size of the synthetic product was determined by size exclusion chromatography.

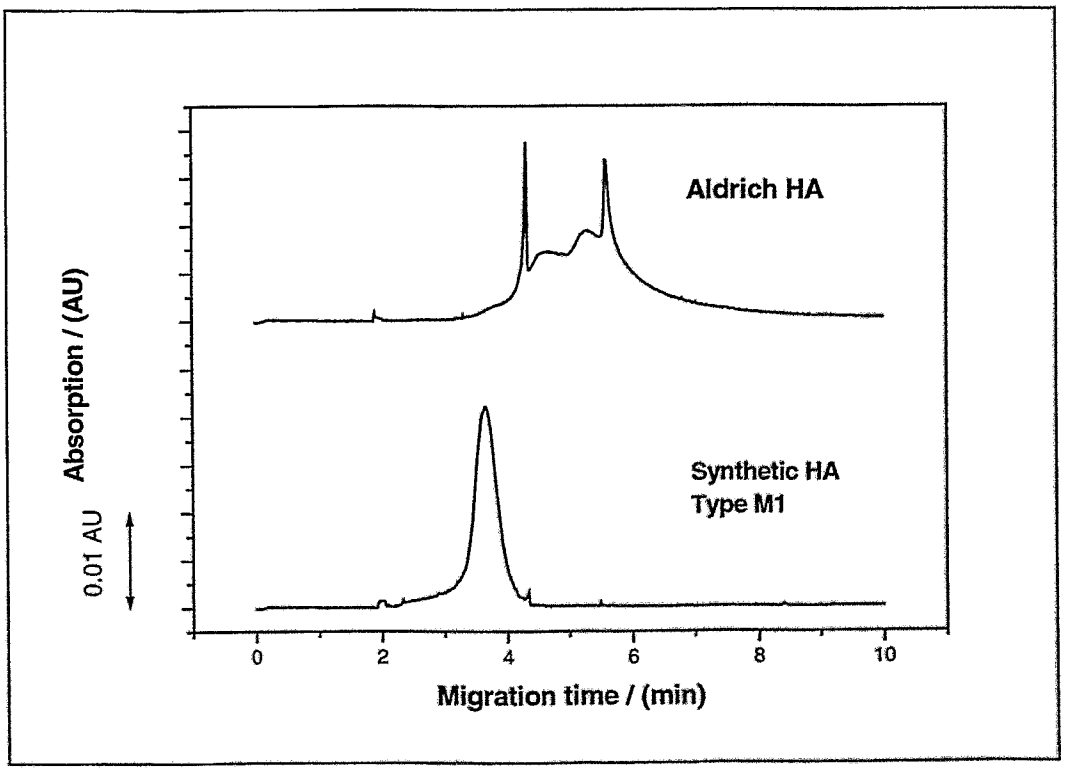

Figure 6.2: Capillary electropherograms of synthetic humic acid (HA) type M1 and purified Aldrich humic acid. Separation conditions: buffer KH_2PO_4 (3 mM) - $Na_2B_4O_7$ (6 mM), pH 8.9; fused silica capillary 75 µm i.d. x 50 cm effective length, 57 cm total length; separation voltage 30 kV; temperature 30 °C; 15 s pressure injection; detection wavelength 214 nm.

FTIR spectroscopy

Fig. 6.3 shows the FTIR spectra of synthetic humic acid type M1 and Aldrich humic acid. In general synthetic humic acid type M1 shows IR absorption bands which are characteristic for natural humic acids [9,16]. Both humic acids differ in their aromatic and aliphatic carbon content. The synthetic product exhibits a greater amount of mono-substituted aromatic carbon structures than Aldrich humic acid, which is indicated by the IR absorption bands at 700 cm^{-1} and 750 cm^{-1}. These structural elements are caused by the use of phenylalanine as precursor substance. Aldrich humic acid possesses a higher content of aliphatic structural elements indicated by the higher intensities of the corresponding absorption bands at 2920 cm^{-1} and 2850 cm^{-1}.

Furthermore, the FTIR spectra point to the higher carboxylic group content of Aldrich humic acid in contrast to synthetic humic acid type M1. The IR absorption band at 1720 cm^{-1} which corresponds to carboxylic groups is stronger pronounced in the spectrum of Aldrich humic acid. This result corresponds to the result of the functional group determination (Tab. 6.3).

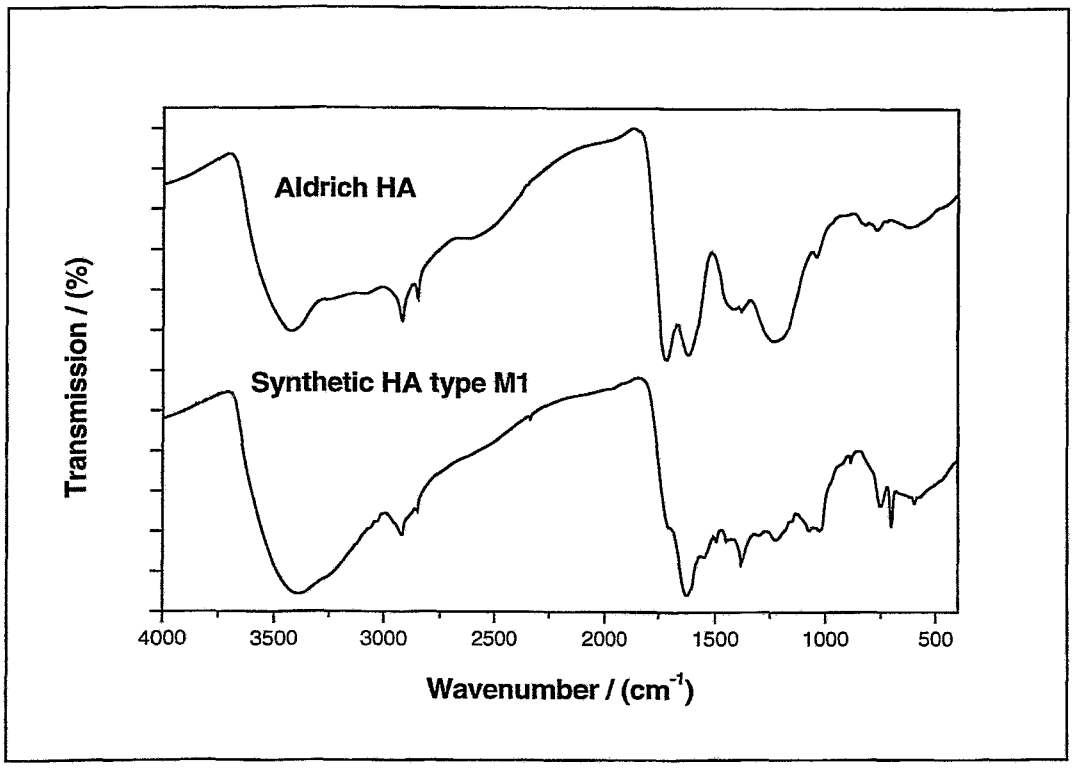

Figure 6.3: FTIR spectra of synthetic humic acid type M1 and Aldrich humic acid.

^{13}C-CP/MAS-NMR-spectroscopy

Fig. 6.4 shows the ^{13}C-CP/MAS-NMR spectrum of synthetic humic acid type M1. The spectrum shows ^{13}C chemical shifts which are characteristic for humic acids [9,17,18]. This result points to structural and functional similarities between the synthetic product and natural humic acids and agrees with the FTIR results.

The spectrum of the synthetic humic acid shows an intensive resonance signal at 129 ppm, corresponding to mono-substituted aromatics due to the use of phenylalanine as precursor substance. The small half-width of this signal indicates similar aromatic structural elements and/or free-movable aromatic end groups. The diffuse, not well-resolved resonance signals can be attributed to aliphatic carbon (20-50 ppm) and aliphatic C-O groups (60-90 ppm). The width of these signals indicates a high heterogeneity and/or a rigid binding of these structural elements. The weak signal at 172 ppm is caused by carboxylic-, ester- and amide groups. A differentiation between these functional groups is not possible with this spectrum. The resonance signals at 110 and 150 ppm indicate the presence of phenolic structural elements.

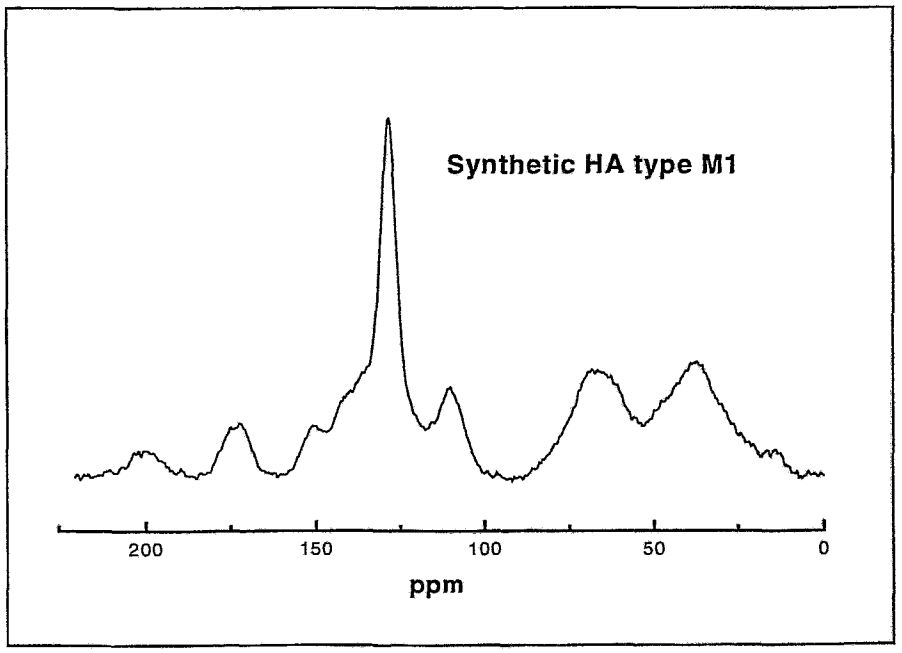

Figure 6.4: ^{13}C-CP/MAS-NMR spectrum of synthetic humic acid type M1.

The ^{13}C-CP/MAS-NMR spectrum of Aldrich humic acid is not shown because this spectrum is hampered by the relatively large concentration of residual iron, which could not be separated during the purification of the humic acid.

Pyrolysis-Gas chromatography/Mass spectrometry (Py-GC/MS)

The pyrolysis gas chromatograms of synthetic humic acid type M1 and Aldrich humic acid are depicted in Fig. 6.5 a and 6.5 b, respectively. The dominant carbon dioxide peaks are due to decarboxylation reactions, mainly of carboxylic groups. The difference in the peak intensities between the synthetic humic acid and Aldrich humic acid corresponds to the analysis of the carboxylic group concentration.

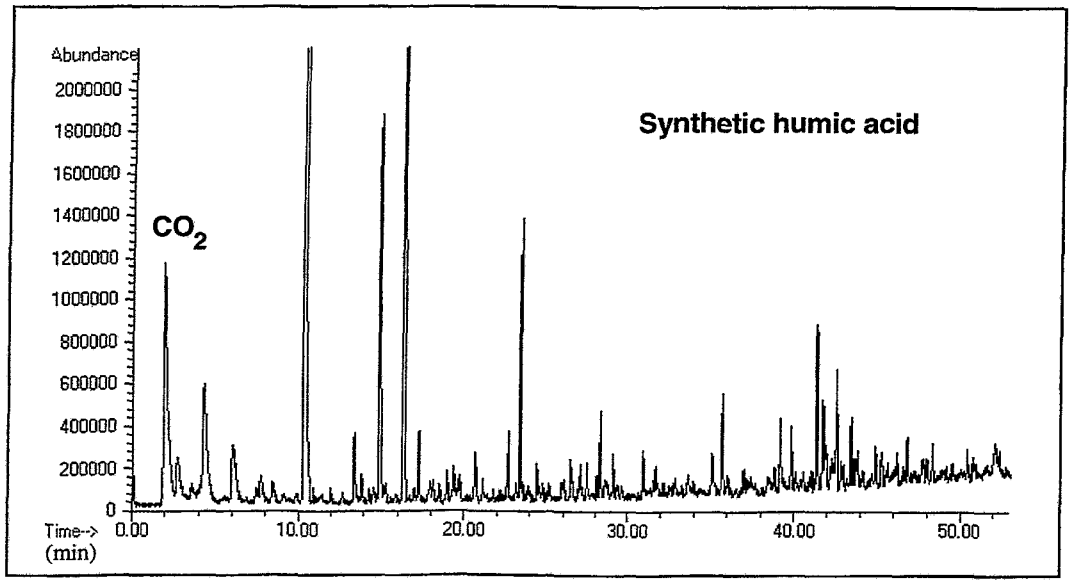

Figure 6.5 a: Pyrogram of synthetic humic acid type M1.

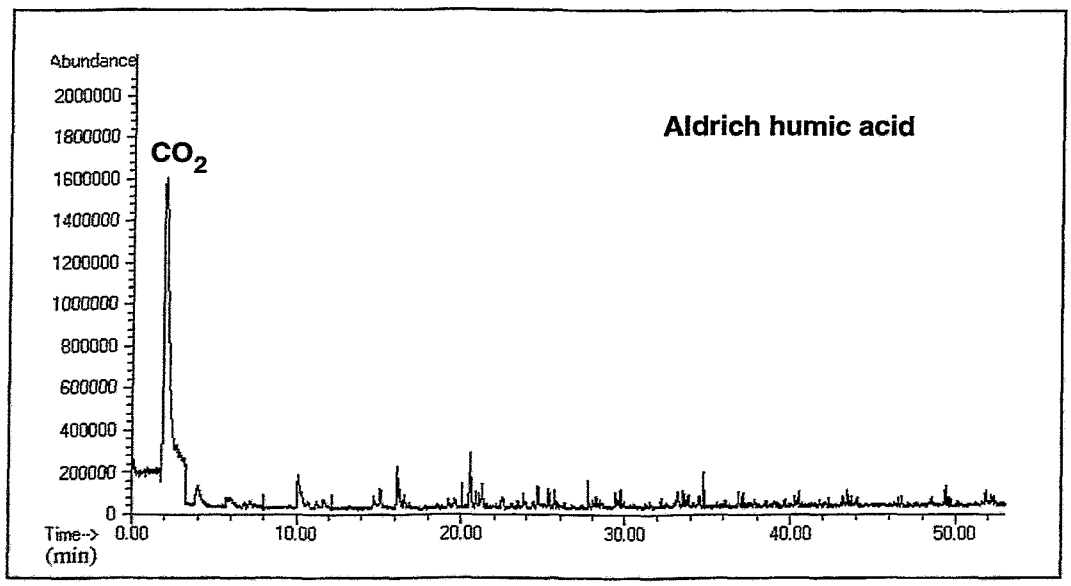

Figure 6.5 b: Pyrogram of the natural humic acid from Aldrich.

The pyrogram of synthetic humic acid type M1 shows intensive peaks in the range between 4 and 12 minutes originating from aromatic fragments such as, for example, benzene, toluene, ethyl benzene, and styrene. These organic structures are due to the use of phenylalanine for the synthesis. Such fragments are also present in the pyrogram of Aldrich humic acid but to a lesser extent. Aldrich humic acid shows a large number of aliphatic pyrolysis fragments, i.e., alkanes and alkenes up to C_{21}, detected between 20 and 50 minutes retention time, which were not detected for the synthetic product type M1.

The pyrolysis fragments of synthetic humic acid type M1 consist of several nitrogen-containing components. Thus, we identified aromatic amines, e.g., 2-aminonaphthalene and N-methyl-N-phenylbenzylamine, as well as substitution products of pyridine, e.g., 3-phenylpyridine and 4-phenyl-N-methylpyridine. Again, this structural elements can be explained by the use of phenylalanine as a synthesis precursor. The pyrogram of Aldrich humic acid did not show any nitrogen-containing product because of its low nitrogen content (0.7 %).

6.2 Synthesis of humic acid type M1 with an ultra high purity

As already mentioned above natural humic acids, e.g., Aldrich humic acid, contain a considerable quantity of non-removable bound inorganic elements, especially iron, which can influence the structure and functionality of humic acids and which can compete to other metal ions during complexation processes. A great advantage of the synthetic humic acids is their low content on inorganic impurities, especially iron. The use of these substances offers the possibility to minimize or to exclude competition reactions during basic studies of the complexation behavior of humic acids with metal ions.

Although synthetic humic acid type M1 shows a lower iron content than Aldrich humic acid, it still contains inorganic impurities resulting from chemicals and glassware applied during the synthesis (cf. Tab. 6.2). To reduce the amount of inorganic impurities of the synthetic product we developed a special synthesis method for extremely pure humic acid type M1.

Based on the synthesis described in 6.1.1 we synthesized a humic acid type M1 using highly purified precursors and likewise ultra pure auxiliaries, e.g., highly purified water, hydrochloric acid (Merck) and sodium hydroxide (Merck) solution. The synthesis was carried out in a apparatus made of Teflon.

6.2.1 Characterization

As a result of the „high-purity" chemistry the amount of inorganic impurities of the humic acid was strongly reduced in comparison to the conventional synthesis. Iron was not detectable in the humic acid fractions. Furthermore, the content of other inorganic constituents was partially reduced by a factor of 10 to 100 and reaches the range of the detection limit. The ash content of this humic acid amounts to < 0.05 %.

The ultra pure synthetic humic acid type M1 shows a somewhat higher content of carboxylic and phenolic OH groups than synthetic humic acid type M1 synthesized by the conventional method (cf. Tab. 6.3). The carboxylic group content determined by calcium acetate exchange amounts to 1.36 ± 0.08 meq/g and the radiometric determined content of phenolic OH groups amounts to 2.5 ± 0.3 meq/g. This result points to the fact, that inorganic impurities of the conventional humic acid type M1 may influence the humic acid functionality by masking functional groups.

Investigations by FTIR spectroscopy show that the ultra pure humic acid of type M1 shows a comparable structure to the conventional humic acid of type M1. FTIR spectra of both humic acids are depicted in Fig. 6.6.

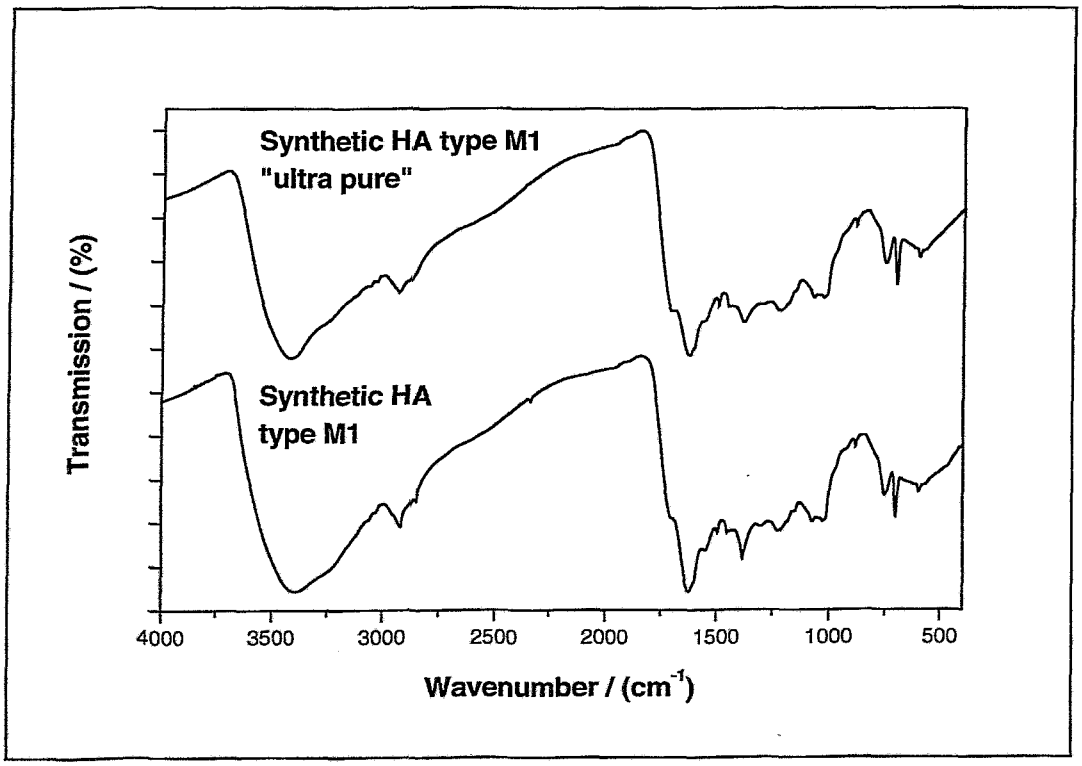

Figure 6.6: FTIR spectra of synthetic humic acid type M1 synthesized by the conventional method and by a special synthesis method for ultra pure humic acids.

6.3 Synthesis of humic acid type M42 with a carboxylic group content comparable to most natural humic acids

In order to simulate the functionality of most natural humic acids, it is necessary to synthesize humic acids with higher amounts of functional groups, especially carboxylic groups compared to synthetic humic acid type M1. Thus we developed a synthesis method for a humic acid with a higher amount of carboxylic groups.

6.3.1 Synthesis

A mixture of 22 g DL-glutamic acid monohydrate (Fluka), 33.3 g xylose (Merck), and 60 mL water was continuously heated for 90 hours at 80 ± 2 °C under reflux and inert gas. The precursor substances are depicted in Fig. 6.7.

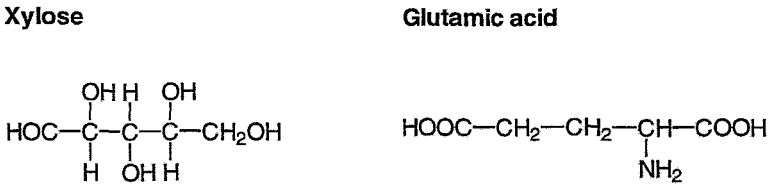

Figure 6.7: Precursor substances of synthetic humic acid type M42.

During the reaction a dark-brown solid and solution were formed. After centrifugation the solid reaction product was ground with ethanol (Merck) and ether (Merck), and then again centrifuged. The solid product was stirred with 150 mL 2 M NaOH (Merck) for 8 hours under inert gas. After centrifugation the remaining solid product was stirred once more with 100 mL 2 M NaOH for 8 hours under inert gas. The alkaline solution, containing the humic acid-like melanoidin fraction, was acidified with 2 M HCl (Merck). The resulting precipitate was washed, dialyzed using dialysis tubes (Thomapor®, exclusion limit MWCO <1000) against purified water, and then lyophilized.

This synthesis was repeated four times. The synthesis products were combined. The yield amounts to 25 g synthetic humic acid type M42 (charge M81).

6.3.2 Characterization

Elemental analysis

The elemental composition of synthetic humic acid type M42 (charge M81), summarized in Tab. 6.4, is comparable to natural humic acids. Differences in the nitrogen and sulfur content compared to Aldrich humic acid are attributed to the precursor substances of the synthetic product.

Table 6.4: Elemental composition of synthetic humic acid type M42 (charge M81) in comparison to natural humic acids.

Element / (%)	Synthetic humic acid type M42 (charge M81)	Aldrich humic acid (charge A2)	Literature [13]
C	58.41 ± 0.53	54.47 ± 1.42	50 - 60
H[a]	4.30 ± 0.22	3.82 ± 0.14	4 - 6
N	4.54 ± 0.12	0.75 ± 0.04	2 - 6
S	-	3.80 ± 0.10	0 - 2
O[b]	27.24 ± 0.53	29.26 ± 1.53	30 - 35
Ash content / (%)	0.3	3.7	-
Moisture content / (%)	5.2	4.2	-

[a] Corrected for water content of the humic acid. [b] The oxygen content was calculated from the difference to 100 %.

Inorganic constituents

The inorganic main constituents of synthetic humic acid type M42 are summarized in Tab. 6.5 in comparison to Aldrich humic acid.

Comparable to synthetic humic acid type M1 humic acid type M42 has only a low amount of inorganic impurities. A great advantage of the synthetic product is the low iron content compared to Aldrich humic acid.

Functional groups

The results of the functional group analysis with different methods are comprised in Tab. 6.6. Due to the fact that this humic acid does not form an insoluble barium salt, the barium hydroxide method for the determination of the total acidity was not applied.

Table 6.5: Inorganic main constituents of synthetic humic acid type M42 in comparison to the purified Aldrich humic acid.

Element / (ppm)	Synthetic humic acid type M42 (charge M81)	Aldrich humic acid (charge A2)
Na	1393 ± 151	2465 ± 418
Mg	19 ± 9	10 ± 5
Al	38 ± 16	78 ± 9
Si	86 ± 40	372 ± 187
Ca	815 ± 357	126 ± 95
Fe	**< 20**	**3651 ± 224**

Table 6.6: Functional groups of synthetic humic acid type M42 (charge M81) determined by different methods.

Functional groups/(meq/g)	Synthetic humic acid type M42 (charge M81)			Aldrich humic acid (charge A2)	Literature [14]
	Radiometric determination	Calcium acetate exchange	Direct titration		
COOH + acidic OH [a]	6.01 ± 0.11	-	-	6.9 ± 0.7	5.6 – 8.9
COOH	3.72 ± 0.28	4.10 ± 0.10	-	4.74 ± 0.05	1.5 – 5.7
acidic OH [a]	2.30 ± 0.36	-	-	3.2 ± 0.7	2.1 – 5.7
PEC [b]	-	-	3.90 ± 0.18	5.33 ± 0.12	-

[a] Acidic hydroxyl groups, e.g., substituted to five-membered heterocycles and aromatics.
[b] PEC = Proton exchange capacity.

In contrast to our synthesized humic acid of type M1, which has only 1.02 ± 0.06 meq/g carboxylic groups, the synthetic humic acid of type M42 shows a carboxylic group content which is comparable to most naturally occurring humic acids. With this results it is shown, that by varying the precursor substances different synthetic humic acids with variable functionality can be designed.

Considering the precursor substances, the unexpectedly high quantity of functional groups determined by the radiometric method, which are capable for methylation and are not hydrolyzable, probably results from H-acidic heterocyclic structures as well as phenolic structural elements. Phenolic structural elements were determined by pyrolysis-gas chromatography/mass spectrometry.

Capillary electrophoresis

Fig. 6.8 depicts the electropherogram of synthetic humic acid type M42. This synthetic product shows in comparison to synthetic humic acid type M1 (Fig. 6.2) a more heterogeneous charge-to-size-ratio distribution. The higher proton exchange capacity of this humic acid may be a potential reason for this observation. The humic acid carboxylic groups are deprotonated at the experimental conditions applied. A mutual repulsion of the deprotonated carboxylic groups can occur, which can cause an unfolding of the molecule and also a cleavage of smaller fragments due to the overcoming of van der Waals forces.

Due to the higher carboxylic group content of synthetic humic acid type M42 in comparison to humic acid type M1 this humic acid shows a longer migration time. However, in comparison to Aldrich humic acid and other natural humic acids synthetic humic acid type M42 shows a smaller charge-to-size-ratio distribution. This indicates a greater homogeneity of the synthetic product regarding their molecule fractions.

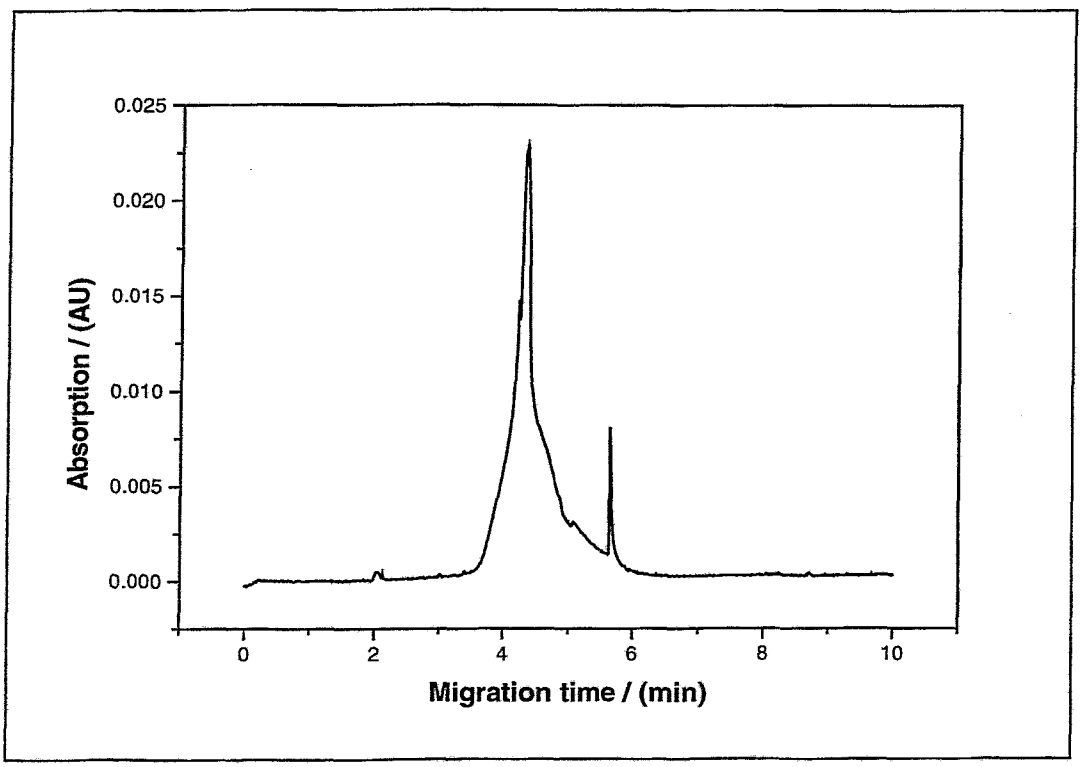

Figure 6.8: Capillary electropherograms of synthetic humic acid type M42 (charge M81). Separation conditions: buffer KH_2PO_4 (3 mM) - $Na_2B_4O_7$ (6 mM), pH 8.9; fused silica capillary 75 µm i.d. x 50 cm effective length, 57 cm total length; separation voltage 30 kV; temperature 30 °C; 15 s pressure injection; detection wavelength 214 nm.

FTIR spectroscopy

Fig. 6.9 compares the FTIR spectra of synthetic humic acid type M42 and type M1. These spectra confirm once more that synthetic humic acid type M42 shows a higher carboxylic group content than synthetic humic acid type M1. The IR absorption band at 1707 cm^{-1} is more pronounced than in the spectrum of humic acid type M1. Furthermore, one can conclude that humic acid type M42 shows IR absorption bands which are characteristic for natural humic acids [9,16].

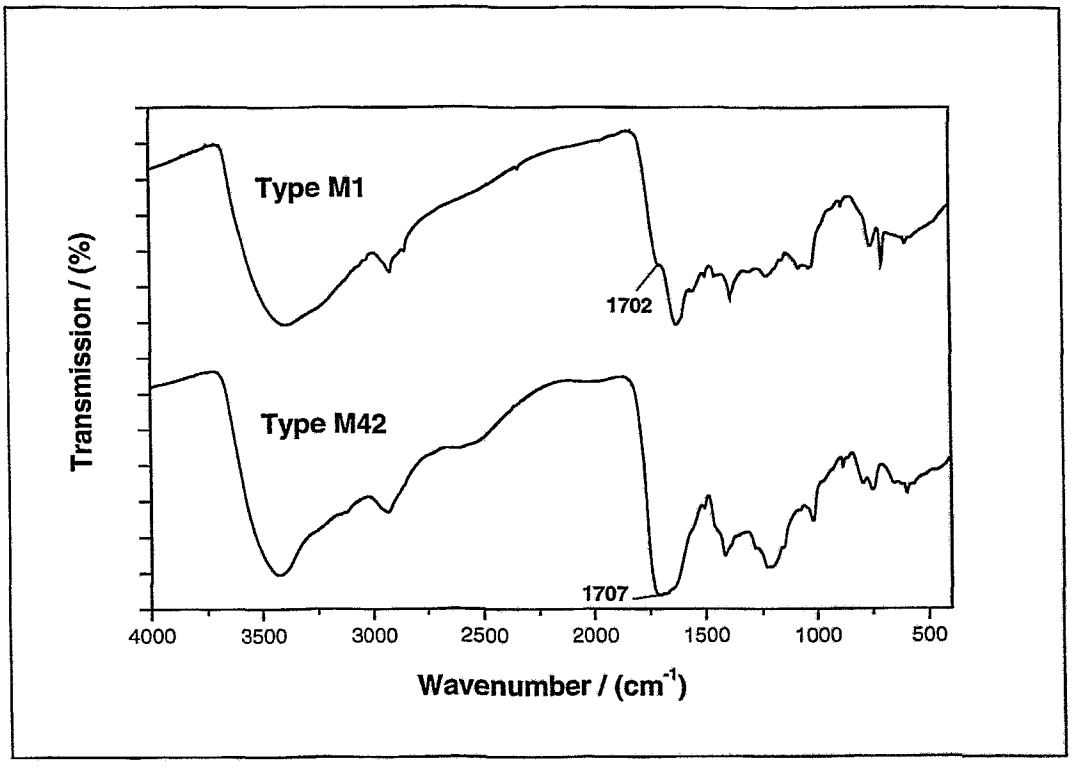

Figure 6.9: FTIR spectrum of synthetic humic acid type M42 (charge M81) in comparison to synthetic humic acid type M1.

6.4 Synthesis of a nitrogen-free humic acid

The ability of humic acids to complex metal ions is mainly due to their high concentration of oxygen-containing functional groups, especially carboxylic and phenolic OH groups. However, also other functional groups, such as nitrogen-containing groups, may contribute as electron-donors to the complexation process. Defined synthetic humic acid model substances, with or without nitrogen may help to elucidate the influence of nitrogen-containing functional groups on the overall complex formation capability. Therefore, we synthesized a non-

nitrogenous humic acid according to our melanoidin concept. Reducing sugars, such as glucose and galactose, can undergo the "Maillard reaction" in hot alkaline solution in absence of amino acids and form the so-called nitrogen-free "pseudo melanoidins" [19].

6.4.1 Synthesis

A mixture of 12 g D(+)-glucose (Fluka), 0.2 g Na_2CO_3 (p.a., Merck) and 18 mL water was refluxed for 15 days under nitrogen (Fig. 6.10). The starting pH was 8.9. In the initial phase of the reaction, the pH decreased to about pH 5 after 24 hours for about one week. Therefore, we adjusted the pH of the reaction mixture to pH 8 by addition of Na_2CO_3 once a day for the first 8 days of the synthesis. The humic acid-like fraction of the reaction product was extracted with 2 M NaOH (Merck) and then precipitated with 2 M HCl (Merck). The resulting precipitate was washed, dialyzed and lyophilized. The synthesis yielded 996 mg of non-nitrogenous synthetic humic acid.

Glucose

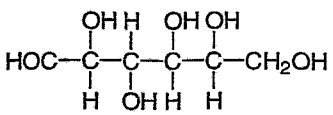

Figure 6.10: Glucose - Precursor for the nitrogen-free humic acid.

6.4.2 Characterization

Elemental analysis

Tab. 6.7 shows the elemental composition of the non-nitrogenous synthetic humic acid and a comparison to literature values for natural humic acids [13]. The synthetic product compares well with natural humic acids.

Table 6.7: Elemental composition of the synthesized non-nitrogenous humic acid in comparison to natural humic acids [13].

Element [a] / (%)	Non-nitrogenous synthetic humic acid	Natural humic acids [13]
C	57.55 ± 0.03	50 – 60
H	5.26 ± 0.01	4 – 6
N	-	2 – 6
O	37.14 ± 0.03	30 – 35

[a] Not corrected for ash and moisture content.

Functional groups

Tab. 6.8 summarizes the functional group content of the non-nitrogenous synthetic product compared to natural humic acids [14]. It is remarkable that the non-nitrogenous synthetic humic acid prepared from glucose shows a higher carboxylic group content than other synthetic humic acids prepared from reducing sugars and α-amino acids. For instance, the synthetic humic acid from type M1 that was discussed in paragraph 6.1, shows only a concentration of 1.0 meq/g carboxylic groups. We conclude from the radiometric determination of the functional groups that the non-nitrogenous product contains both phenolic OH and carboxylic groups.

Table 6.8: Functional group content of the synthesized non-nitrogenous humic acid in comparison to natural humic acids [14].

Functional groups / (meq/g)	Non-nitrogenous synthetic humic acid		Aldrich humic acid (charge A2)	Natural humic acids [14]
	Calcium acetate exchange	Radiometric determination		
COOH + phenolic OH	-	7.23 ± 0.81	6.9 ± 0.7	5.6 – 8.9
COOH	2.64 ± 0.12	2.38 ± 0.14	4.74 ± 0.05	1.5 – 5.7
phenolic OH	-	4.86 ± 0.83	3.2 ± 0.7	2.1 – 5.7

FTIR spectroscopy

Fig. 6.11 shows the FTIR spectrum of the non-nitrogenous synthetic humic acid, which shows characteristic absorption bands for humic acids [9,16]. It is to emphasize that this spectrum

shows IR absorption bands which are characteristic for phenolic OH groups (deformation vibrations of phenolic OH groups, e.g., 1281 cm^{-1}).

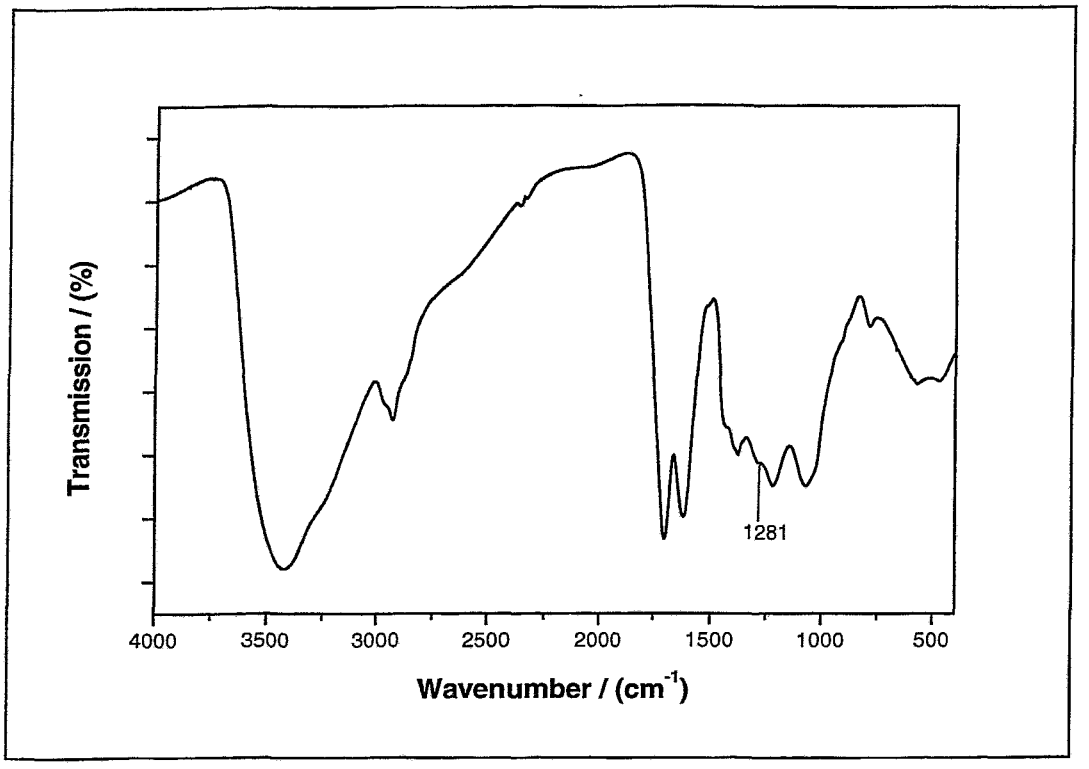

Figure 6.11: FTIR spectrum of the non-nitrogenous synthetic humic acid.

Additionally, the fact that this humic acid contains phenolic OH groups was confirmed by pyrolysis-gas chromatography/mass spectrometry. With this method we detected phenol and phenolic substitution products as thermolysis fragments.

Capillary electrophoresis

Capillary zone electrophoresis showed that the non-nitrogenous humic acid has a more homogeneous charge-to-size ratio distribution than natural humic acids. Fig. 6.12 depicts an electropherogram for the synthetic product.

The results of the different characterization methods show that it is possible to synthesize non-nitrogenous humic acid model substances from glucose.

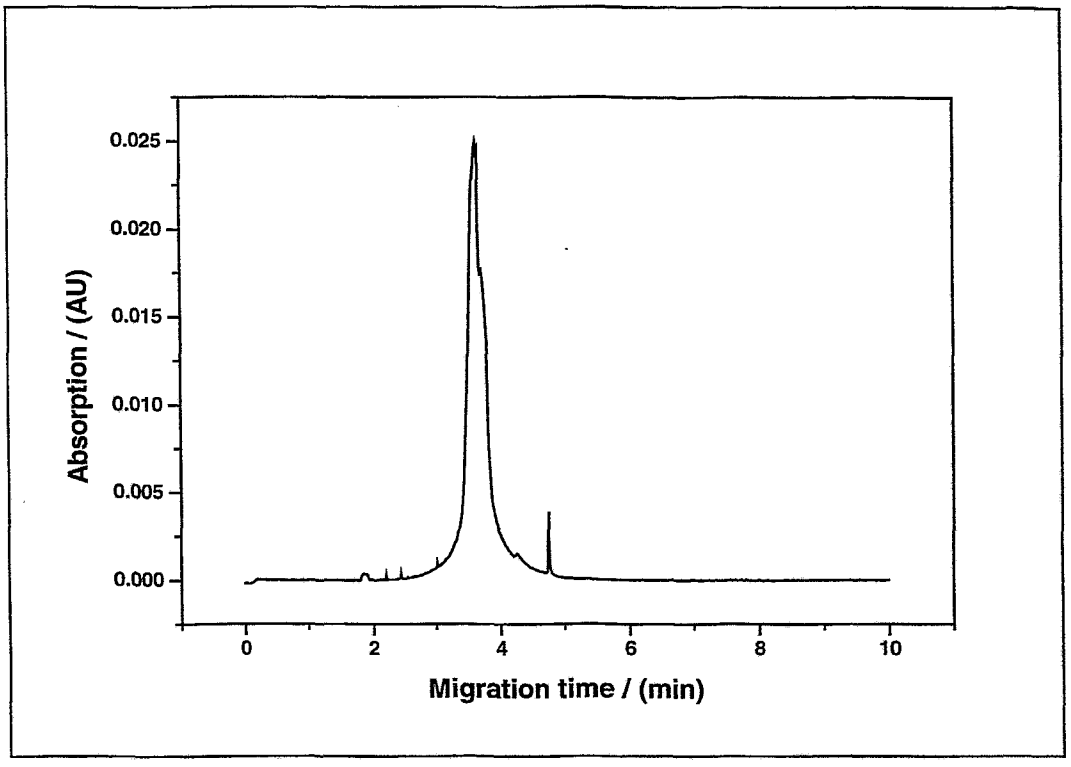

Figure 6.12: Capillary electropherograms of the non-nitrogenous synthetic humic acid. Separation conditions: buffer KH_2PO_4 (3mM) – $Na_2B_4O_7$ (6mM), pH 8.9; fused silica capillary 75 µm i.d. x 50 cm effective length, 57 cm total length; separation voltage 30 kV; temperature 30 °C; 15 s pressure injection; detection wavelength 214 nm.

6.5 Conclusions

We have shown that the synthesis of melanoidins starting from reducing sugars and α-amino acids results in humic acid-like substances. These can be used as humic acid model substances. The humic acid-like melanoidins show functional and structural properties which are comparable to natural humic acids. Nevertheless, they show a higher homogeneity regarding their molecule fractions and a lower amount of inorganic constituents than their natural analogous. It was shown experimentally that the amount of inorganic constituents can be decreased to the detection limit applying an "high purity" synthesis method. "Ultra-pure" synthetic humic acids can be used to study the influence of inorganic impurities and constituents on humic acid properties, for instance on the complexation behavior.

The functional and structural properties of synthetic humic acids can be varied by varying the precursor substances. We have shown that the synthesis starting from xylose, glycine and phenylalanine results in a synthetic humic acid type M1 having a high amount of mono-substituted aromatic structural elements and only a low number of carboxylic groups. Starting

from xylose and glutamic acid it is possible to synthesize a humic acid, which shows a carboxylic group content comparable to most natural humic acids. Besides the functional group content, the elemental composition of the synthetic humic acids can also be varied. A nitrogen-free synthetic humic acid model substance was synthesized from an aqueous glucose solution.

7 Synthesis of modified humic acids with blocked phenolic hydroxyl groups

We synthesized modified humic acids with blocked phenolic OH groups with regard to the investigation of the influence of phenolic OH groups on the complexation behavior of humic acids with metal ions.

The modification process is comparable to the radiometric determination of functional groups (cf. paragraph 5) and comprised two steps (Fig. 7.1): a) the permethylation of carboxylic and phenolic OH groups with diazomethane resulting in methyl ester and methyl ether groups and b) the hydrolysis of the ester groups in alkaline solution.

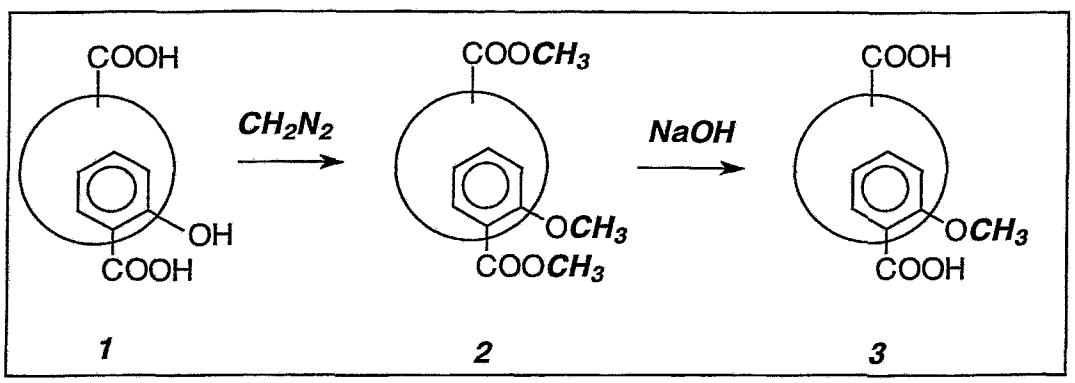

Figure 7.1: Reaction scheme for the synthesis of humic acids with blocked phenolic OH groups. (1) – unmodified humic acid, (2) – permethylated humic acid, (3) – humic acid with blocked phenolic OH groups.

7.1 Synthesis

We synthesized modified humic acids with blocked phenolic OH groups starting from the synthetic humic acids type M1 and M42 and from Aldrich natural humic.

First, the suspension of the original humic acid in methanol was reacted under stirring for three hours at –5 to 5 °C with diazomethane, generated from Diazald® (Sigma-Aldrich). After

three hours the solvent was distilled. The permethylation procedure was repeated for several times and stopped when the incorporation of diazomethane into the humic acid was completed. The solvent, that was distilled from the reaction mixture then showed the yellow color of the non-reacted excess of diazomethane. Then the permethylated sample was lyophilized. The functional group content of the permethylated humic acid, was determined radiometrically.

For hydrolysis of the ester groups we applied two different pathways, (a) the hydrolysis with methanolic NaOH under reflux and (b) the hydrolysis with 2 M NaOH at room temperature.

(a) The permethylated humic acid was refluxed under stirring for 8 hours with an excess of methanolic NaOH solution. Following, the methanol was removed by distillation. The distillation residue was taken up in water. The alkali non-soluble components were separated by centrifugation and the modified synthetic humic acid was precipitated from the aqueous solution by adding 1 M HCl. This method was exclusively used for the permethylated humic acid type M1.

(b) The permethylated humic acid was stirred for 8 hours with 2 M NaOH in a nitrogen atmosphere. The alkali non-soluble residue was separated by centrifugation. Following, the modified humic acid was precipitated by addition of 2 M HCl. This method was applied for all permethylated humic acids.

In both cases the modified humic acid precipitate was centrifuged, washed, dialyzed using dialysis tubes (Thomapor®, exclusion limit MWCO < 1000), and then lyophilized.

It is to consider that with this method also other H-acidic OH groups, e.g., OH groups substituted to five-membered heterocycles may be methylated with diazomethane, resulting in nonhydrolizable methyl ether groups.

7.2 Characterization

The permethylated humic acids as well as the humic acids with blocked phenolic OH groups were characterized for their functional group content using different methods. Tab. 7.1 summarizes the results of these investigations. The humic acids were also investigated by FTIR spectroscopy.

From the results summarized in Tab. 7.1 one can conclude that the phenolic OH groups are only partially modified during the derivatization process. The humic acids with blocked phenolic OH groups have 52 % to 74 % less phenolic OH groups compared to the original

humic acids. In the permethylated humic acids we still determined by the radiometric method functional groups which are capable for methylation but are not hydrolyzable, i.e., these are no carboxylic groups. However, it is still not confirmed if these functional groups are unmodified phenolic OH or other unmodified H-acidic OH groups or functional groups which are produced during the derivatization of the humic acids and that are capable for methylation but not hydrolyzable. It is obvious that in some cases the number of functional groups that are capable for methylation and not hydrolyzable is increased during the saponification step.

Table 7.1: Functional group content of the modified humic acids (HA) in comparison to the unmodified humic acids.

Humic acid	Modification	Phenolic OH / (meq/g)	COOH / (meq/g)	PEC / (meq/g) [a]
Aldrich (charge A2/97)	original	3.4 ± 0.5	4.41 ± 0.11	5.06 ± 0.17
	permethylated	0.6 ± 0.3	< 0.1 [b]	n.m. [c]
	blocked phenolic OH groups	1.1 ± 0.4	3.25 ± 0.05	3.58 ± 0.21
Type M1 (charge R36/95) [d]	original	2.3 ± 0.1	1.02 ± 0.06	1.36 ± 0.08
	permethylated	0.3	< 0.1 [b]	n.m.
	blocked phenolic OH groups	1.1 ± 0.2	1.91 ± 0.07	1.94 ± 0.13
	original HA saponified	1.7 ± 0.1	2.03 ± 0.02	2.12 ± 0.06
Type M1 (charge M100A) [e]	original	2.4 ± 0.1	1.34 ± 0.05	1.69 ± 0.10
	permethylated	0.3	< 0.1 [b]	n.m.
	blocked phenolic OH groups	0.9 ± 0.3	1.16 ± 0.03	1.35 ± 0.23
Type M42 (charge M81)	original	2.3 ± 0.4 [f]	4.10 ± 0.10	3.90 ± 0.18
	permethylated	0.6 ± 0.1	< 0.1 [b]	n.m.
	blocked acidic OH groups [g]	0.6 ± 0.3	3.21 ± 0.08	3.28 ± 0.06

[a] PEC: Proton Exchange Capacity. [b] Radiometrically determined. [c] n.m. : not measured. [d] Hydrolysis method (a). [e] Hydrolysis method (b). [f] cf. chapter 6.3. [g] Blocked acidic OH groups, e.g., substituted to five-membered heterocycles and aromatics (cf. chapter 6.3).

Applying method (a) for the hydrolysis of ester groups, the carboxylic group content of the humic acid was increased probable due to the hydrolysis of ester groups of the original humic acid (see Tab. 7.1). Also hydrolysis of amide groups may occur under the applied conditions which also results in the formation of carboxylic groups. Therefore, an alkaline treatment of the original humic acid type M1 was performed in the same manner as the saponification of the permethylated humic acid of type M1. The functional group analysis of the resulting humic acid (original humic acid saponified) is also shown in Tab. 7.1. The resulting humic acid has a carboxylic group content that is comparable with the modified synthetic humic acid with blocked phenolic OH groups but has a higher content of phenolic OH groups. The amount of phenolic OH groups is somewhat lower than in the original humic acid. This may be caused by condensation reactions during refluxing with methanolic NaOH.

The hydrolysis method (b) represents a more sensitive method. However, comparing the amount of carboxylic groups of the modified humic acids with the unmodified humic acids one can observe that the modified humic acids show a lower carboxylic group content than the original humic acids. Possible causes may be:

- a decomposition of the humic acid molecules in acid-soluble components during the modification;
- a leaching of smaller humic acid molecules with higher carboxylic group content from the humic acid mixture during reprocessing of the modified humic acids or
- decarboxylation reactions during the derivatization process.

The smallest differences in the carboxylic group content were observed for the modified synthetic humic acid type M1 (-13 %) and type M42 (-22 %) compared to the original humic acids. This points to the fact that both humic acid materials are more homogenous than Aldrich humic acid.

The modification process of phenolic OH groups was further investigated by FTIR spectroscopy, which allows the observation of the two different derivatization steps, i.e., first the formation of the permethylated humic acid and second the saponification of the permethylated product resulting in the humic acid with blocked phenolic OH groups.

IR absorption bands, which point to the formation of methyl ether groups, including phenylmethylethers, were identified especially in the finger-print region of the spectra of the modified humic acids with blocked phenolic OH. However, due to the overlapping of IR absorption bands of different humic acid functional groups resulting in a few broad IR

absorption bands as well as due to strong interactions between different functional groups of the humic acid it is difficult to clearly establish these absorption bands in some cases.

Fig. 7.2 shows the FTIR spectra of the unmodified and the modified humic acid type M1. An indication for the modification of phenolic OH groups is the absence of the absorption band at 1292.8 cm^{-1} in the spectrum of the modified humic acid, which corresponds to these functional groups. The spectrum of the unmodified humic acid type M1 shows this band. The ether group absorption bands (1023.9 cm^{-1}, 1097.4 cm^{-1} and 1246.8 cm^{-1}) present in the spectrum of the modified humic acid also confirm that phenolic OH groups are blocked. Additionally, the increase of the intensity of the absorption band at 2862.8 cm^{-1} indicates the formation of methyl ethers. The increase of the intensity of the absorption band at 1453.5 cm^{-1} (C-H deformation vibrations) results from the incorporation of CH_3-groups into the molecule as a result of the methyl ether formation. Furthermore, the synthetic humic acid type M1-B has a significantly higher amount of carboxylic groups (1712.2 cm^{-1}) than the original humic acid.

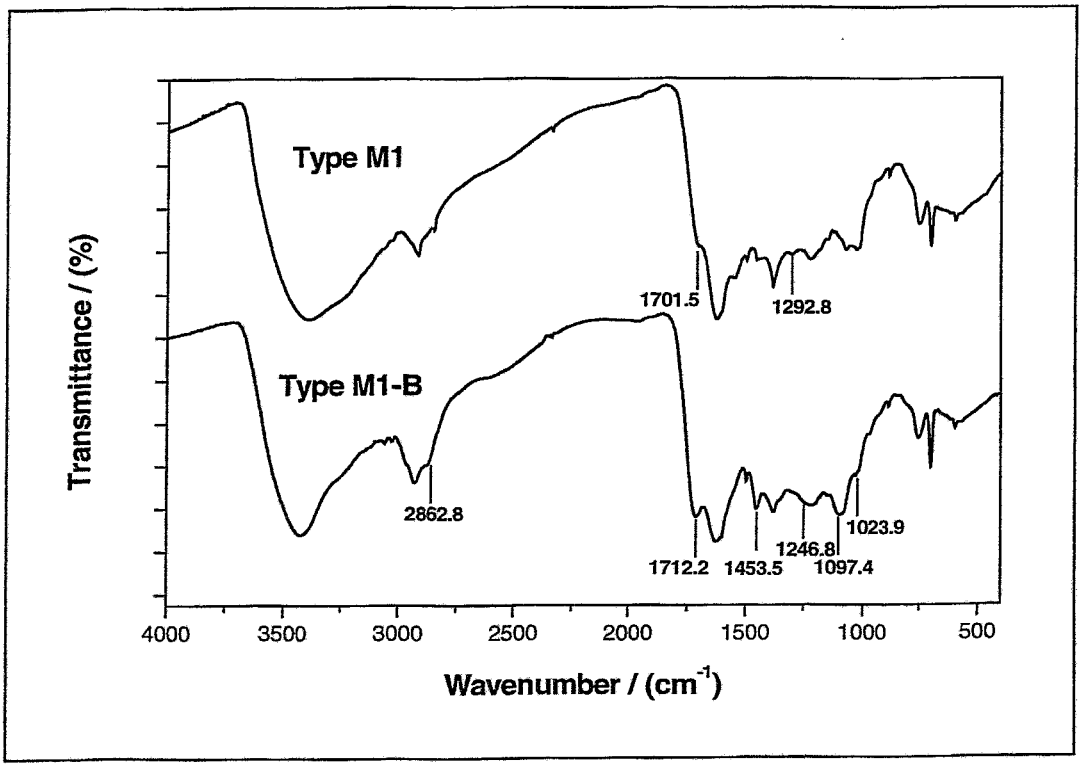

Figure 7.2: FTIR spectra of the unmodified synthetic humic acid of type M1 and the synthetic humic acid with blocked phenolic OH groups (Type M1-B; hydrolysis (a)).

From the characterization results one can conclude that there is the possibility to synthesize humic acids with blocked phenolic OH groups. With the modified humic acid type M1 we

investigated for the first time the influence of phenolic OH groups on the complexation behavior of humic acids with UO_2^{2+} ions. These investigations are described in paragraph 11.

8 Synthesis of isotopically labelled humic acids

Migration and sorption experiments are performed to predict the migration behavior of radionuclides in the presence of humic substances. One of the decisive questions, that has to be answered concerns the fate of humic acids during the interaction of humic-acid-metal-complexes with sediments. In order to study the migration and sorption behavior of actinides in the presence of humic acids, i.e., in laboratory batch and column experiments it is advantageous to label the humic material with radionuclides. Thus, it is possible to detect and to balance very precisely the fate of humic acids in the investigated system.

Requirements on a radioactive labelling of humic acids are the use of long-living radionuclides, e.g., ^{14}C, the irreversibility of the labelling, the preservation of the humic acid functionality and a high isotopic enrichment. The stability of the labelled material is essential for its successful use in experiments over long times. Decomposition of the labelled humic acid and loss of radioactivity during such experiments would lead to incorrect results and an incorrect interpretation of the processes under investigation. The incorporation of a radioactive label into humic materials must be accomplished by methods which do not change the characteristics of the humic material.

There are some possibilities to introduce radioactive labels, e.g., ^{14}C, ^{125}I, into the humic acid molecule. For instance, the chemical derivatization of functional groups using a radioactive reagent, e.g., [^{14}C]methylamine or the enzymatically mediated incorporation of [^{14}C]phenol in the humic material [20,21]. However, this reactions may alter the humic acid, especially the functionality of humic acids by derivatization of functional groups. Such derivatives often are not sufficiently stable for long-time experiments [20,22]. Furthermore, there is the possibility to synthesize isotopically labelled humic acid model substances according to our melanoidin concept using isotopically labelled precursor substances, e.g., α-amino acids. The greatest advantages of the synthesis of isotopically labelled melanoidins compared to other labelling methods are the stable labelling of the humic acid in the backbone structure without any changes in the humic acid functionality and the possibility to synthesize humic acids with different functionalities as described in chapter 6.1. to 6.4.

Within the scope of this project, we investigated the synthesis of ^{14}C-labelled humic acid model substances with different functionalities starting from ^{14}C-labelled α-amino acids. The aim of this work was the selection of the optimal labelling position of the amino acid to obtain humic acids with high specific radioactivity [23].

8.1 Synthesis and results

We synthesized ^{14}C-labelled humic acids of type M1 and type M42 according to the synthesis procedures described in 6.1 and 6.3, respectively. The ^{14}C-labelled α-amino acids used are depicted in Fig. 8.1.

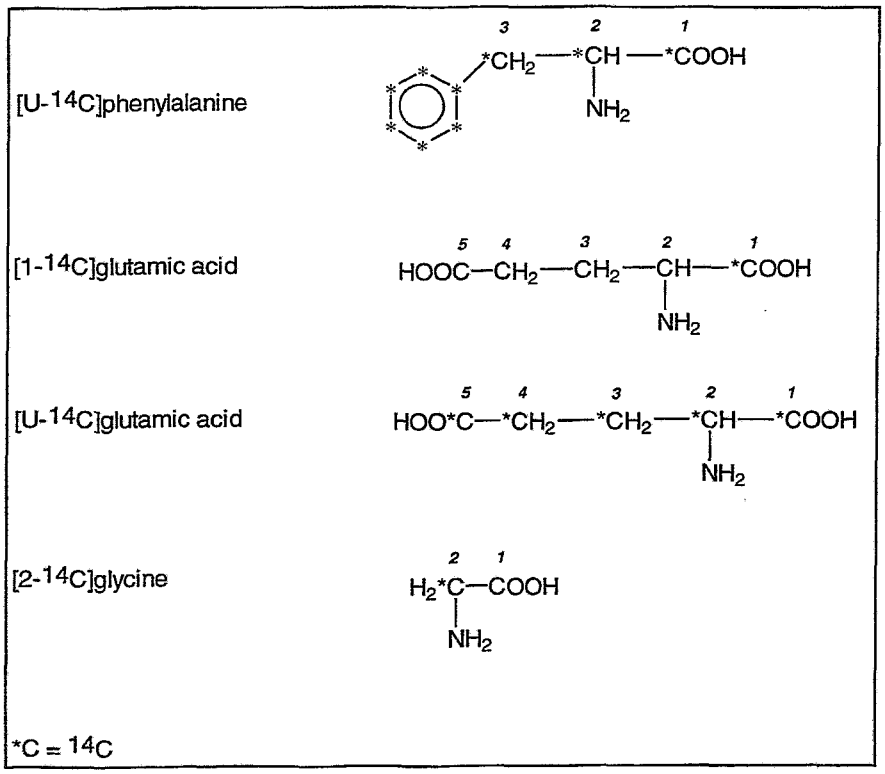

Figure 8.1: ^{14}C-labelled amino acids used for the synthesis of ^{14}C-labelled synthetic humic acids type M1 and type M42.

Tab. 8.1 summarizes the starting materials, the specific activities of the amino acids and the activity yields of the synthesized humic acids.

The radiochemical yield depends on the experimental conditions and is limited by the formation of insoluble humin-like substances. The yields as well as the specific activity of

CO_2 which is eliminated during the reaction allow conclusions with regard to the reaction course. The nitrogen content of the humic acid molecule corresponds to the amount of incorporated amino acid. In all cases, the C-1 carboxylic group of the amino acid is eliminated during the melanoidin formation. This elimination is a precondition for the incorporation of the amino acid in the melanoidin molecule. Therefore, [1-^{14}C]-labelled amino acids, e.g., [1-^{14}C]glutamic acid, are not suitable for the synthesis of ^{14}C-labelled humic acids. However, the CO_2 which is released during the reaction originates not only from the amino acid because the specific activity of the eliminated CO_2 is smaller than the specific activity of the amino acid related to the labelling position. CO_2 from xylose is also eliminated during the reaction.

Table 8.1: Starting materials and activity yields for the synthesis of different humic acids. Xylose was the sugar component used in all cases.

Humic acid type	Precursors		Humic acid Yield	
	Amino acids	(MBq/mmol)	(% ^{14}C)	(MBq/g)
M1	[U-^{14}C]phenylalanine, glycine	40	12	36
M1	[2-^{14}C]glycine, phenylalanine	40	30	104
M42	[1-^{14}C]glutamic acid	40	0	0
M42	[U-^{14}C]glutamic acid	40	5	102

The highest activity yields for humic acid type M1 are reached using [2-^{14}C]glycine as precursor substance. Calculations have shown that the maximal specific activity of humic acid type M1, that can be reached starting from [2-^{14}C]glycine with a maximal specific activity of 1.85 GBq/mmol, amounts to 4.8 GBq/g. With this specific activity 100 ng of ^{14}C-labelled humic acid can exactly be detected. That means, that about 1 µg ^{14}C-labelled humic acid per liter can be detected. This detection limit allows the use of this ^{14}C-labelled humic acid in batch and migration experiments.

Furthermore, using [U-^{14}C]glutamic acid, synthetic humic acid type M42 can be synthesized with a comparable high specific activity (like humic acid type M1 starting from [2-^{14}C]glycine). This fact enables us to synthesize ^{14}C-labelled humic acids with a high carboxylic group content comparable to most natural humic acids. However, the yield of ^{14}C of this synthesis is smaller compared to the synthesis of humic acid type M1.

9 Stability of synthetic and natural humic acid stock solutions

Natural humic acids are subjected to permanent alteration reactions. Nevertheless, comparable chemical properties are necessary for all comparative investigations with humic acids. Alterations of humic acids are especially possible in solutions with extreme pH conditions after long storage periods.

The stability of stock solutions from synthetic and natural humic acids were investigated regarding their temperature and light sensitivity under different pH conditions.

9.1 Experimental

Alkaline conditions

Stock solutions of synthetic humic acid type M1 and type M42 as well as Aldrich humic acid were prepared under aerobic conditions with a humic acid concentration of 1 g/L and a NaOH concentration of 10^{-2} mol/L. Three samples of each stock solution were stored under the following conditions:

a) at room temperature and daylight,
b) at room temperature under exclusion of daylight and
c) at 5 °C under exclusion of daylight.

Periodically the absorption of the humic acid solutions at 465 nm were measured with a spectrophotometer (Spekol 11, VEB Carl Zeiss Jena, Germany). Furthermore, the pH values of the solutions were determined.

Acid conditions

A stock solution of synthetic humic acid type M1 (0.5 g HA/L) was investigated at pH 6. Furthermore, stock solutions of synthetic humic acid type M42 and Aldrich humic acid (1 g HA/L) were investigated at pH 4.

The storage conditions and the absorption measurements of the solutions were the same as in the investigations under alkaline conditions.

9.2 Results

Alkaline conditions

Fig. 9.1 shows the absorption intensities at 465 nm for stock solutions of synthetic humic acid type M1 stored under different conditions versus storage time. For all stock solutions a decrease in the absorption intensities was observed with increasing storage time. The highest decrease was determined for solutions which were stored at room temperature and daylight.

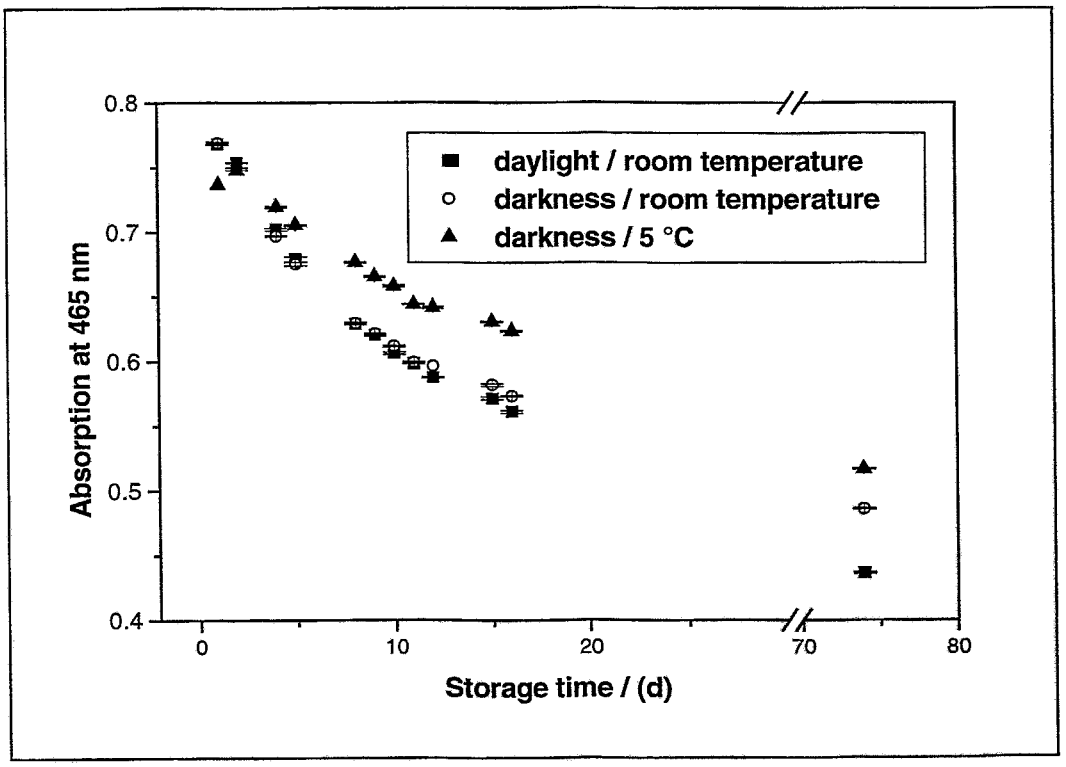

Figure 9.1: Absorption of stock solutions of synthetic humic acid type M1 at 465 nm at different storage conditions versus storage time ([HA]: 1 g/L; [NaOH]: 10^{-2} M).

Comparable trends were determined for synthetic humic acid type M42 and Aldrich humic acid. Fig. 9.2 depicts a comparison of the absorption trend for the investigated humic acid stock solutions stored at room temperature and daylight. For all humic acid solutions a decrease of the absorption at 465 nm with increasing storage time was observed. The lowest percentage decrease in dependence on the storage conditions and storage time was observed for Aldrich humic acid.

Significant changes in the pH values of the solutions of Aldrich humic acid and synthetic humic acid type M1 were not observed. The solutions of synthetic humic acid type M42 show a permanent decrease of their pH values.

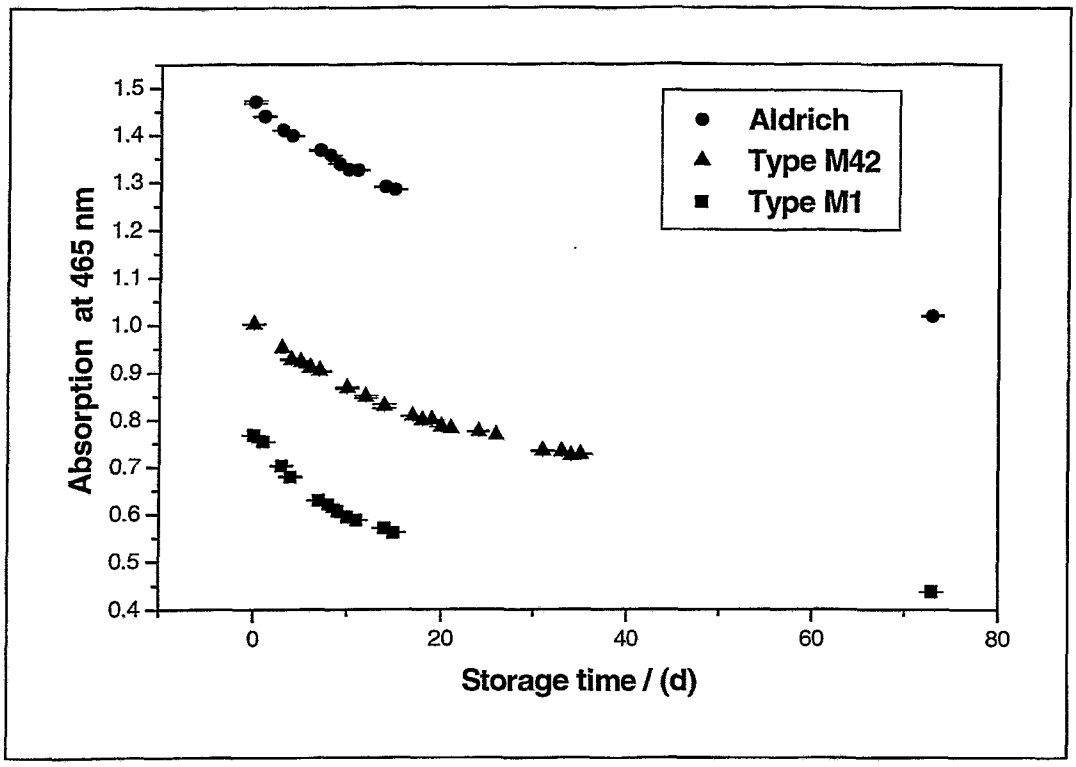

Figure 9.2: Absorption of humic acid stock solutions at 465 nm versus storage time ([HA]: 1 g/L; [NaOH]: 10^{-2} M; storage at room temperature and daylight).

The decrease in the absorption intensities points to the fact that the stock solutions are subjected to alterations under the applied conditions. The alterations may be caused by a hydrolytic decomposition of the humic acids, e.g., due to the hydrolysis of ester groups, because of the high pH values. The alterations of the solutions can be retarded by storing the solutions under cooling and exclusion of daylight.

Acid conditions

Under acid pH conditions all solutions show only an insignificant decrease in the absorption intensities at 465 nm, which lies in the range of the experimental error. Fig. 9.3 shows the trend of the absorption at 465 nm for the humic acid solutions stored at room temperature and daylight versus storage time.

Significant changes in the pH values were not observed for the solutions of synthetic humic acid type M1. Solutions of humic acid type M42 and Aldrich humic acid only show a negligible increase in their pH values.

In contrast to the storage at alkaline conditions no significant dependency between the storage conditions and the stability of the solution was observed.

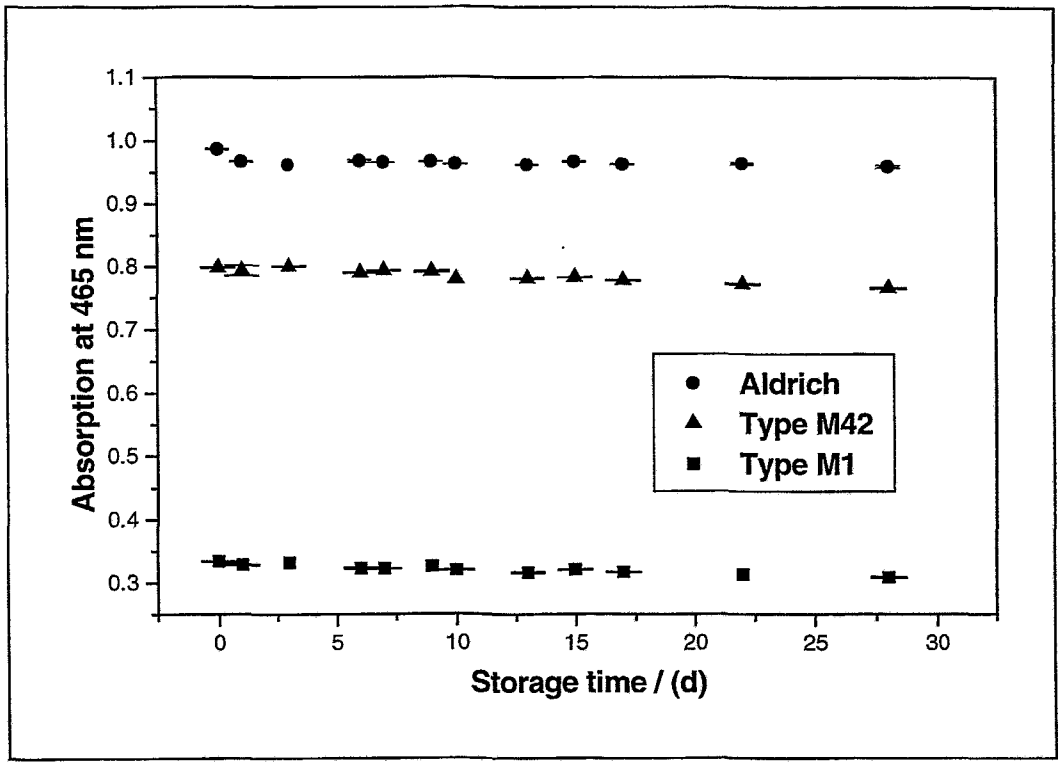

Figure 9.3: Absorption of humic acid solutions at 465 nm versus storage time ([HA]: 1 g/L for Aldrich HA and HA type M42; 0.5 g/L for HA type M1; pH 4 for Aldrich HA and HA type M42; pH 6 for HA type M1; storage at room temperature and daylight).

From that one can conclude, that humic acid stock solutions show a higher stability under acid conditions. However, instabilities of the solutions are expected with increasing storage time, which may be caused by chemical reactions and/or by the growth of fungi.

9.3 Conclusions

Aqueous stock solutions of synthetic and natural humic acids show comparable stabilities under similar storage conditions. They show alterations during the storage over long periods of time, whereby acid solutions show higher stabilities than alkaline solutions. For alkaline solutions we observed a strong dependency between the storage conditions and the stability of the solutions.

Freshly prepared stock solutions of synthetic and natural humic acids should be used to ensure comparable experimental conditions for the investigations of humic acids in solution.

10 Interaction of synthetic and natural humic acids with uranium(VI)

10.1 EXAFS investigations for the determination of structural parameters of uranyl(VI) humates [24]

Extended X-ray absorption fine structure analysis (EXAFS) is an useful tool for analyzing the complexation behavior of humic substances on a molecular level. EXAFS is a standard technique, providing molecular-level information on the nearest neighbor structure of a chosen absorbing atom [25], which also allows the investigation of amorphous materials and liquid substances.

The objective of the EXAFS investigations was to obtain information about the structure of uranyl-humic acid complexes, in particular about the binding of the UO_2^{2+} ion onto humic acid. The EXAFS investigations performed included the following focal points:

- comparison of the interaction between the purified natural humic acid from Fluka and the synthetic humic acid type M1 with UO_2^{2+} ions,
- comparison of uranyl humates with different uranyl loadings,
- comparison of uranyl humates prepared under different conditions and
- comparison of uranyl humates that were measured in the wet or dry form.

10.1.1 Experimental

Sample preparation

We studied uranyl humate complexes prepared under different conditions. The humic acid was either dissolved in aqueous solution or prepared as an aqueous suspension of solid humic acid. These were then reacted with solutions containing varying UO_2^{2+} amounts. After isolation and purification of the uranyl humates the samples were lyophilized. One sample was not dried completely, but measured in the form of a wet paste.

A list of the samples investigated, the concentration of uranyl ions per weight humic acid in the reaction solution during the preparation, the uranyl loadings of the samples regarding their carboxylic group contents and the general preparation method are given in Tab. 10.1. A detailed description of the sample preparation is given in [24].

Table 10.1: Sample preparation and UO_2^{2+} loadings of the uranyl humate complexes investigated.

Sample	Sample preparation		Uranyl humate	
	mg U/g HA in reaction solution	Method of sample preparation	UO_2^{2+} loading[a] (mg U/g HA)	UO_2^{2+} loading[b] (% COOH)
1	540	reaction of UO_2^{2+} with dissolved Fluka-HA; pH = 3.5	392	87
2	400	sorption of UO_2^{2+}; onto an aqueous suspension of Fluka-HA; pH < 1	160	35
3	45	reaction of UO_2^{2+} with dissolved Fluka-HA; pH = 4.0	36	8
4	48	reaction of UO_2^{2+} with dissolved Fluka-HA; pH = 4.0	44	10
5	21	reaction of UO_2^{2+} with dissolved synthetic HA type M1; pH = 4.0	18	14

[a] The UO_2^{2+} loadings of the samples were determined using ICP-MS following digestion of the uranyl humates in HNO_3. The average values from two ICP-MS determinations are shown.
[b] UO_2^{2+} loadings expressed in percent of carboxylic group capacity calculated assuming charge neutralization. The humic acid carboxylic group content was determined by the calcium acetate method.

Although similar amounts of uranyl ions per weight humic acid were used in the preparation of samples 1 and 2, their uranyl loadings differ significantly due to the different pH conditions during sample preparation.

EXAFS measurements

Uranium L_{III}-edge EXAFS transmission spectra were measured at room temperature at the Hamburger Synchrotronstrahlungslabor HASYLAB, experimental station RÖMO II, beamline X1.1, using a Si(311) double-crystal monochromator detuned ~ 50 % of the maximum incident flux. Fig. 10.1 shows schematically the experimental set-up.

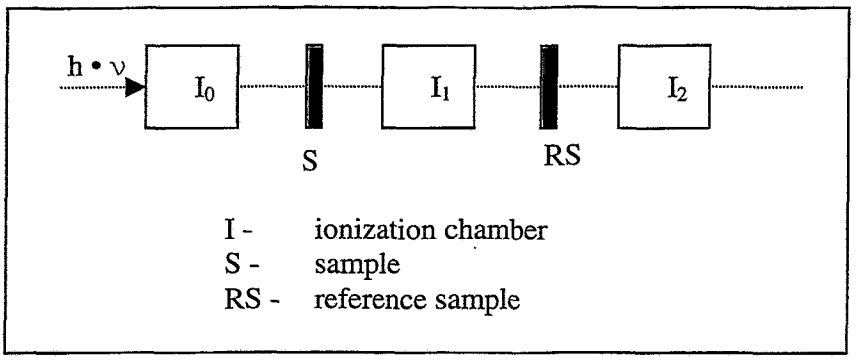

Figure 10.1: Experimental set-up of the EXAFS measurements.

The samples were dispersed in Teflon and pressed as 1.3 cm diameter pellets. The amount of sample corresponding to 18-30 mg U, calculated from the experimentally determined uranyl loadings given in Tab. 10.1, was introduced into the pellets. The jump over the U L_{III}-edge for these samples averaged 0.8. Sample 4 was measured as a wet paste, loaded into a polyethylene sample holder having thin windows in the direction of the synchrotron beam. The edge jump for this sample was only 0.2 so that the signal-to-noise ratio limited the upper range of the spectrum to ~ 17900 eV. To calibrate the energy of the sample spectra, a spectrum from a 0.2 M UO_2Cl_2 solution which was placed behind the sample, was recorded simultaneously. The energy of the first inflection point in the reference spectrum was defined as 17166 eV. Three spectra were recorded for each sample and then averaged. The ionization energy for the U L_{III} electron (E_0) was arbitrarily defined as 17185 eV for all averaged sample spectra.

Data reduction and analysis were performed using the suite of programs EXAFSPAK [26]. Scattering amplitude and phase-shift functions were calculated using the theoretical EXAFS modeling code FEFF6 [27]. A more detailed description of the data analysis is given in [24].

IR spectroscopy

IR spectra of the dried uranyl humate samples as well as the untreated humic acids were measured. Spectra from KBr pellets containing equal amounts of sample were recorded at room temperature between 200 and 4000 cm^{-1}.

10.1.2 Results and discussion

IR Spectroscopy

All IR spectra of the uranyl humate complexes show, in comparison to the uncomplexed humic acids, a decrease in the absorption bands characteristic for C=O and C-O vibrations of carboxylic groups at 1720 cm^{-1} and 1200 cm^{-1}, respectively. At the same time the intensity of bands associated with asymmetric and symmetric stretching vibrations of COO^- groups, found between 1560 cm^{-1} and 1520 cm^{-1} and at 1380 cm^{-1}, increases. As example, the IR spectra of the untreated Fluka humic acid and sample 1 are depicted in Fig. 10.2. For some samples the observed changes were not as great due to the low uranyl loadings. However, the combined decrease in carbonyl band intensity and increase in COO^- band intensity indicate the conversion of humic acid carboxylic groups to carboxylate ions through the loss of protons upon reaction with uranyl ions. This strongly suggests a direct interaction/complexation of the humic acids with the uranyl ions. Furthermore, the results from IR spectroscopy point to a monodentate coordination of the COO^- group onto the UO_2^{2+} ion [24].

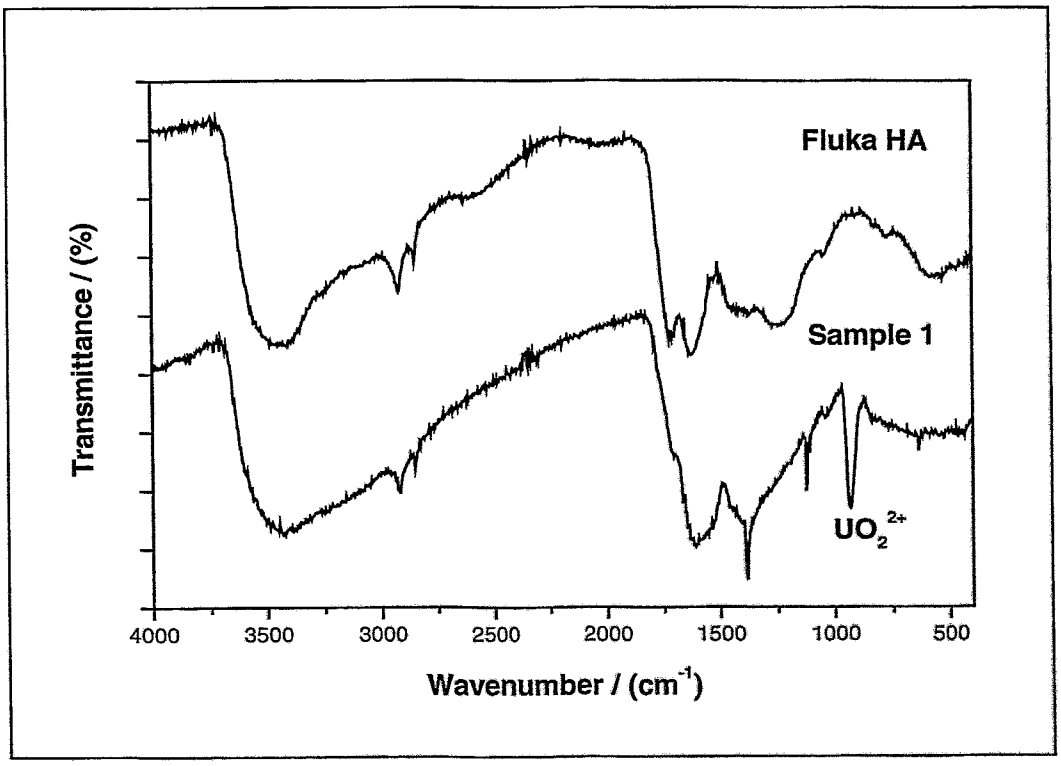

Figure 10.2: IR Spectra of the untreated, purified Fluka humic acid and sample 1, Fluka HA following complexation with uranyl ions.

EXAFS results

The EXAFS oscillations were isolated from the raw, averaged data by removal of the pre-edge background, followed by μ_0-removal via spline fitting techniques and normalization using a Victoreen falloff [25]. As example, Fig. 10.3 shows the U L_{III} absorption spectrum of sample 5, which is already energy calibrated and corrected relative to the pre-edge background.

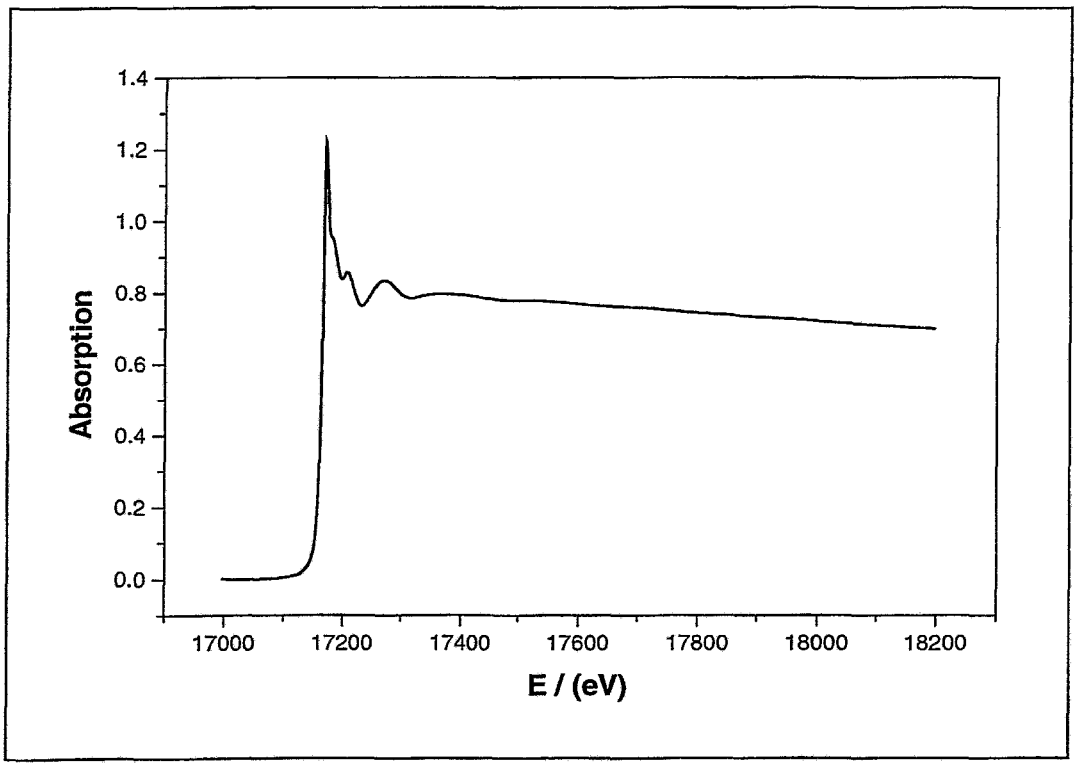

Figure 10.3: U L_{III}-edge absorption spectra of sample 5.

The k^3-weighted EXAFS oscillation of all investigated uranyl humate samples of Fluka humic acid and synthetic humic acid type M1 are depicted in Fig. 10.4.

The contribution of the different coordination shells to the EXAFS oscillation can be separated by Fourier transformation. Fig. 10.5 shows the corresponding Fourier transforms (FT's). The FT's represent pseudo-radial distribution functions of atoms surrounding the central, absorbing uranium atom. The intensity of the peaks corresponds to the coordination number. The peak position gives information about the distances of the atoms. The FT's are not corrected for EXAFS phase-shifts causing peaks to appear at shorter distances (R + Δ) relative to the true near-neighbor distances R.

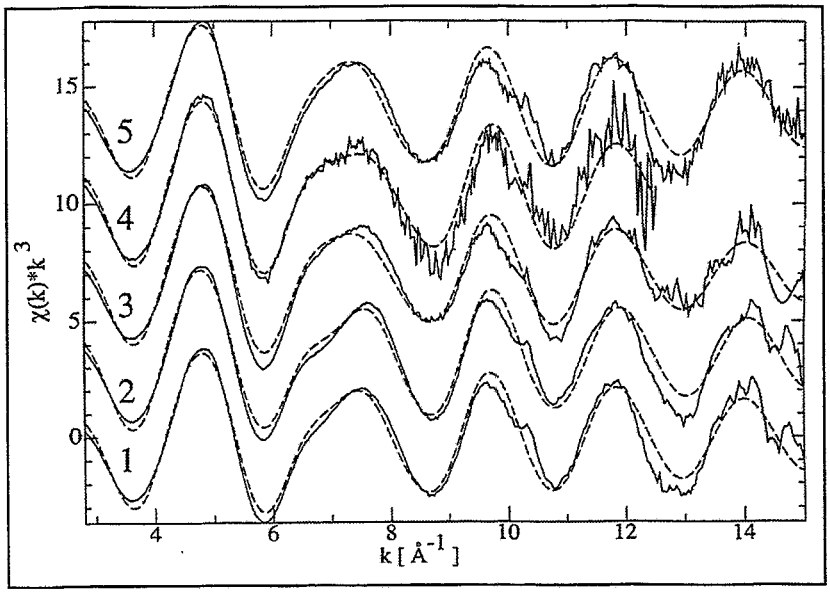

Figure 10.4: k^3-weighted U L_{III}-edge EXAFS for samples 1 – 5 (Tab. 10.1). The solid lines are the experimental spectra, the dashed lines result from the fit described in the text. For clarity, the spectra have been shifted along the y-axis.

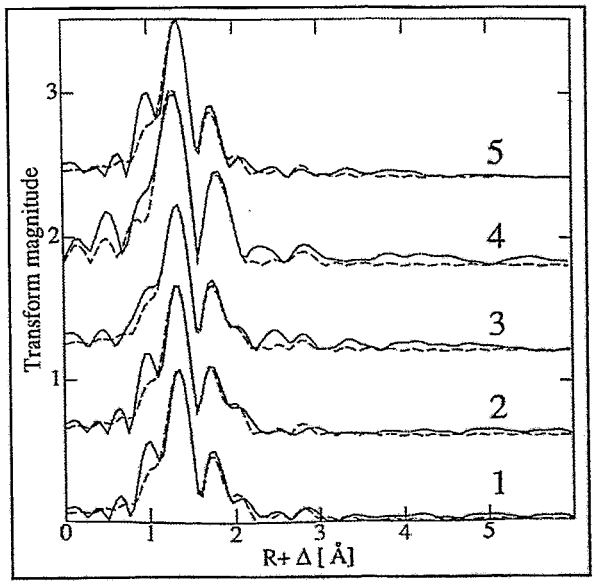

Figure 10.5: Fourier transforms of the EXAFS depicted in Fig. 10.4. The transformation in the k-region shown was performed using a rectangular window. The solid lines are the experimental spectra, the dashed lines results from their fit. For clarity, the spectra have been shifted along the y-axis.

The EXAFS oscillations in Fig. 10.4 show no significant differences except for slight variations in the structure of the shoulder centered at about 7 $Å^{-1}$. Two coordination shells are evident in the FT's in Fig. 10.5. All samples investigated show comparable FT's which are dominated by a peak at approximately 1.3 Å. This peak corresponds to the axial oxygen atoms

(O_{ax}) of the uranyl unit. The next peak represents the equatorial oxygen atoms (O_{eq}) coordinated to uranium. The weak peak in the FT's at about 2.9 Å is not from a true coordination shell. It results from multiple scattering along the uranyl unit [28,29]. No peaks with significant intensity indicative of scattering on a strong backscatterer, e.g., a U-U interaction are evident in the spectra.

The EXAFS oscillations were fitted to the EXAFS equation using a structural model with the two coordination shells observed in the FT's, containing oxygen atoms as backscatterer. In addition, multiple scattering involving both axial oxygen atoms of the uranyl unit was included in the fit. The k-range of the fits was 2.8 – 15 $Å^{-1}$. For sample 4 the k-range was limited to 2.8 – 12.5 $Å^{-1}$. The coordination number for the axial oxygen atoms (N_{ax}) was held constant at 2. The shift in threshold energy (ΔE_0) was varied as single value for all paths. A more detailed description of the evaluation of the experimental data including a test of the accuracy of the EXAFS analysis and an exemplary deconvoluted fit of an uranyl humate spectrum is given in [24].

The structural parameters obtained from the fits of the EXAFS oscillations are given in Tab. 10.2.

Table 10.2: Fit parameters for U L_{III}-edge EXAFS data for samples 1-5 (cf. Tab. 10.1) using the model described in the text (N_{ax} = 2). Errors in bond length (R) and coordination numbers (N) are ± 0.02 Å and ~20 %, respectively. (ΔE_0: shift in threshold energy, σ^2 : EXAFS-Debye-Waller factor).

Sample	U-O_{ax}		U-O_{eq}			ΔE_0
(cf. Tab. 10.1)	R (Å)	σ^2 ($Å^2$)	N	R (Å)	σ^2 ($Å^2$)	(eV)
1	1.78	0.002	5.0	2.38	0.013	- 7.5
2	1.77	0.002	5.4	2.39	0.013	- 8.3
3	1.78	0.003	5.2	2.37	0.013	- 8.5
4	1.78	0.002	5.0	2.37	0.010	- 7.9
5	1.78	0.002	5.1	2.37	0.014	- 8.5

The axial U-O_{ax} distances in all samples investigated were determined to be 1.77 – 1.78 Å, equatorial U-O_{eq} distances amount to 2.37 - 2.39 Å. Within the experimental error there are no differences in the U-O bond distances between the samples with large loadings (sample 1 and 2) compared to those with relatively low loadings (sample 3 and 4). Furthermore, the structural parameters obtained for the sample prepared by sorption of UO_2^{2+} onto a suspension of natural humic acid (sample 2) are the same as those for the samples prepared from humic

acid in solution. The sample measured as a wet paste (sample 4) shows the same results as the samples measured in the dried form. This indicates that the presence of excess water does not change the average equatorial bond distance surrounding uranium in the uranyl humate complexes. The comparison of the fit results obtained for the samples prepared from Fluka humic acid and the uranyl humate prepared from synthetic humic acid type M1 shows that the synthetic humic acid behaves similarly towards the binding of UO_2^{2+} ions as the natural humic acid. This was already found in former studies of the interaction of UO_2^{2+} ions with the same synthetic humic acid and Fluka humic acid with higher UO_2^{2+}-loadings [10].
The high Debye-Waller-factors are attributed to a high disorder in the arrangement of atoms in the equatorial shell which is caused by the high variety of binding sites of the humic acids. Additional measurements at low temperatures are necessary to distinguish between static disorder, such as the presence of two U-O_{eq} distances close in proximity and thermal disorder.

Assuming that carboxylic groups are the most important functional groups of the humic acid for the complexation of metal ions at pH 4, essentially three important bonding modes of carboxylate ions to metal ions are possible, as depicted in Fig. 10.6.

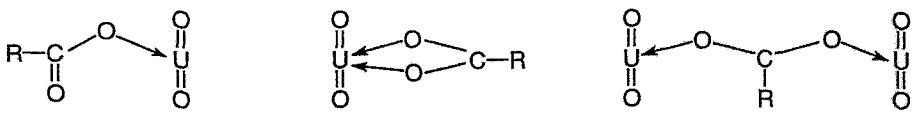

Figure 10.6: Schematic representation of the possible coordination modes of the carboxylate ion onto the UO_2^{2+} unit.

Nineteen crystalline uranyl carboxylate complexes with known structures, having ligands that may serve as models for humic acid structural elements, were considered regarding their axial and equatorial U-O bond distances [24]. The averaged bond distances are 1.76 ± 0.03 Å for U-O_{ax}, 2.48 ± 0.05 Å for U-O_{eq} (bidentate carboxylate oxygen atoms), 2.39 ± 0.05 Å for U-O_{eq} (monodentate carboxylate oxygen atoms) and 2.36 ± 0.05 Å for U-O_{eq} (bridging carboxylate oxygen atoms).
The observed binding distances for the axial oxygen atoms of the uranyl unit for sample 1 – 5 are comparable to the averaged bond distance observed for the crystalline uranyl carboxylate complexes [24]. Furthermore, the U-O_{eq} distances in the uranyl humates lie closer to the averaged values typical for monodentate or bridging carboxylate groups, than to the averaged value for bidentate coordination. So we conclude that the number of monodentate and/or

bridging carboxylate ligands must be greater than the number of bidentate ligands. Otherwise the average U-O_{eq} distance would exceed the measured value of 2.37 ± 0.02 Å. Nevertheless, this result is in contrast to IR results published by Koglin et al. [30], who interpreted a bidentate coordination of humic acid carboxylic groups onto uranium.

The EXAFS fits of the uranyl humate spectra show the presence of five oxygen atoms in the equatorial sphere around the uranyl unit. Assuming charge neutralization two negative charged complexing groups are required to neutralize the charge of the uranyl unit. If two monodentate carboxylate groups are considered as the bonding partners three neutral ligands are necessary to fulfill the coordination requirement of five equatorial atoms. The binding of two bidentate carboxylate anions or four bridging groups would also attain charge neutralization. In both cases, four equatorial oxygen atoms are contributed by the carboxylate ligands and the coordination number of five is still not reached. However, in the case of bidentate ligation the resulting average bond distance would be much longer. This is of course assuming that the bond length between any neutral ligands and uranium is not extremely short. As example, the average U-O_{eq} bond distance for water ligands in the crystalline complexes considered in [24] is 2.43 Å. If water is considered as the neutral ligand/s then the average U-O_{eq} bond length from a neutral complex involving bidentate carboxylate groups is exceedingly longer than the distances observed for samples 1-5.

If not only carboxylate ligands but also acidic hydroxyl groups, e.g., phenolic OH or hydroxyl groups in α-position to a carboxyl group, are included as possible ligands for charge neutralization several neutral ligands must be present to obtain a coordination number of five. Which kind of neutral ligands contribute to the coordination is not known. However, it is possible that protonated phenolic OH groups contribute to the complexation process.

The possibility of any coordination involving bridging of two uranyl ions via a single carboxylate oxygen atom (μ-oxo-bridging) was excluded because no typical U-U distance for such coordination was observed. However, from our analysis the presence of bridging carboxylate groups cannot be excluded [24].

10.2 Determination of uranyl complexation constants with natural and synthetic humic acids at pH 4

Laser-induced fluorescence spectroscopy offers a very good possibility to investigate the complexation behavior of metal ions with humic acids. This method renders the possibility for a direct quantification and characterization of the investigated system with very low detection limits. In contrast to other methods like ultrafiltration, ion exchange or solvent extraction, a further advantage of this method represents the possibility for a direct determination of the metal ion speciation without any disturbance of the thermodynamic equilibrium.
The objective of the investigation was to determine the ability of synthetic humic acid type M42, which has a carboxylic group content comparable to most natural humic acids, to mimic the complexation behavior of natural humic acids with UO_2^{2+} ions.

10.2.1 Experimental

Preparation of uranyl humate solutions
To characterize the interaction of the UO_2^{2+} ion with synthetic and natural humic acids, we measured the fluorescence signal of the UO_2^{2+} ion as a function of the total uranyl concentration at a constant humic acid concentration. All experiments were performed in air at 20 ± 1 °C in 0.1 M $NaClO_4$ at pH 3.98 ± 0.01 for synthetic humic acid type M42 (charge M81) and pH 3.96 ± 0.03 for Aldrich humic acid. The humic acid concentration was kept constant at 5 mg/L. The uranyl concentration was varied from $1.0 \cdot 10^{-6}$ to $9.7 \cdot 10^{-6}$ M for synthetic humic acid type M42 and $6.5 \cdot 10^{-7}$ to $8.3 \cdot 10^{-6}$ M for Aldrich humic acid. The sample solutions were prepared from stock solutions of humic acid and $UO_2(ClO_4)_2$. The concentration of UO_2^{2+} in the solutions was determined with ICP-MS analysis. The ionic strength was adjusted to 0.1 M with 1 M $NaClO_4$ (p.a., Merck). Calibration of the relative fluorescence signal as a function of the UO_2^{2+} concentration was done with solutions that were identical to the solutions of the complexation experiments but did not contain any humic acid. The pH values were adjusted with NaOH (Merck) and $HClO_4$ (Merck).

The uranyl species distribution from pH 3 to 9 ($[UO_2^{2+}]$: $1 \cdot 10^{-5}$ M; pCO_2: $10^{-3.5}$ atm; 0.1 M $NaClO_4$) was calculated with the EQ3/6 program [31] based on complex formation constants compiled by Grenthe et al. [32] (NEA data base). Under these conditions, the first uranyl

hydrolysis species, UO_2OH^+, occurs besides the free UO_2^{2+} ion at pH 4 with a relative concentration of 2.7 %. Thus, the uranyl hydroxo species concentrations in the experiments performed are lower than the experimental error and were therefore not considered for calculating the complexation constants.

Laserfluorescence spectroscopic measurements

A detailed description of the laser instrumentation is given in [33]. The spectroscopic light source was a Nd:YAG laser, pulsed with a repetition rate of 10 Hz (GCR 230, Spectra Physics, Mountain View, CA, USA). The fourth harmonic oscillation of the Nd:YAG laser (266 nm) at laser energies below 700 µJ was applied to excite the uranyl fluorescence. At these energies, no significant photolytic decomposition of the humic acid occurs [33]. The emission signal was focused into the spectrograph (Model 1235 Acton Research, Acton, MA, USA) by a fiber optic cable. For fluorescence detection, we used a time controlled photodiode array detector (Model 1455 EG&G Instruments, Princeton Applied Research, Princeton, NJ, USA), cooled to – 30 °C. Using a delay generator (Model 9650, EG&G Instruments), the time gate of fluorescence detection was set to open at 200 ns after the excitation pulse for an interval of 1000 ns. Time resolved measurements allow the discrimination of uranyl fluorescence signal against excitation pulse and short humic acid fluorescence emission (fluorescence lifetime < 10 ns [10]). The fluorescence signal was measured from 408 to 634 nm. Ten spectra of each sample were collected over 100 laser pulses in each case. The spectra were standardized relative to the pulse energy. An average spectrum was calculated from 10 emission spectra.

10.2.2 Results and discussion

The measured fluorescence spectra represent the sum of the free UO_2^{2+} ion fluorescence, the fluorescence of the first hydrolytic uranyl species (UO_2OH^+) and a residue of scattered laser light of the excitation pulse (second order) at 532 nm produced in the spectrograph. The spectra were deconvoluted by a non-linear least square method using spectra from earlier measurements [33] to calculate the contribution of the free UO_2^{2+} ion to the fluorescence signal. The spectrum of UO_2OH^+ was included in the peak deconvolution because of the strong fluorescence yield of UO_2OH^+ in comparison to the free UO_2^{2+} ion. The amount of

UO_2OH^+ (< 2.7 %) that was present in the experiment was neglected in the stability constant calculations because its concentration was below the experimental error for the UO_2^{2+} concentration determination. For all cases no emission of the uranyl humate complex was directly observed. Furthermore, we did not observe any quenching effects of the UO_2^{2+} ion by self quenching or quenching by the humic acid in the investigated concentration range.

The uranyl fluorescence intensity for each sample was integrated between 465 and 570 nm. Equivalent results from the solutions without humic acid were used to determine the free UO_2^{2+} concentration when uranyl humate is present.

The evaluation of the experimental data was performed based upon the metal ion charge neutralization model [34], which considers the complexation reaction of a given metal ion with humic acid as a metal ion charge neutralization process. According to this model, the UO_2^{2+} ion occupies two proton exchanging sites of the humic acid molecule [Eq. (10.1)]:

$$UO_2^{2+} + HA(II) \rightleftharpoons UO_2HA(II) \qquad (10.1)$$

where HA(II) represents the humic acid ligand and $UO_2HA(II)$ stands for the uranyl humate complex.

$$\beta = \frac{[UO_2HA(II)]}{[UO_2^{2+}]_{free} \cdot [HA(II)]_{free}} \qquad (10.2)$$

β - complexation constant; $[UO_2HA(II)]$ - uranyl humate concentration; $[UO_2^{2+}]_{free}$ – free uranyl ion concentration; $[HA(II)]_{free}$ – free humic acid concentration

The model was chosen because it offers the possibility to determine complexation constants which are independent of the humic acid origin, the metal ion concentration, and the pH value. Based on this concept, stability constants of uranyl complexes with natural humic acids and their synthetic analogues are expected to be similar.

Because not all complexing sites of the humic acid are available for the UO_2^{2+} ion binding the loading capacity (LC), which represents the mole fraction of maximal available complexing sites of the humic acid, is introduced by this model. The LC represents a humic acid specific value which depends on the experimental conditions.

The LC and the complexation constants were determined graphically by linear regression of the experimental data after rearranging Eq. (10.3) for the free UO_2^{2+} ion concentration [34]:

$$\beta = \frac{[UO_2HA(II)]}{[UO_2^{2+}]_{free} \cdot ([HA(II)]_{total} \cdot LC - [UO_2HA(II)])} \qquad (10.3)$$

where β represents the complexation constant, $[UO_2HA(II)]$ the uranyl humate concentration, $[UO_2^{2+}]_{free}$ the free uranyl ion concentration, $[HA(II)]_{total}$ the total molar humic acid concentration [34] and LC stands for the loading capacity.

$$[UO_2^{2+}]_{free} = LC \bullet \frac{[UO_2^{2+}]_{free} \bullet [HA(II)]_{total}}{[UO_2HA(II)]} - \frac{1}{\beta} \qquad (10.4)$$

Fig. 10.7 shows the analysis for synthetic humic acid type M42.

Considering the graphically determined LC, we computed a complexation constant for each experimental point. The results of these calculations, the analytical data of the starting concentrations and the data derived from the spectroscopic measurements are summarized in Tab. 10.3. Tab. 10.4 gives the graphically determined complexation constants and the LC in comparison to the values published by Czerwinski et al. [35] obtained by using a natural humic acid from the Gorleben site.

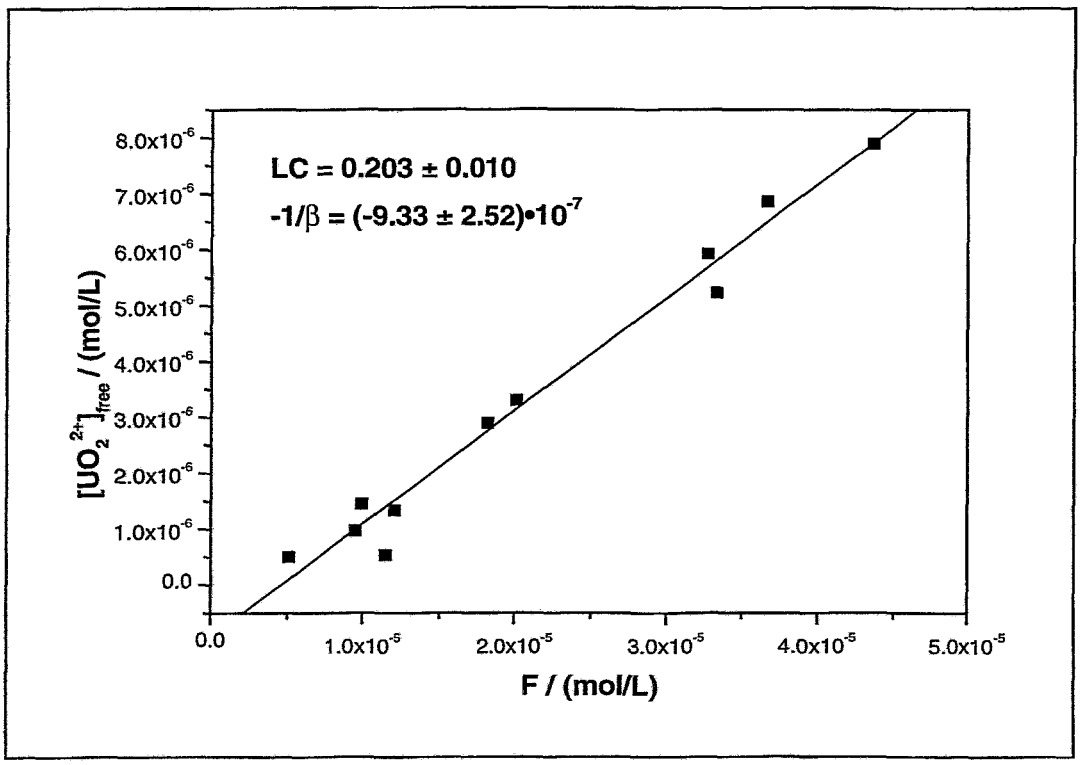

Figure 10.7: Graphically determination of the loading capacity (LC) and the complexation constant for the complexation of synthetic humic acid type M42 with the UO_2^{2+} ion by linear regression of experimental data.

$$F = \frac{[UO_2^{2+}]_{free} \bullet [HA(II)]_{total}}{[UO_2HA(II)]}$$

Table 10.3: Analytical data of the starting concentrations, the spectroscopically determined data of each component, and log β for the complexation of synthetic humic acid of type M42 and Aldrich humic acid.

$[HA(II)]_{total}$ (µmol/L)	$[UO_2^{2+}]_{total}$ (µmol/L)	$[UO_2^{2+}]_{free}$ (µmol/L)	$[UO_2HA(II)]$ (µmol/L)	$[HA(II)]_{free}$ (µmol/L)	log β
Synthetic humic acid type M42 (charge M81)					
(PEC[a]: 3.90 ± 0.18 meq/g; pH 3.98 ± 0.01; I: 0.1 M $NaClO_4$; LC: 0.203 ± 0.010)					
9.8 [b]	1.00	0.54	0.46	1.53	5.74
9.8	1.47	0.51	0.97	1.02	6.27
9.8	1.97	0.97	1.00	0.99	6.02
9.8	2.42	1.34	1.08	0.90	5.95
9.8	2.88	1.45	1.43	0.56	6.25
9.8	4.44	2.89	1.55	0.43	6.09
9.8	4.90	3.30	1.60	0.38	6.10
9.8	6.76	5.23	1.54	0.45	5.82
9.8	7.71	5.93	1.78	0.21	6.16
9.8	8.70	6.86	1.83	0.15	6.24
9.8	9.66	7.89	1.77	0.21	6.03
Aldrich humic acid (charge A2)					
(PEC: 5.33 ± 0.12 meq/g; pH 3.96 ± 0.03; I: 0.1 M $NaClO_4$; LC: 0.217 ± 0.022)					
13.3	0.65	0.27	0.38	2.51	5.76
13.3	1.24	0.48	0.77	2.12	5.88
13.3	2.42	1.23	1.19	1.70	5.76
13.3	2.96	1.45	1.51	1.38	5.88
13.3	4.80	2.87	1.93	0.96	5.84
13.3 [b]	6.07	3.58	2.49	0.40	6.24
13.3	6.99	4.95	2.04	0.85	5.68
13.3	8.27	5.79	2.48	0.41	6.01

[a] PEC: Proton exchange capacity.

[b] Value was not considered for validation.

Table 10.4: Complexation constants and loading capacities of synthetic humic acid type M42 and purified natural humic acid from Aldrich in comparison to a Gorleben humic acid.

	Synthetic humic acid type M42 (charge M81)	Aldrich humic acid (charge A2)	GoHy humic acid GoHy-537 [35]
	Complexation constants log β [a]		
Graphical [b]	6.04 ± 0.24	5.86 ± 0.28	-
Calculated [c]	6.06 ± 0.35	5.88 ± 0.35	6.16 ± 0.13
	Loading capacities (LC) [%] [a]		
Graphical [b]	20 ± 2	22 ± 4	18.5 ± 0.3

[a] Deviations = 2 σ.
[b] Calculated by linear regression of experimental data.
[c] Mean values from Tab. 10.3.

Within the experimental errors we found a remarkable agreement between the LC and complexation constants of the synthetic humic acid type M42 and Aldrich humic acid, which indicates a similar complexation behavior for both investigated systems. This fact was already observed comparing the complexation behavior of the natural humic acids from Fluka and Aldrich with a previous sample of synthetic humic acid type M42 published in [36].
For validation of the postulated complexation reaction [Eq. (10.1)], Eq. (10.2) was rearranged to:

$$\log\frac{[UO_2HA(II)]}{[UO_2^{2+}]_{free}} = \log[HA(II)]_{free} + \log\beta \quad . \tag{10.5}$$

The slope of the linear regression function of Eq. (10.5) represents the metal ion to ligand ratio and will result of unity, when Eq. (10.1) is valid. The determined values are 0.92 ± 0.17 for synthetic humic acid and 0.81 ± 0.16 for Aldrich humic acid. These results verify the postulated complexation reaction.

Although there are several literature values for the uranyl humic acid complexation, a direct comparison of our complexation data is only possible with data published by Czerwinski et al. [35] given in Tab. 10.4, because these were also treated with the metal ion charge neutralization model. The complexation constants of our synthetic humic acid and Gorleben humic acid agree very well within the experimental errors. There are small differences in the loading capacity of our product and of Gorleben humic acid which may be due to their different origin.

From these results we conclude that the synthetic humic acid type M42 appropriately simulates the functionality of natural humic acids although there are differences in their elemental composition and structural elements

10.3 Structure of uranyl(VI) humate complexes of synthetic and natural humic acids studied by FTIR spectroscopy

IR spectroscopy is a useful tool for the characterization of humic acids regarding their functionality. Functional and structural changes of humic acids are reflected by changes in the intensity, position or occurrence of characteristic absorption bands. In addition, IR spectroscopy offers the possibility to investigate functional variations of humic acids due to complex formation processes with metal ions [24].

The objective of this work was to proof the similar coordination of UO_2^{2+} ions onto synthetic and natural humic acids and to confirm previous results obtained by EXAFS and laser-induced fluorescence spectroscopy. For the first time uranyl humate complexes were investigated in the far infrared range (FIR) beside the middle infrared range (MIR) [37].

10.3.1 Experimental

Preparation of uranyl humates

For the preparation of the uranyl humate complexes synthetic humic acid type M1 and type M42 as well as natural humic acid from Aldrich were suspended in water. On the basis of their carboxylic group contents uranyl acetate (type M1, Aldrich) or uranyl perchlorate (type M42) solutions were added to the aqueous humic acid suspensions for the complex formation. The pH values were adjusted to pH 4 for synthetic humic acid type M1 and Aldrich humic acid and to pH 2 for humic acid type M42. The uranyl humate complexes were isolated by centrifugation, purified and lyophilized. The uranyl loadings of the complexes were determined by ICP-MS after digestion of the complexes with HNO_3. Assuming charge neutralization, the uranyl humates of humic acid type M1, type M42 and Aldrich show regarding their carboxyl group contents uranyl loadings of 120 %, 29 % and 129 %, respectively. The low uranyl loading of humic acid type M42 compared to humic acid type M1 and humic acid Aldrich results from the different pH values during sample preparation.

FTIR measurements

FTIR measurements were carried out with the spectrometer mod. SPECTRUM 2000 (Perkin Elmer, Nieuwerke, NL). The humic acids as well as their uranyl complexes were measured in the solid form as KBr pellets (MIR range) and PE pellets (FIR range).

10.3.2 Results and discussion

Fig. 10.8 shows a comparison of the FTIR spectra of the humic acids investigated in the range between 4000 cm^{-1} and 50 cm^{-1} (MIR-FIR).

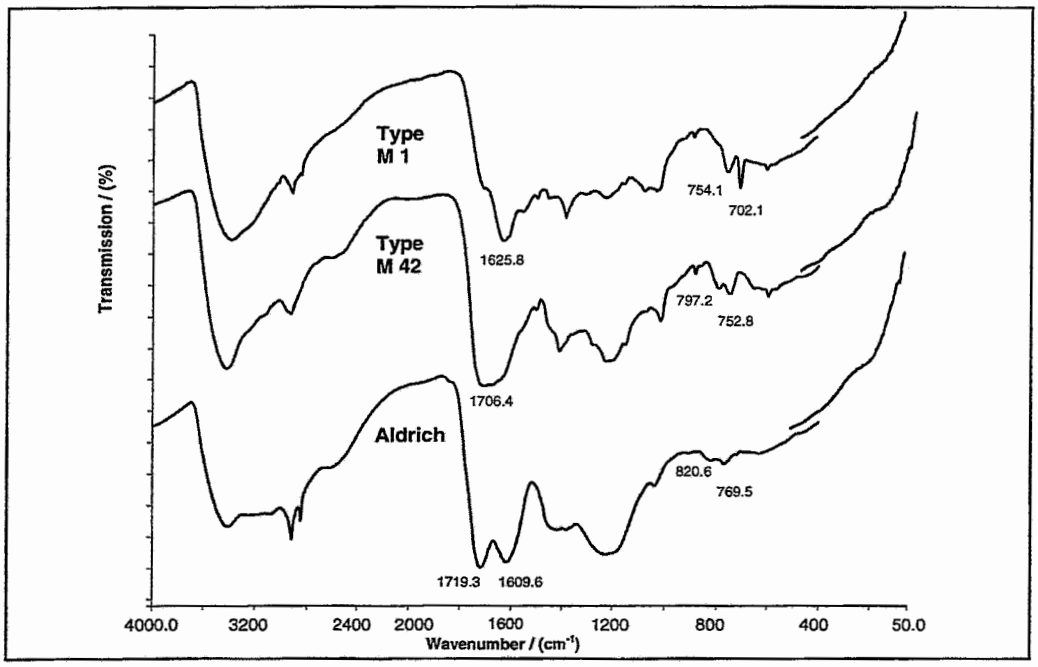

Figure 10.8: FTIR spectra (MIR and FIR) of synthetic humic acid type M1 and type M42 and Aldrich humic acid.

The humic acids show comparable IR absorption bands. However, some differences occur in the MIR. Synthetic humic acid type M1 exhibits clear δ(C-H) out of plane vibrations at 702.1 cm^{-1} and 754.1 cm^{-1} which corresponds to mono-substituted aromatic structures caused by the use of phenylalanine as precursor substance. In contrast to synthetic humic acid type M1, synthetic humic acid type M42 and Aldrich humic acid show more pronounced C=O stretching vibrations at 1706.4 cm^{-1} (M42) and 1609.6 cm^{-1}, 1719.3 cm^{-1} (Aldrich) due to their higher carboxylic group contents. All humic acids show absorption bands which correspond

to aliphatic structural elements. As expected, in the FIR the humic acids exhibit no characteristic absorption bands.

Fig. 10.9 depicts the FTIR spectra of the solid uranyl humate complexes. The FTIR spectra of all uranyl humates show in comparison to the untreated humic acids comparable variations due to the complex formation. All FTIR spectra of the uranyl humate complexes show in consequence of the complexation reaction a decrease of the absorption bands characteristic for C=O and C-O vibrations of non-dissociated carboxylic groups at about 1720 cm^{-1} and 1200 cm^{-1}.

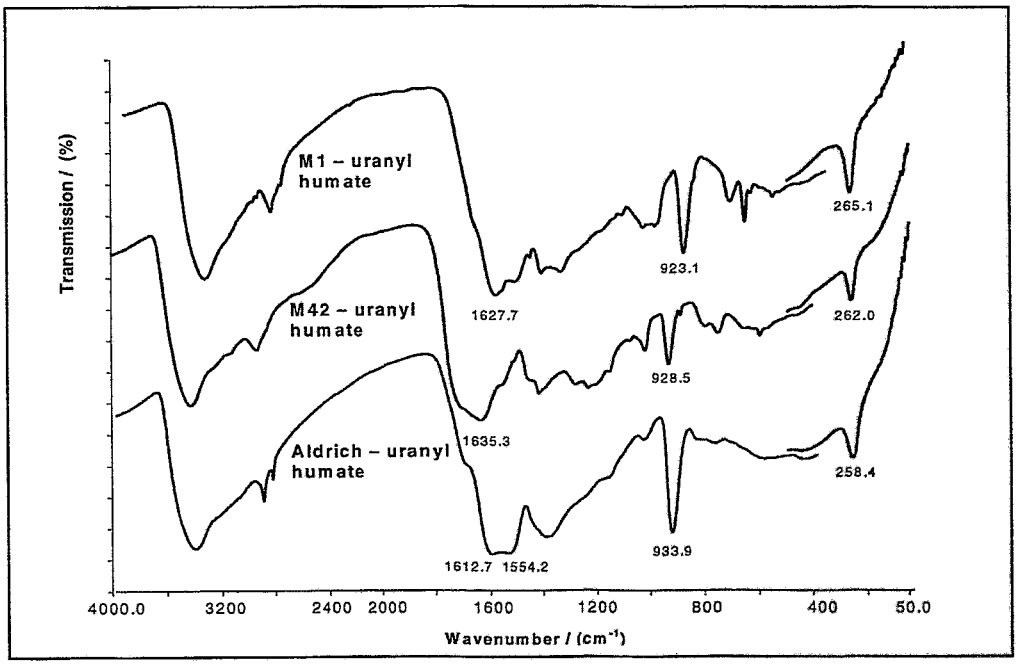

Figure 10.9: FTIR spectra of uranyl humate complexes of synthetic humic acid type M1, type M42 and Aldrich humic acid.

For all complexes the asymmetric UO_2^{2+} stretching vibration was observed in the MIR range (923.1 cm^{-1} (M1), 928.3 cm^{-1} (M42) and 933.1 cm^{-1} (Aldrich)). The position of this band is shifted significantly to higher wavenumbers with decreasing aromatic character of the complexing humic acid. Furthermore, characteristic UO_2^{2+} bending frequencies were first detected in the FIR range at 265.1 cm^{-1} (M1), 262.0 cm^{-1} (M42) and 258.4 cm^{-1} (Aldrich). These bands show a significant shift to lower wavenumbers with decreasing aromatic character of the humic acid.

From the results obtained one can conclude that the UO_2^{2+} coordination onto humic acids is comparable for the investigated synthetic and natural humic acids. The observed shifts of the absorption bands of the UO_2^{2+} unit in the MIR and FIR range may be explained by differences

in the aromaticity of the humic acids. However, these differences do not indicate significant differences in the UO_2^{2+} coordination.

The FTIR spectroscopic results agree with our previous investigations by EXAFS and laser-induced fluorescence spectroscopy and show once more that the synthetic humic acids mimic the functionality of natural humic acids very well.

11 Influence of phenolic hydroxyl groups on the complexation behavior of humic acids with uranium(VI)

The influence of phenolic OH groups on the complexation behavior of humic acids under acid and neutral conditions is not known up to now. Often it is assumed that only humic acid carboxylic groups act as complexing groups in the complexation process with metal ions at pH values lower pH 9 because of the high pK_a values of phenolic OH groups [38]. Nevertheless, phenolic OH groups may contribute to the complexation process as chelating agents. Beyond it they are able to form hydrogen bonds, e.g., with oxygen atoms coordinated to the complexing metal ion.

For the first time, we investigated the influence of phenolic OH groups on the complexation behavior of humic acids with UO_2^{2+} ions using a modified synthetic humic acid type M1 with blocked phenolic OH groups as well as a additional alkali treated synthetic humic acid of type M1 (see paragraph 7; type M1, charge R36/95). The investigations were performed at pH 4 by laser-induced fluorescence spectroscopy.

11.1 Experimental

The preparation of the uranyl humates corresponds to the procedure described in paragraph 10.2.1. The composition of the investigated uranyl humate solutions as well as the main characteristics of the humic acids applied are shown in Tab. 11.1.

The calibration of the relative fluorescence signal as a function of the UO_2^{2+} concentration was done with solutions that were identical to the solutions of the complexation experiments but did not contain any humic acid.

Table 11.1: Characteristics of the applied humic acids and composition of the investigated uranyl humate solutions.

	Type M1-V [a]	Type M1-B [b]
phenolic OH / (meq/g)	1.7 ± 0.1	1.1 ± 0.2
PEC [c] / (meq/g)	2.12 ± 0.06	1.94 ± 0.13
COOH / (meq/g)	2.03 ± 0.02	1.91 ± 0.07
UO_2^{2+} / (µmol/L)	1.1 – 10.3	1.1 – 10.3
HA / (mg/L)	10	10
pH	3.96 ± 0.04	3.94 ± 0.05
I_{NaClO4} / (mol/L)	0.1	0.1

[a] Type M1-V: humic acid type M1 directly saponified. [b] Type M1-B: humic acid type M1 with blocked phenolic OH groups. [c] PEC: Proton exchange capacity.

The experimental conditions of the spectroscopic measurements were the same as described in paragraph 10.2.1.

11.2 Results and discussion

The experimental data were evaluated applying the charge neutralization model by Kim and Czerwinski [34]. This model was chosen because it renders, due to the introduction of the loading capacity as normalizing term, the possibility for the description of the complexation behavior of humic acids independent of the experimental conditions and of the origin of the humic acids. Applying this complexation model comparable complexation constants will be determined for different humic acids. That means, in contrast to other thermodynamic complexation models, differences in the complexation behavior of humic acids will not be reflected in different stability constants. However, differences in the complexation behavior of humic acids will result in different loading capacities, which depend on the humic acid and the experimental conditions.

A significant lower loading capacity for the humic acid with blocked phenolic OH groups should result, if the blocking of the phenolic OH groups shows an influence on the complexation behavior of humic acids with UO_2^{2+} ions.

Tab. 11.2 shows the analytical data of the starting concentrations, the spectroscopically determined data for each component and the complexation constants which were determined for each measurement. The loading capacities (LC, Eq. (11.1)) for both humic acids were

determined graphically as described in paragraph 10.2.2. An illustration of the LC (Eq. (11.1)) for both humic acids with UO_2^{2+} ions, which represents the mole fraction of maximal available complexing sites of the humic acids under the applied experimental conditions, is given in Fig. 11.1.

$$LC = \frac{[UO_2HA(II)]_{max}}{[HA(II)]_{tot}} \qquad (11.1)$$

$[UO_2HA(II)]_{max}$ represents the maximal concentration of humic acid complex which can be formed under the applied experimental conditions and $[HA(II)]_{tot}$ stands for the total molar humic acid concentration.

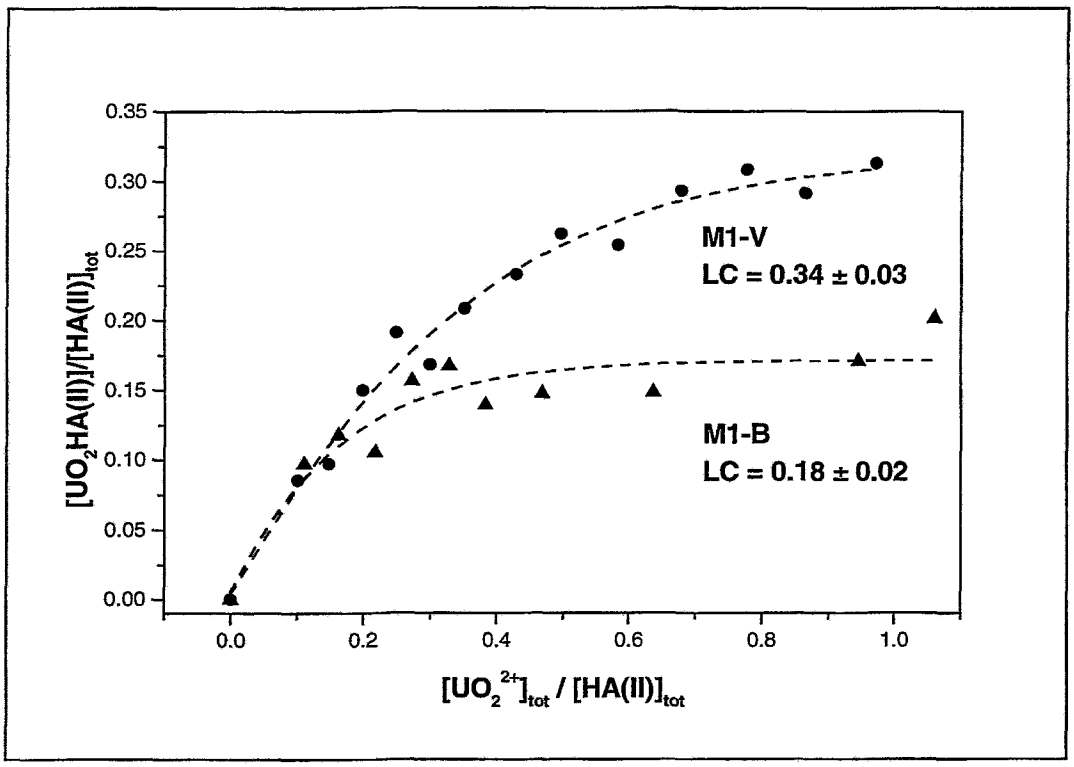

Figure 11.1: Loading capacities for humic acid M1-V and M1-B.

Tab. 11.3 summarizes the LC and the calculated complexation constants for humic acid M1-V and M1-B.

Table 11.2: Analytical data of the starting concentrations, the spectroscopically determined data of each component, and log β for the complexation of the alkali treated synthetic humic acid type M1 (M1-V) and the modified synthetic humic acid type M1 with blocked phenolic OH groups (M1-B).

$[HA(II)]_{total}$ (µmol/L)	$[UO_2^{2+}]_{total}$ (µmol/L)	$[UO_2^{2+}]_{free}$ (µmol/L)	$[UO_2HA(II)]$ (µmol/L)	$[HA(II)]_{free}$ (µmol/L)	log β
Type M1-V (unmodified phenolic OH)					
(PEC[a]: 2.12 ± 0.06 meq/g; pH 3.96 ± 0.04; I: 0.1 M $NaClO_4$; LC: 0.34 ± 0.03)					
10.6	1.07	0.16	0.91	2.69	6.32
10.6	1.56	0.53	1.03	2.56	5.88
10.6	2.10	0.52	1.59	2.01	6.18
10.6	2.63	0.61	2.03	1.57	6.33
10.6	3.17	1.39	1.78	1.81	5.85
10.6	3.70	1.50	2.21	1.39	6.03
10.6	4.54	2.07	2.47	1.13	6.02
10.6	5.25	2.47	2.78	0.82	6.14
10.6	6.18	3.48	2.69	0.90	5.93
10.6	7.18	4.08	3.11	0.49	6.19
10.6	8.23	4.96	3.27	0.32	6.31
10.6	9.16	6.07	3.09	0.51	6.00
10.6	10.29	6.98	3.32	0.28	6.23
Type M1-B (modified phenolic OH groups)					
(PEC: 1.94 ± 0.13 meq/g; pH 3.94 ± 0.05; I: 0.1 M $NaClO_4$; LC: 0.18 ± 0.02)					
9.7	1.07	0.13	0.94	0.86	6.94
9.7	1.56	0.42	1.14	0.65	6.62
9.7	2.10	1.09	1.02	0.78	6.08
9.7	2.63	1.12	1.52	0.28	6.69
9.7	3.17	1.54	1.62	0.17	6.78
9.7	3.70	2.36	1.35	0.45	6.11
9.7	4.54	3.10	1.43	0.36	6.10
9.7	6.18	4.74	1.44	0.36	5.93
9.7	9.16	7.50	1.66	0.14	6.20
9.7 [a]	10.29	8.34	1.96	-	-

[a] Value was not considered for determination of log β and validation.

Table 11.3: Complexation constants and loading capacities of the synthetic humic acid with unmodified phenolic OH groups (M1-V) and with blocked phenolic OH groups (M1-B).

	Synthetic humic acid M1-V	Synthetic humic acid M1-B
	Complexation constants log β [a]	
Calculated [b]	6.11 ± 0.34	6.38 ± 0.74
	Loading capacities (LC) [%] [a]	
Graphical [c]	34 ± 3	18 ± 2

[a] Deviations = 2 σ.
[b] Mean values from Tab. 9.2.
[c] Determined by linear regression of experimental data.

Within their experimental errors both humic acids show comparable complexation constants. Nevertheless, humic acid M1-B shows a significant lower LC at pH 4 than humic acid M1-V. This indicates that the blocking of the phenolic OH groups changes the complexation behavior of the humic acid. From these results one can conclude that phenolic OH groups may be involved in the complexation process with UO_2^{2+} ions under the applied conditions.
At pH 4, the humic acid phenolic OH groups are likely protonated due to their high pK_a values. We assume that intermolecular hydrogen bonds between the hydrogen atoms of the unmodified phenolic OH groups and the oxygen atoms of the UO_2^{2+} ions contribute to the complex formation. However, also steric effects, i.e., steric hindrances, may contribute to the change of the complexation behavior of the humic acid after blocking the phenolic OH groups. Currently we are investigating the influence of phenolic OH groups on the complexation behavior of humic acids using other modified synthetic and natural humic acids. Furthermore, EXAFS investigations are planned to confirm this result.

12 Complexation behavior of uranium(VI) with humic acids at pH 7

Predicting the environmental behavior of uranium in aquifer systems requires knowledge about the complexation behavior of uranium in the presence of humic substances at environmental relevant pH values, i.e., in the neutral pH range. Up to now the uranium complexation with humic substances has been mostly studied under conditions where competing reactions such as carbonate complexation and hydrolysis are excluded. The investigations were carried out at pH ≤4. However, it is known, that in the environmental

relevant pH range the uranium speciation is determined by carbonate complexation and hydrolysis. Thus, mixed ligand complexes consisting of uranium, humic acid and a secondary ligand, e.g., carbonate or hydroxide can be formed. From that the requirement for the investigation of the complexation behavior of uranium in the presence of humic acids at pH values greater than pH 4 results.

There are only few studies describing the formation of ternary uranium complexes in the presence of humic acids. Zeh et al. [39] described a ternary complex of uranyl hydroxo humate ($UO_2(OH)HA$, $\log \beta = 14.7 \pm 0.5$). Glaus et al. [40] reported a UO_2CO_3HA complex with a stability constant of $\log \beta \approx 5$.

Within this project we investigated the complexation behavior of uranium in the presence of humic acids at pH 7 by means of time-resolved laser-induced fluorescence spectroscopy. The experiments were performed under exclusion of CO_2 to prevent the formation of carbonate complexes.

12.1 Experimental

Sample preparation

We investigated the complexation behavior of uranium with the purified natural humic acid from Aldrich at pH 7.00 ± 0.04 in 0.1 M $NaClO_4$ solution. The fluorescence signal of the uranium species as a function of the total uranium concentration was measured at a constant humic acid concentration (5 mg/L). The uranium concentration was varied from $4.8 \cdot 10^{-6}$ to $1.8 \cdot 10^{-5}$ mol/L. The calibration of the relative fluorescence signal as a function of the uranium concentration was done on solutions that were identical to the solutions of the complexation experiments but did not contain any humic acid.

To exclude the formation of carbonate complexes the sample preparation was performed using CO_2 free water as well as carbonate-free chemicals in a glove box under inert gas conditions (N_2). The uranium concentration of the solutions was determined by ICP-MS analysis.

Laserspectroscopic measurements

The spectroscopic investigations were performed in a glove box under inert gas conditions (N_2). For fluorescence excitation we used a excitation wavelength of 410 nm produced in an optical parametric oscillator (MOPO-730-10, Spectra Physics, USA), which was pumped with

the third harmonic (355 nm) of a Nd:YAG laser. The laser light was transferred into the glove box applying a fiber optic cable. The laser energies for fluorescence excitation only reached amounts of about 150 µJ because of an energy loss in the fiber optic cable. The fluorescence signal was focused into the spectrograph (Model 1235 Acton Research, Acton, MA, USA) by a fiber optic cable. For the detection we used a time controlled photodiode array detector (model 1455 EG&G Instruments, Princeton Applied Research, Princeton, NJ, USA), cooled to –30 °C. The time gate of fluorescence detection was set to open at 200 ns after the excitation pulse for an interval of 2 µs. The fluorescence signal was measured from 408 to 634 nm. Ten spectra of each sample were collected over 100 laser pulses in each case. The spectra were standardized relative to the pulse energy. An average spectrum was calculated from 10 emission spectra. Because of the excitation wavelength of 410 nm and the low laser energies used for the excitation we only observed a weak fluorescence signal. The errors of the fluorescence measurements amounted to about 10 %.

Uranium species distribution

The uranium species distribution from pH 2 to 12 ($[UO_2^{2+}]$: $1 \cdot 10^{-5}$ mol/L; I: 0.1 M $NaClO_4$) in absence of humic acid and CO_2 was calculated (Fig. 12.1) with the EQ3/6 program [31] based on complexation constants compiled by Grenthe et al. (NEA data base) [32].

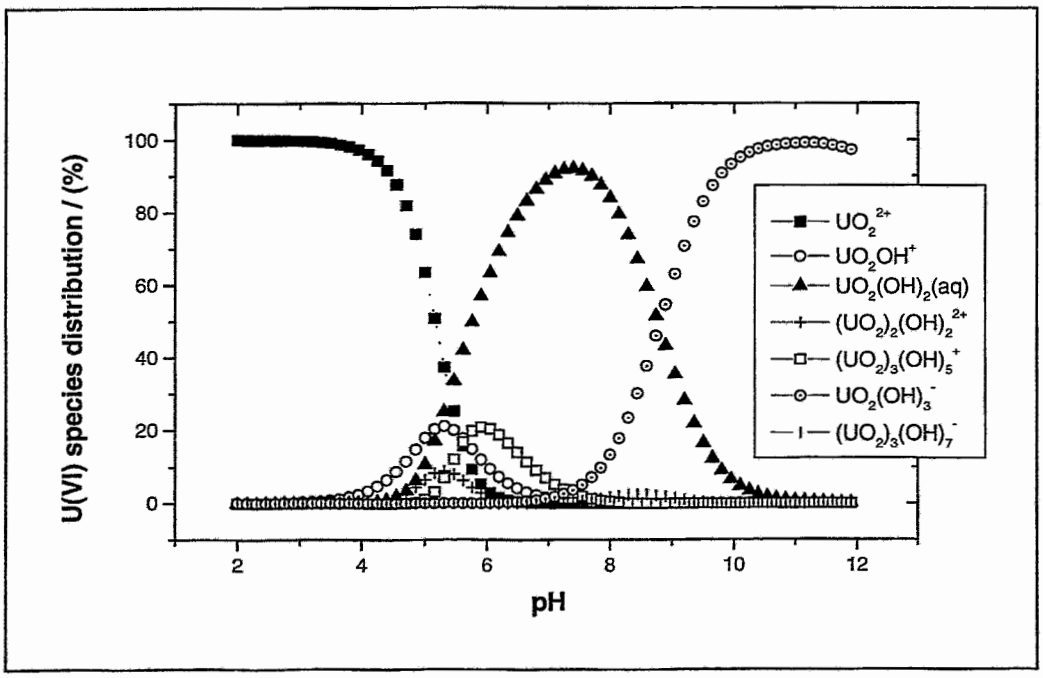

Figure 12.1: Uranium(VI) species distribution in aqueous solution in the absence of CO_2 and humic acid ($[UO_2^{2+}]$: $1 \cdot 10^{-5}$ mol/L; I: 0.1 M $NaClO_4$).

In absence of CO_2 and humic acid, the uranium speciation in the neutral and alkaline pH range is dominated by uranyl hydroxo complexes. At pH 7 uranium occurs to 89.6 % as $UO_2(OH)_2(aq)$, 6.4 % as $(UO_2)_3(OH)_5^+$, 1.5 % as UO_2OH^+, and 1.4 % as $UO_2(OH)_3^-$.

12.2 Results and discussion

The measured uranyl fluorescence intensities of the solutions with humic acid as well as without humic acid were integrated between 450 and 570 nm. Fig. 12.2 shows the results of this integration in dependence on the total uranium concentration.

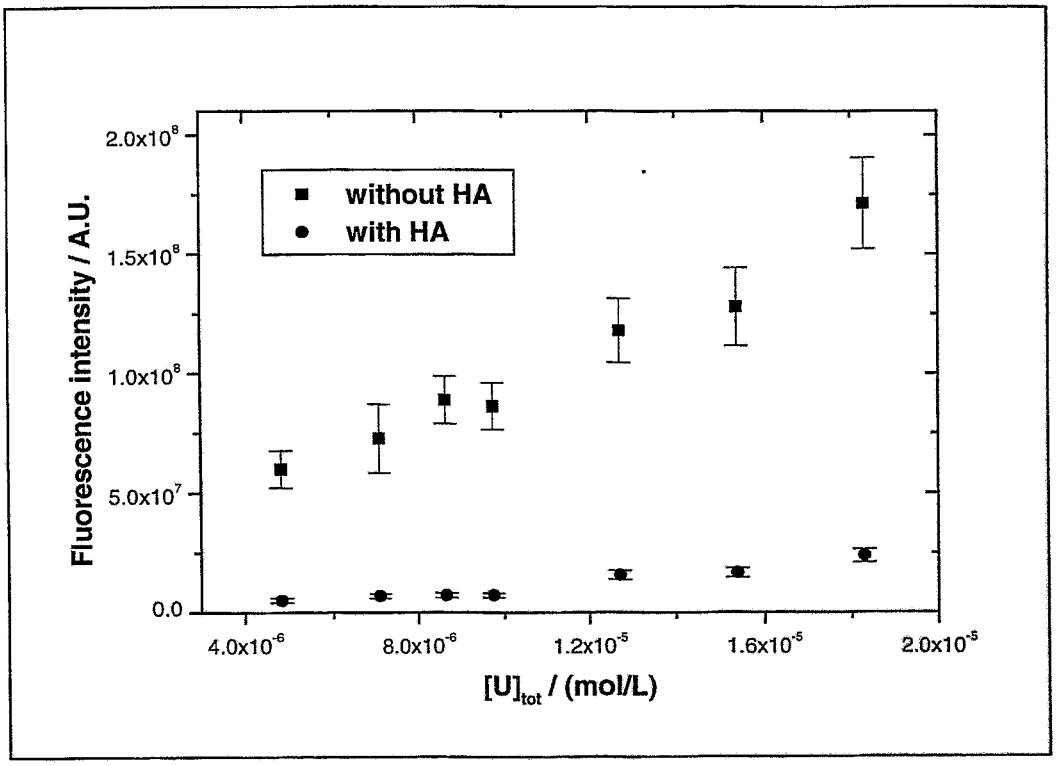

Figure 12.2: Integral fluorescence intensities of U(VI) of the investigated solutions with and without humic acid in dependence on the total uranium concentration.

Due to the complex formation between humic acid and uranium species at pH 7 a strong decrease in the fluorescence intensities of the solutions containing humic acid compared to the fluorescence intensities of the solutions without humic acid was obtained.

Under consideration of the uranium speciation at pH 7 we assume that the complex formation with humic acid starts from the aqueous $UO_2(OH)_2$ complex, that reacts with the humic acid

under ligand exchange to a ternary uranyl hydroxo humate complex. The strong decrease in the fluorescence intensities of the solutions with humic acid compared to the solutions without humic acid confirms the assumption that the aqueous $UO_2(OH)_2$ complex basically contributes to the complex formation between uranium(VI) and humic acid at pH 7. Nevertheless, it is not known to which extent other uranium species, that are also present in the solution (with about 10 %) besides the main species $UO_2(OH)_2$, contribute to the complex formation with humic acid. However, in our evaluation we did not consider these additional complex formation possibilities because the amounts of these species are lower than the experimental errors of the fluorescence measurements used for the determination of the concentration of non-complexed uranium as well as for the determination of the total uranium concentration.

For the individual complexation reaction we assumed, comparable to Zeh et al. [39], that UO_2OH^+ reacts with the humic acid under charge neutralization [Eq. (12.1)].

$$UO_2OH^+ + HA(I)^- \rightleftharpoons UO_2(OH)HA(I) \qquad (12.1)$$

The complex stability constant for the postulated complex formation can be defined as follows:

$$\beta = \frac{[UO_2(OH)HA(I)]}{[UO_2OH^+]_{free} \bullet [HA(I)^-]_{free}} \qquad (12.2)$$

where $[UO_2(OH)HA(I)]$ represents the concentration of the postulated ternary uranyl hydroxo humate complex, $[UO_2OH^+]_{free}$ stands for the free uranium hydroxide concentration in solution and $[HA(I)^-]_{free}$ represents the concentration of the free humic acid ligand in solution. The concentration of $UO_2(OH)HA(I)$ can be derived according to Eq. (12.3).

$$[UO_2(OH)HA(I)] = [UO_2OH^+]_{tot} - [UO_2OH^+]_{free} \qquad (12.3)$$

$[UO_2OH^+]_{tot}$ represents the total uranium concentration in solution determined by ICP-MS. The concentration of free uranium hydroxide, $[UO_2OH^+]_{free}$, was calculated from the fluorescence intensities of the solutions without and with humic acid (Fig. 12.2).

The total humic acid concentration $[HA(I)]_{tot}$ in mol/L was determined according to the definition in the metal ion charge neutralization model [34]:

$$[HA(I)]_{tot} = \frac{[HA] \bullet PEC}{1} \tag{12.4}$$

where [HA] is the concentration of humic acid in g/L, PEC is the proton exchange capacity of the humic acid in eq/g and 1 stands for the charge of the postulated complexing uranium species, UO_2OH^+. Introducing the loading capacity (LC) according to Eq.(12.5), whereby $[UO_2(OH)HA(I)]_{max}$ represents the maximal concentration of the uranyl hydroxo humate complex which can be formed under the applied conditions, the free humic acid concentration in solution can be defined according to Eq. (12.6).

$$LC = \frac{[UO_2(OH)HA(I)]_{max}}{[HA(I)]_{tot}} \tag{12.5}$$

$$[HA(I)]_{free} = [HA(I)]_{tot} \bullet LC - [UO_2(OH)HA(I)] \tag{12.6}$$

The combination of Eqs. (12.2) and (12.6) results in:

$$\beta = \frac{[UO_2(OH)HA(I)]}{[UO_2OH^+]_{free} \bullet ([HA(I)]_{tot} \bullet LC - [UO_2(OH)HA(I)])} \tag{12.7}$$

As already shown in paragraph 10.2.2 the LC as well as the complexation constant can be determined graphically by rearranging Eq. (12.6) for the free $[UO_2OH^+]$ concentration in solution (Fig. 12.3).

Applying the graphically determined LC we calculated for each experimental point a complexation constant according Eq. (12.7). The results of these calculations are summarized in Tab. 12.1 together with the analytical data of the initial concentrations as well as the data derived from the laserspectroscopic measurements.

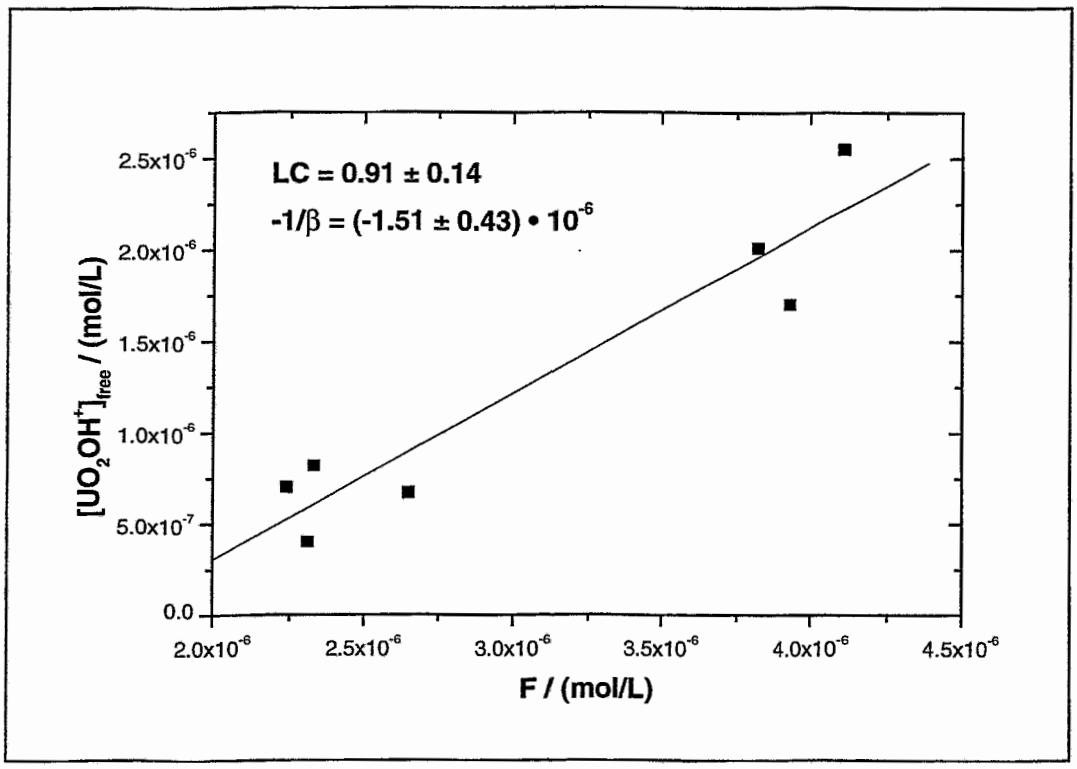

Figure 12.3: Graphical determination of the loading capacity (LC) and the complexation constant for the complexation of Aldrich humic acid with U(VI) at pH 7 by linear regression of experimental data.

$$F = \frac{[UO_2OH^+]_{free} \bullet [HA(I)]_{tot}}{[UO_2(OH)HA(I)]}$$

Table 12.1: Analytical data of the initial concentrations, the spectroscopically determined data of each component, and log β for the complexation of Aldrich humic acid with U(VI) at pH 7.

$[HA(I)]_{tot}$ (µmol/L)	$[UO_2OH^+]_{tot}$ (µmol/L)	$[UO_2OH^+]_{free}$ (µmol/L)	$[UO_2(OH)HA(I)]$ (µmol/L)	$[HA(I)]_{free}$ (µmol/L)	log β
Aldrich humic acid (charge A2/97)					
PEC: 5.06 ± 0.17 meq/g; pH 7.00 ± 0.04; I: 0.1 M $NaClO_4$; LC: 0.91 ± 0.14					
25.4	4.83	0.40	4.43	18.67	5.77
25.4	7.10	0.67	6.43	16.67	5.76
25.4	8.65	0.70	7.95	15.14	5.87
25.4	9.75	0.82	8.93	14.17	5.89
25.4	12.73	1.70	11.02	12.07	5.73
25.4	15.38	2.01	13.37	9.73	5.84
25.4[a]	18.32	2.55	15.77	7.33	5.93

[a] Value was not considered for validation.

The results of the evaluation of the experimental data applying the metal ion charge neutralization model are summarized in Tab. 12.2.

Table 12.2: Results of the laserspectroscopic investigation of the complexation between U(VI) and Aldrich humic acid at pH 7, I: 0.1 M $NaClO_4$.

Complexation data	Aldrich humic acid (± 2 σ)
Loading capacity (LC)	0.91 ± 0.28
log β – calculated[a]	5.83 ± 0.14
log β – graphical[b]	5.83 ± 0.25

[a] Mean value from Tab. 12.1.
[b] Calculated by linear regression of experimental data.

The graphical as well as the calculated complex formation constants agree very well. For validation of the postulated complexation reaction, Eq. (12.2) was rearranged to:

$$\log\frac{[UO_2(OH)HA(I)]}{[UO_2OH^+]_{free}} = \log[HA(I)]_{free} + \log\beta \qquad (12.8)$$

The slope of the linear regression function of Eq. (12.8) for our experimental data was determined with 0.9. The deviation of this value from the ideal value of one and also the relatively high standard deviations obtained for log β (graphical) and for LC are mainly due to the propagation of experimental errors, which were described above. Nevertheless, the result of the validation verifies the postulated complexation reaction.

In addition to the described evaluation of the experimental data applying the metal ion charge neutralization model, we determined a conventional complex stability constant without the introduction of the loading capacity. With this method we determined a complex stability constant of log β = 5.76 ± 0.28 (± 2 σ). This result agrees very well with the complexation constants summarized in Tab. 12.2.
A direct comparison of our complexation constant with the complexation constant published by Zeh et al. [39] is not possible because the stability constant determined by Zeh et al. was calculated using other presumptions.

The total reaction for the complexation of $UO_2(OH)_2$ with humic acid can be divided into different partial reactions [Eq. (12.9)-(12.13)]. Under consideration of the complex stability constants of the partial reactions as well as the dissociation constant of the humic acid the

stability constant of the total reaction can be derived. Therefore, the complexation constants for the hydrolysis of uranium [32] were converted for an ionic strength of 0.1 M applying the Davies equation [41]. The dissociation constant pKa (I: 0.1 M) of Aldrich humic acid was determined from the direct titration of the humic acid (cf. paragraph A.2.4) at half deprotonation and amounts to 4.58 ± 0.03.

Reaction			***log $\beta_{0.1\,M}$***	
$UO_2(OH)_2 + 2\,H^+$	⇌	$UO_2^{2+} + 2\,H_2O$	*10.08*	(12.9)
$UO_2^{2+} + H_2O$	⇌	$UO_2OH^+ + H^+$	*-4.98*	(12.10)
$HHA(I)$	⇌	$H^+ + HA(I)^-$	*-4.58 ± 0.03*	(12.11)
$UO_2OH^+ + HA(I)^-$	⇌	$UO_2(OH)HA(I)$	*5.83 ± 0.14*	(12.12)
$UO_2(OH)_2 + HHA(I)$	⇌	***$UO_2(OH)HA(I) + H_2O$***	***6.35***	**(12.13)**

From the partial reactions above we derived a complex stability constant for the total complexation reaction of $UO_2(OH)_2$ with Aldrich humic acid of log $\beta_{0.1M} = 6.35$.
However, to verify these first results and to determine the contribution of the other uranium species present in the solution to the complexation process at pH 7 it is necessary to continue these investigations with additional laserspectroscopic measurements above and below pH 7. Furthermore, EXAFS investigations should be performed to validate the formation of the $UO_2(OH)HA(I)$ complex.

13 Migration behavior of uranium in an aquifer system rich in humic substances[1]

Laboratory flow through column experiments contribute essential knowledge to assess the influence of humic substances on the migration behavior of actinide ions. There is the possibility to investigate the migration behavior of actinides depending on different parameters, e.g., groundwater flow velocity and column length.
There are some publications which describe flow through column experiments for the investigation of the migration behavior of radionuclides in geological formations, for instance investigations regarding the migration behavior of Am(III) [42], Eu(III), Np(IV)/(V) and

[1] This work was performed in cooperation with Dr. R. Artinger (INE, Forschungszentrum Karlsruhe).

Pa(IV)/(V) [43]. Up to now, the migration behavior of uranium was studied by Kim et al. by means of column experiments [44,45]. Migration experiments with a sediment/groundwater (GoHy-2227) system from the Gorleben site (Germany) were performed. The investigations were carried out under inert gas conditions (Ar + 1 % CO_2) with columns of 25 cm length and 5 cm inner diameter.

The present study focuses on flow through column experiments to investigate the migration behavior of uranium in a sandy humic colloid-rich aquifer system, i.e., in the system sediment/groundwater GoHy-532 from Gorleben. We investigated the uranium migration behavior as a function of uranium/groundwater equilibration time before injection into the column, groundwater flow velocity and column length. Ultrafiltration experiments were used for the determination of the uranium size distribution.

13.1 Experimental

Experimental set-up

The experiments were performed in a glove box under inert gas conditions (Ar + 1 % CO_2, 22 ± 2 °C). The columns were tightly packed with sand and equilibrated with groundwater (GoHy-532) from the Gorleben site over several months. The sediment and groundwater characterization was described by Artinger [42,46]. The groundwater has a dissolved organic carbon content (DOC) of about 30 mg C/L, a pH value of 7.2 ± 0.1 and a Eh value of - 220 mV. The monitoring of the experiments and the recording of the experimental data was performed on-line by a personal computer. The experimental set-up is shown in Fig. 13.1.

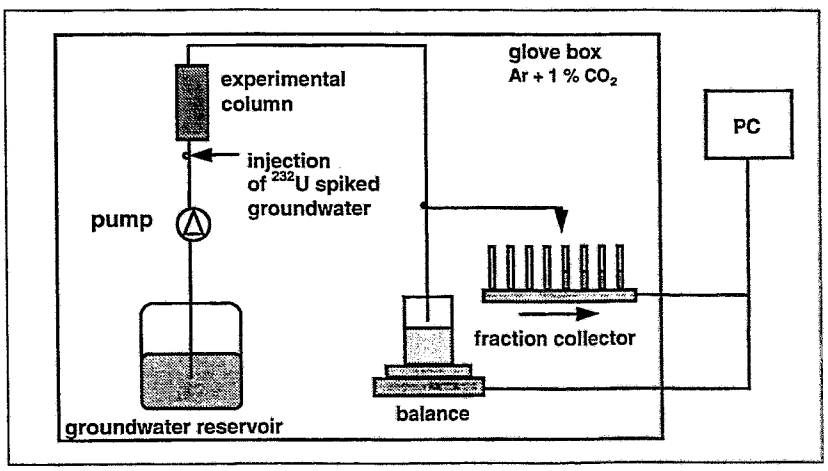

Figure 13.1: Experimental set-up of the column experiments.

Tracers

The uranium isotope Uranium-232 ($t_{1/2}$ = 72 years) in form of $^{232}UO_2Cl_2$ (Isotopendienst M. Blaseg GmbH, Waldburg, Germany) was applied because of its high specific activity. The ^{232}U stock solution showed a specific activity of 841 kBq/mL which corresponds to an uranium concentration of $4.6 \cdot 10^{-6}$ mol/L. Furthermore, tritiated water (HTO) was used as a conservative tracer to determine the hydraulic properties of the columns.

Procedure

The column experiments were performed in dependence on:

- ^{232}U/groundwater pre-equilibration time before the injection into the column,
- groundwater flow velocity and
- column length.

Prior to the experiments aliquots of the ^{232}U stock solution were reacted with the groundwater corresponding to the studied pre-equilibration time. Different pre-equilibration times from 1 hour to 82 days were investigated. The groundwater flow velocity was varied from 0.04 m/d to 2.03 m/d. The column length was varied between 25 cm and 75 cm. The experimental parameters and the hydraulic properties of the individual migration experiments are summarized in Tab. 13.1.

For all experiments 1 mL of the ^{232}U spiked initial solution and 200 µL HTO were simultaneously injected into the column. The eluted water was collected in a polypropylene flask. In addition to this, fractions of the eluate were collected by a fraction collector at certain times during the experiment. The eluate, the eluate fractions and the initial solutions were analyzed for their ^{232}U and HTO concentrations by liquid scintillation counting. Additionally, alpha-spectroscopy was applied to determine the concentration of ^{232}U daughter nuclides. Thus, it was possible to correct the alpha-activities determined by liquid scintillation counting with regard to the alpha-activity contributed by the daughter nuclides. The breakthrough curves for HTO and ^{232}U result from the ^{232}U and HTO concentration in the eluate fractions.

Furthermore, investigations regarding the size distribution of uranium in the initial solutions and in different eluate fractions were performed by ultrafiltration. Ultrafilters with molecular weight cutoffs of 1 kD to 1000 kD (MICROSEP, Filtron, Northborough, MA, USA) were applied.

Table 13.1: Experimental conditions for the column experiments.

Experiment number	U / groundwater equilibration time (d)	Column length (cm)	Uranium concentration (mol/L)	Darcy velocity v_D (m/d)	Pore water flow velocity v (m/d)	Effective porosity ε	Longitudinal dispersion coefficient D_L (cm^2/s)
1	0.04	25	$5.1 \cdot 10^{-7}$	0.321	0.970	0.331	$8.64 \cdot 10^{-5}$
2	0.63	25	$4.5 \cdot 10^{-7}$	0.314	0.949	0.331	$3.73 \cdot 10^{-5}$
3	11	25	$4.9 \cdot 10^{-7}$	0.312	0.943	0.331	$3.70 \cdot 10^{-5}$
4	82	25	$4.2 \cdot 10^{-7}$	0.310	0.934	0.332	$3.34 \cdot 10^{-5}$
5	5	25	$4.4 \cdot 10^{-7}$	2.030	6.078	0.334	$2.14 \cdot 10^{-4}$
6	6	25	$4.7 \cdot 10^{-7}$	0.038	0.114	0.333	$1.58 \cdot 10^{-5}$
7	5	50	$4.1 \cdot 10^{-7}$	0.241	0.724	0.333	$2.55 \cdot 10^{-5}$
8	5	75	$4.3 \cdot 10^{-7}$	0.239	0.697	0.343	$3.24 \cdot 10^{-5}$

^{232}U species distribution

Species calculations for the groundwater GoHy-532 ([UO_2^{2+}]: $5 \cdot 10^{-7}$ mol/L, pH 7.2 ± 0.1, 1 % CO_2) were performed to determine the distribution of uranium species in the investigated groundwater/sediment system. The calculations based on complex formation constants compiled by Grenthe et al. [32] (NEA data base) and stability constants for the complex formation of UO_2^{2+} with humic acids published by Czerwinski et al. ($UO_2HA(II)$) [35] and Zeh et al. ($UO_2OHHA(I)$) [39]. Two calculations were performed at Eh = 800 mV and Eh = -220 mV, respectively. Uranium(VI) occurs at Eh = 800 mV and pH 7.2 to about 72 % as $UO_2(CO_3)_2^{2-}$, 21 % as $UO_2(CO_3)_3^{4-}$, 2 % as $UO_2(OH)_{2(aq)}$ and only to about 3 % as $UO_2OHHA(I)$ complex. Considering the experimental determined redox potential of the groundwater of –220 mV and assuming thermodynamic equilibration uranium shows a totally different species distribution. The initially added U(VI) should be present in reduced form as U(IV) in form of the $U(OH)_{4(aq)}$ complex. Possibly occurring U(IV) humate complexes were not considered in the calculation because there are no reliable thermodynamic data. Generally it is known from literature that tetravalent actinides like Th(IV) [1] interact stronger with humic substances than hexavalent uranium.

In contrast to the calculated species distribution, ultrafiltration experiments of the ^{232}U labelled groundwaters showed for uranium roughly the size distribution of the humic substances in the groundwater [46]. Fig. 13.2 shows the ^{232}U size distribution in different initial solutions (alpha-activity contribution by daughter nuclides ≤10 %). From this one can conclude that ^{232}U is mainly associated with humic colloids. Approximately 85 - 90 % of ^{232}U are associated with colloids greater than 1000 D and about 20 - 30 % occur in form of ionic species, probable carbonato complexes.

Up to now it can not definitely be stated whether and to what extend the humic colloid-bound uranium is present in the reduced tetravalent state. From neptunium experiments performed recently [47] it is known that the oxidation state has an essential influence on the neptunium size distribution. The reduction of Np(V) causes a decrease of ionic NpO_2^+ species in solution. Np(IV) is almost quantitatively associated to humic colloids. From that one may expect that the reduction of U(VI) to U(IV) also influences the uranium size distribution. However, no significant changes in the ^{232}U size distribution were observed. Therefore, it can be concluded that there is no significant uranium reduction in the initial solutions.

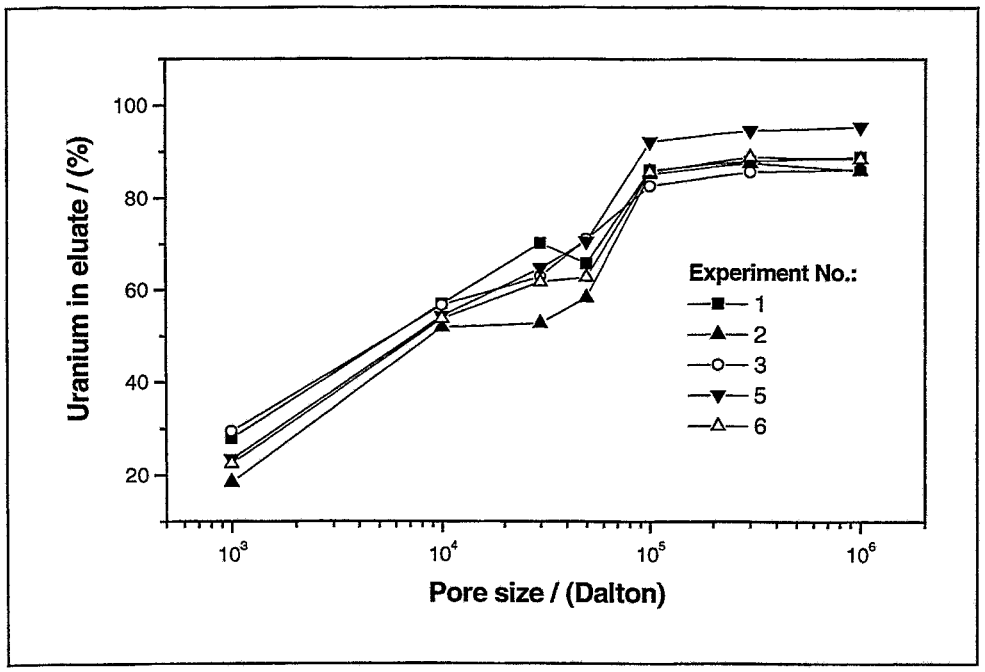

Figure 13.2: ^{232}U size distribution in the initial solutions (GoHy-532, 1 % CO_2, [U]: $4.1 \cdot 10^{-7}$–$5.1 \cdot 10^{-7}$ mol/L, activity contribution of daughter nuclides ≤ 10 %).

13.2 Results and discussion

13.2.1 Comparison of ^{232}U and HTO breakthrough curves

From the breakthrough curves of ^{232}U and HTO one can conclude how far the ^{232}U migration differs from the groundwater flow.

The migration behavior is characterized by the retardation factor, R_f [Eq. (13.1)], where V represents the volume of the eluate and V_P stands for the effective pore volume of the column.

$$R_f = \frac{V}{V_P} \tag{13.1}$$

$R_f > 1$ indicates a delayed transport of an injected metal ion trough the column compared to that of the conservative tracer with a retardation factor of one, whereas $R_f < 1$ means an accelerated migration.

For example, the ^{232}U and HTO breakthrough curves of experiment No. 7 are depicted in Fig. 13.3. These curves are typical for the experiments carried out under varied experimental conditions. In addition, a ^{241}Am breakthrough curve is shown in Fig. 13.3 that was measured under comparable conditions [42].

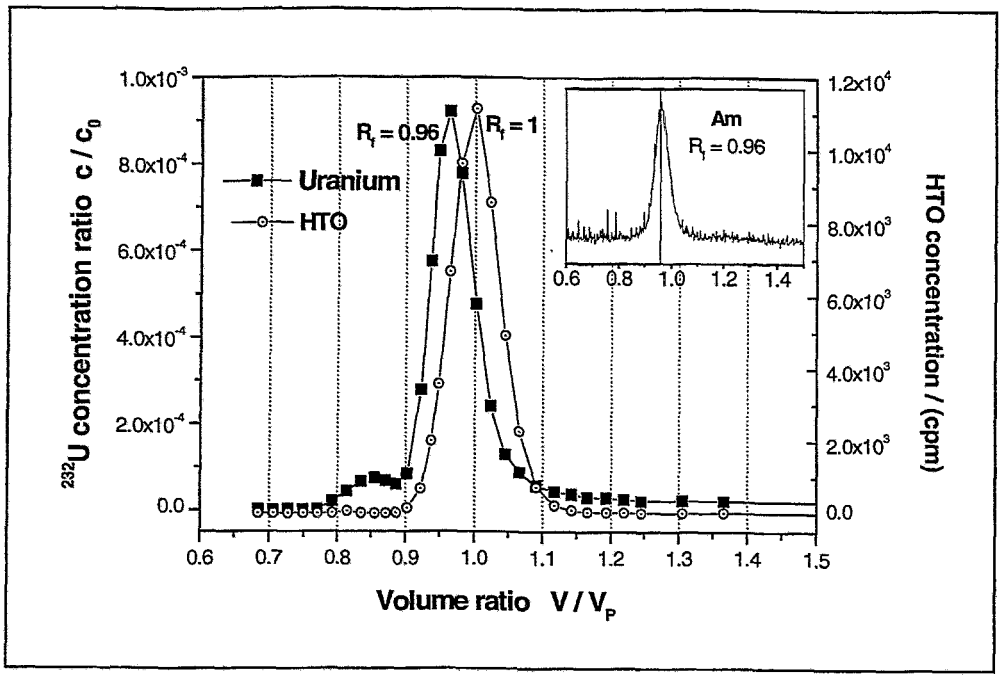

Figure 13.3: ^{232}U and HTO breakthrough curves in comparison to an ^{241}Am breakthrough curve determined under comparable conditions [42].

Fig. 13.3 shows that a fraction of ^{232}U is eluted with the retardation factor $R_f = 0.96$ meaning that this part of uranium is transported slightly faster through the column than the conservative tracer. This accelerated transport is attributed to the association of uranium with humic colloids, which move faster than the conservative water-tracer due to size exclusion processes.

The humic colloid-borne transport is confirmed by ultrafiltration experiments. Fig. 13.4 shows exemplary for experiment No. 7 the size distribution of uranium in fraction 13, eluted at $R_f = 0.92$. In this fraction ^{232}U shows roughly the size distribution of the DOC in the groundwater [46]. No significant fraction of ionic uranium species was obtained.

In addition, the humic colloid-borne ^{232}U transport is confirmed by the R_f value of 0.96 ± 0.01 which is also found in ^{241}Am migration experiments.

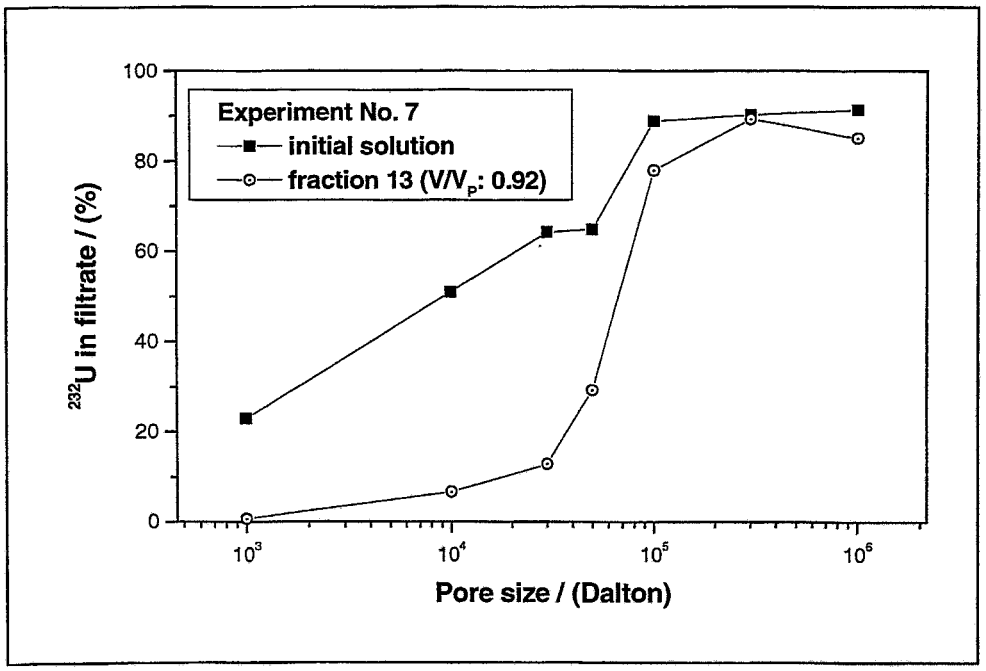

Figure 13.4: Size distribution of ^{232}U in fraction 13, experiment No. 7.

Furthermore, the ^{232}U breakthrough curves show the elution of a smaller fraction of ^{232}U at $R_f = 0.84 \pm 0.01$ and a different strong pronounced tailing after the breakthrough maximum (Fig. 13.3). The early eluted uranium fraction at $R_f = 0.84 \pm 0.01$ is attributed to the association of uranium with much larger colloids, that was shown by filtration experiments. For example, in experiment No. 4 about 50 % of ^{232}U and its daughter nuclides, eluted from $R_f = 0.78$ to $R_f = 0.88$, are bound to colloids > 450 nm. Merely 20 % of the nuclides are associated with colloids smaller than 10^6 Dalton, which is typical for humic colloids. Whether this transport is mediated by enlarged coagulated humic substances, inorganic colloids, or eventual microorganisms, is not known up to now.

There are some indications that the uranium transport with larger colloids is related to a reduction of U(VI) to U(IV). An example for this is the enhancement of the $^{228}Th/^{232}U$ isotope ratio in the early eluted fraction at $R_f = 0.84 \pm 0.01$. Breakthrough curves of ^{228}Th, which was formed during the experiments with concentrations between 10^{-10} and 10^{-9} mol/L from the radioactive decay of ^{232}U, were determined for two experiments by alpha-spectrometry. As illustrated in Fig. 13.5 the maximum of the ^{228}Th breakthrough curves occurs at a R_f value of about 0.9. This thorium fraction migrates distinctly faster through the column than the humic colloid-bound non-retarded ^{232}U fraction at $R_f = 0.96 \pm 0.01$. This points to the fact that the tetravalent ^{228}Th migrates with larger colloids.

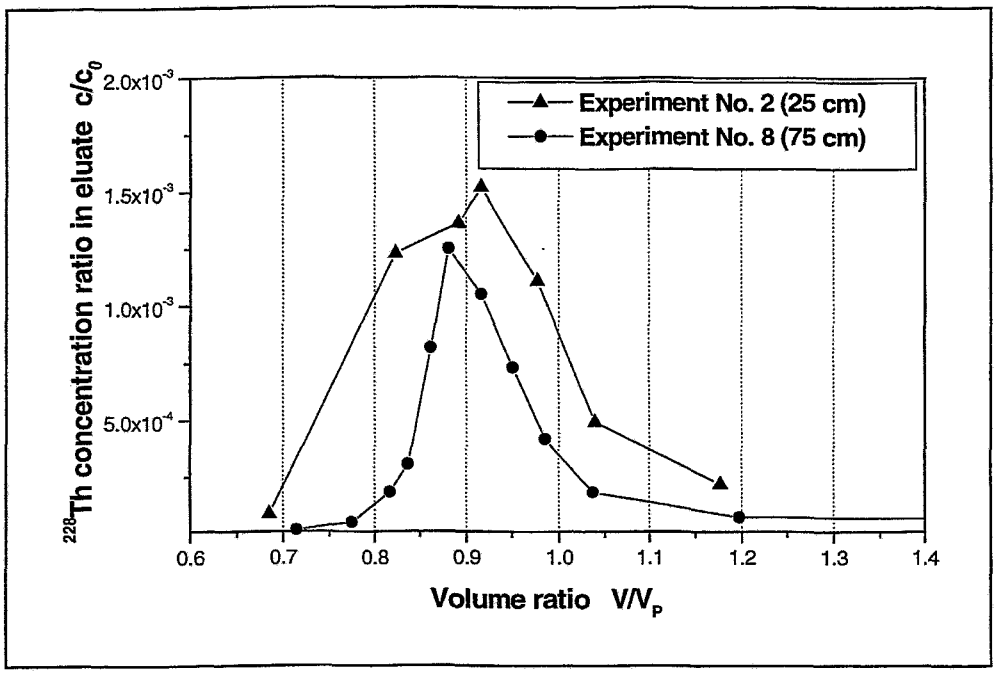

Figure 13.5: ^{228}Th breakthrough curves determined by alpha-spectrometry.

Experiment No. 4 with the highest ^{232}U/groundwater pre-equilibration time of 82 days gives another indication for the possible accelerated transport of U(IV). Here, the uranium fraction with $R_f = 0.84$ is especially pronounced (cf. Fig. 13.7), which points to a faster migration of ^{232}U associated to larger molecules.

13.2.2 Determination of the ^{232}U recovery

As mentioned before, colloid-borne ^{232}U is not only eluted with $R_f = 0.96 \pm 0.01$ (mean value for all experiments) but also earlier at $R_f = 0.84 \pm 0.01$. Beyond it, a different strong pronounced tailing is observed after the breakthrough maximum. To be able to compare the recovery of humic colloid-borne uranium with $R_f = 0.96 \pm 0.01$ for all experiments, a Gaussian distribution with $R_f = 0.96 \pm 0.01$ as center, and a dispersion derived from the HTO migration was taken as a basis. As second component a Gaussian distribution with $R_f = 0.84 \pm 0.01$ (exception experiment No. 8: $R_f = 0.88$) as center was fitted. For example, Fig. 13.6 shows the analysis of the breakthrough curves regarding the recovery of humic colloid-borne ^{232}U for experiment No. 4.

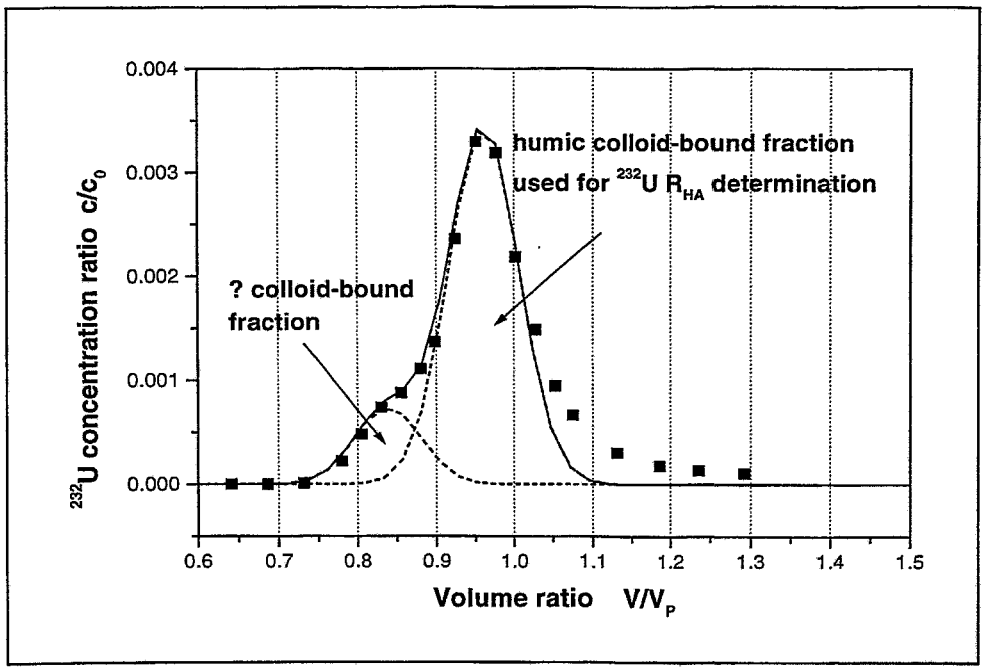

Figure 13.6: Determination of the humic colloid-borne ^{232}U fraction.

Furthermore, we determined the total recovery of ^{232}U after about 5 pore volumes, which includes the recovery of colloid-borne uranium fractions with R_f values of 0.84 ± 0.01 and 0.96 ± 0.01 as well as the recovery of retarded ^{232}U in the tailing. It is calculated according to Eq. (13.2):

$$R = \frac{U_{eluted}}{U_{injected}} \bullet 100\% \qquad (13.2)$$

where U_{eluted} represents the eluted uranium after about 5 pore volumes and $U_{injected}$ stands for the injected uranium.

The total recoveries (R_{tot}) and the recoveries of humic colloid-borne ^{232}U (R_{HA}), which includes only the fraction eluted at R_f = 0.96 ± 0.01 are summarized in Tab. 13.2 for all experiments. As mentioned before, the attachment of the ^{232}U fraction with R_f= 0.96 ± 0.01 to the humic colloid-borne fraction was confirmed by ^{241}Am experiments [42].

Table 13.2: Recovery of ^{232}U in column experiments.

Experiment number	Pre-equilibration time (d)	Darcy velocity v_D (m/d)	Column length (cm)	Total ^{232}U recovery R_{tot} (%)	Humic colloid-borne ^{232}U recovery R_{HA} (%)	Retardation of humic colloid-borne ^{232}U R_f (± 0.01)
Variation of pre-equilibration time						
1	0.04	0.321	25	2.0 ± 0.5	0.4 ± 0.1	0.97
2	0.63	0.314	25	3.5 ± 0.9	1.4 ± 0.3	0.97
3	11	0.312	25	5.2 ± 1.3	3.3 ± 0.8	0.96
4	82	0.310	25	14.2 ± 3.6	7.6 ± 1.9	0.96
Variation of Darcy velocity						
5	5	2.030	25	9.1 ± 2.3	6.5 ± 1.6	0.95
3	11	0.312	25	5.2 ± 1.3	3.3 ± 0.8	0.96
6	6	0.038	25	6.0 ± 1.5	1.5 ± 0.4	0.97
Variation of column length						
3	11	0.312	25	5.2 ± 1.3	3.3 ± 0.8	0.96
7	5	0.241	50	3.5 ± 0.9	2.4 ± 0.6	0.96
8	5	0.239	75	6.4 ± 1.6	2.0 ± 0.5	0.96

13.2.3 Influence of the pre-equilibration time on the migration behavior of uranium

Fig. 13.7 depicts the ^{232}U breakthrough curves for the experiments applying different ^{232}U/groundwater pre-equilibration times before injection into the column. The ^{232}U recoveries are summarized in Tab. 13.2.

Fig. 13.7 shows that a significant increase of the humic colloid-bound ^{232}U fraction occurs with increasing ^{232}U/groundwater pre-equilibration. This observation is confirmed by the recoveries summarized in Tab.13.2. The comparison of the recovery of colloid-borne uranium and the total recovery after about 5 pore volumes as a function of the pre-equilibration time (Tab. 13.2) shows that both recoveries increase with increasing pre-equilibration time. This fact suggests that uranium binding onto the humic colloids becomes stronger with increasing equilibration time. Consequently, uranium becomes less available for an interaction with the sediment surface during the migration through the column. Comparable results were found for americium [42]. In addition, Rao et al. [48] studied the interaction between Eu(III) and humic acids using cation exchange. They described a time-dependent stronger binding of trivalent metal ions with humic substances. However, the cause of this phenomenon is not known up to now.

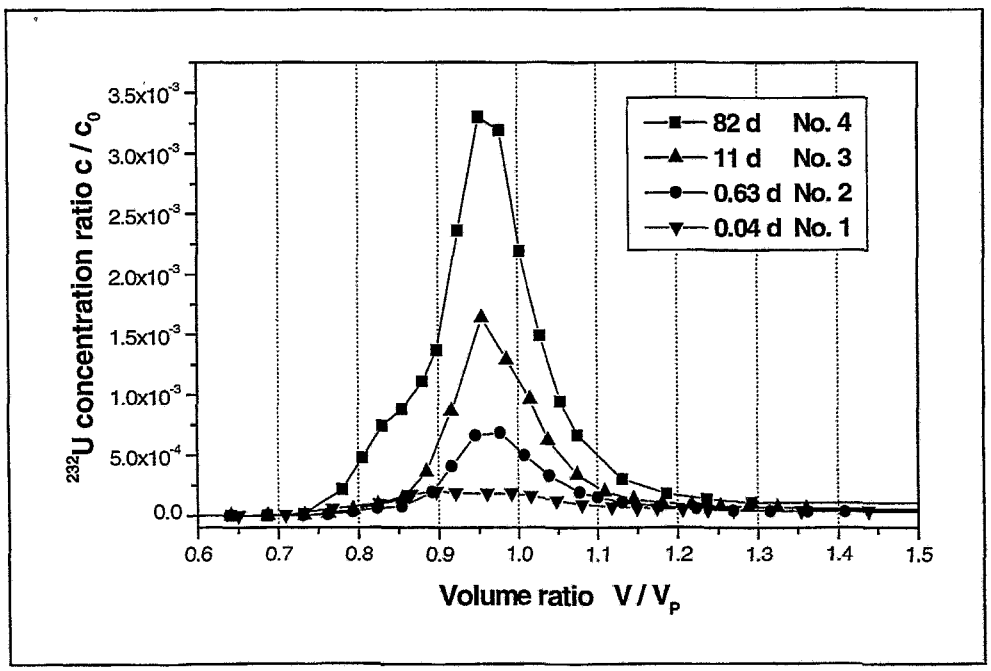

Figure 13.7: ^{232}U breakthrough curves in dependence on the ^{232}U/groundwater equilibration time before injection into the column.

The relatively large fraction of ^{232}U eluted at $R_f = 0.84$ after a equilibration time of 82 days (experiment No. 4) can possibly be attributed to the reduction of uranium(VI) to uranium(IV). The fact that the breakthrough curve of the tetravalent uranium daughter nuclide thorium shows a maximum at $R_f \sim 0.9$ (cf. paragraph 13.2.1) represents a possible reference for that. Nevertheless, an experimental proof for a reduction of uranium(VI) does not exist.

13.2.4 Influence of the groundwater flow velocity and the column length on the migration behavior of uranium

Variations in the groundwater flow velocity and the column length cause variations in the residence time of the colloid-bound uranium in the column. Fig. 13.8 shows the ^{232}U breakthrough curves obtained with different groundwater flow velocities. Increasing the groundwater flow velocity from 0.04 m/d to 2.03 m/d, an increase of the recovery of colloid-bound ^{232}U from 1.5 % to 6.5 % was obtained (Tab. 13.2). This tendency was also found for Am(III) [42].

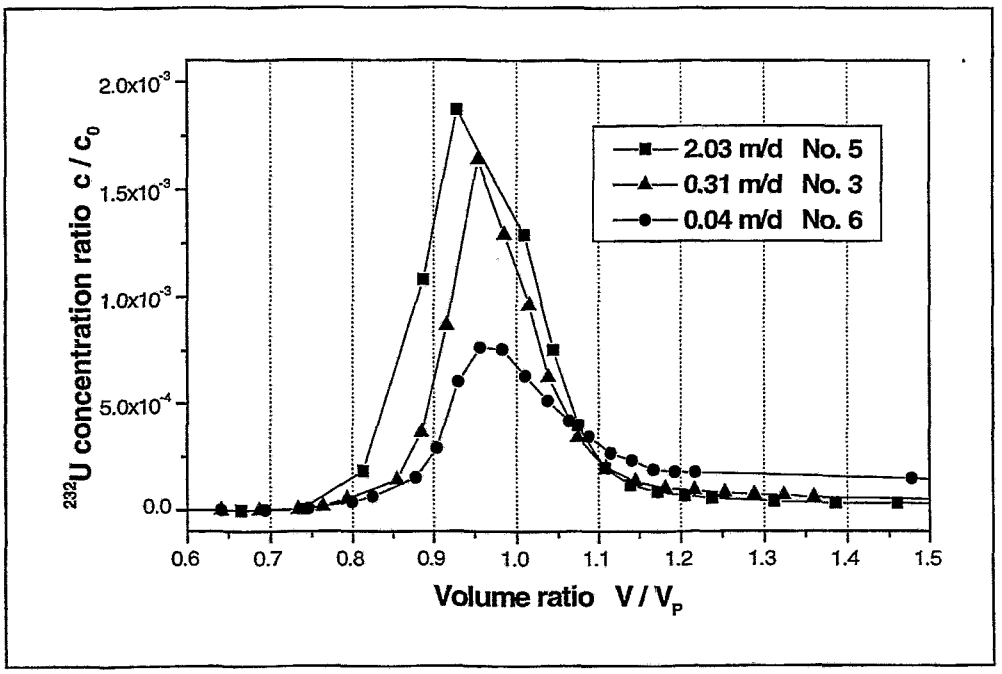

Figure 13.8: ^{232}U breakthrough curves in dependence on the groundwater flow velocity.

Furthermore, a decrease in the recovery of colloid-borne uranium was observed with increasing column length (Tab. 13.2).

Fig. 13.9 depicts the recovery of non-retarded colloid-borne ^{232}U as a function of the residence time in the column. The results consists of the results obtained by varying the groundwater flow velocity and the column length. The recovery of non-retarded colloid-bound transported uranium decreases continuously with increasing residence time in the column, which points to a time-dependent stronger interaction of uranium with the sediment surface. This dependence may be explained by a time-dependent dissociation of uranium from the colloids followed by an interaction with the sediment surface.

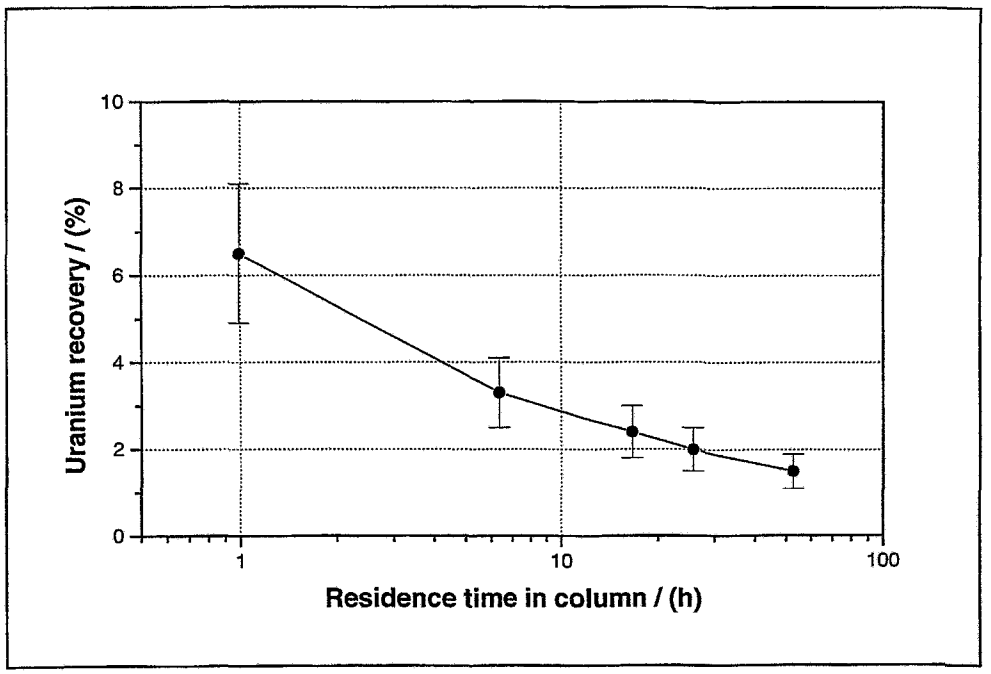

Figure 13.9: Recovery of humic colloid-borne ^{232}U ($R_f = 0.96 \pm 0.01$) in dependence on the residence time in the column. The pre-equilibration time is constant.

In contrast to this fact, the total recovery of eluted ^{232}U shows no distinct trend depending on the migration period (Tab. 13.2). This may be due to the different strong tailing and the varying amount of the colloid-borne uranium fraction at $R_f = 0.84 \pm 0.01$. From data in Fig. 13.8 one can derive that the tailing of the breakthrough curves increases with increasing migration time. That means the interaction of uranium with the sediment shows an increasing influence on the uranium migration.

13.3 Conclusions

The results of the migration experiments in a sandy humic colloid rich groundwater/sediment system show that depending on the experimental conditions a portion of 0.4 up to 7.6 % of the injected uranium migrates non-retarded and colloid bound. Due to size exclusion effects, the migration velocity of the humic colloid-borne uranium is found to be up to 5 % faster than the groundwater flow velocity.

The migration behavior of uranium is strongly influenced by kinetically controlled processes. The recovery of humic colloid-borne uranium depends on the uranium/groundwater equilibration time prior to the injection into the column. The recovery increases with increasing pre-equilibration time, which is attributed to a time-dependent binding of uranium onto the humic colloids with different strength. Furthermore, the recovery of uranium depends on the residence time of humic colloid-borne uranium in the column, determined by the groundwater flow velocity and the column length. With increasing residence time a decreasing recovery of humic colloid-borne uranium was observed. These observations are due to a time-dependent dissociation of uranium from the humic colloids followed by an interaction of uranium with the sediment. Up to now it is not known to what extent U(VI) is reduced to U(IV) during the experiments. First indications point to the reduction of uranium and a colloid-borne transport of U(IV).

^{228}Th, which was formed from ^{232}U by radioactive decay during the migration experiments, also migrates colloid-bound through the groundwater/sediment system. The mean migration velocity of the colloid-borne thorium fraction is about 10 % higher than the groundwater flow velocity.

The column experiments reveal important kinetic effects controlling the humic colloid-borne migration of uranium. These kinetic effects are comparable to those found for instance for the migration behavior of Am(III). Consequently one can conclude that the K_D concept, which is based on thermodynamic equilibrium, is not suitable to describe the humic colloid-borne uranium migration. Therefore, the uranium migration experiments provide a first basis to describe and to predict the subsurface migration of colloidal uranium in natural aquifers. Additional experiments are necessary to further improve the understanding of the basic processes controlling uranium migration, especially experiments investigating the influence of the uranium reduction to the tetravalent oxidation state on the migration behavior of uranium.

14 Effect of humic acid on the uranium(VI) sorption onto phyllite

For the safety assessment of uranium mining areas and for the far field of nuclear waste repositories it is crucial to understand the interaction of uranium with site-specific rock material and furthermore, to know all processes and substances that may influence this interaction. Such processes are, for instance, possible chemical reactions inside a rock pile. Organic materials, such as humic and fulvic acids, may interact with dissolved inorganic contaminants and may affect the sorption behavior of such contaminants on geological materials. Due to complex formation reactions between radionuclides and humic substances the solubility of contaminants can be enhanced. The sorption of the formed species can be either stronger or weaker than the sorption of the uncomplexed species. Thus, the uranium migration in aquifers is affected. Consequently, it is necessary to quantify the influence of humic material on radionuclide sorption.

Phyllite was chosen as a site-specific rock material because it is quite common in the Western Erzgebirge in Saxony, Germany, and because it is closely associated with the uranium deposits of the uranium mining areas in East Germany. Phyllite is a low-grade metamorphic rock that is mainly composed of the minerals quartz, muscovite, chlorite, and albite.

Batch experiments were conducted in order to determine the effect of humic acid on the uranium(VI) sorption onto phyllite in the pH range of 3.5 to 9.5. A site-specific natural humic acid (Kranichsee humic acid), isolated from the bog 'Kleiner Kranichsee' [49], and a ^{14}C-labelled synthetic humic acid type M1 (^{14}C-M1) were used for the experiments. Both humic acids were compared with regard to their sorption behavior on phyllite and their influence on the uranium sorption onto phyllite.

The effect of humic substances of different origin on the uranium(VI) sorption onto various rock materials and minerals, e.g., clay, hematite, silica and ferrihydrite, has been described in the literature [50-55].

14.1 Experimental

Materials

The light-colored phyllite, used for the sorption experiments, was obtained from the uranium mine 'Schlema-Alberoda' near Aue in Western Saxony (Germany). It was collected at a depth of 540 m. The phyllite is composed of 48 vol.% of quartz, 25 vol.% of chlorite, 20 vol.% of muscovite, 5 vol.% of albite, and 2 vol.% of brownish opaqueous material, identified as Ti-

and Fe-oxides [56]. The 63 to 200 µm grain size fraction of the phyllite was used for batch sorption experiments. Its specific surface area, determined by means of the BET method, is 4.0 m^2/g.

The natural humic acid (Kranichsee humic acid) used for the sorption experiments was isolated from surface water of the mountain bog 'Kleiner Kranichsee' that is located in the vicinity of uranium mining sites at Johanngeorgenstadt in Western Saxony (Germany) [49].

The ^{14}C-labelled synthetic humic acid type M1 (^{14}C-M1) was synthesized as described in paragraph 8.

Sorption experiments

The sorption experiments were conducted under atmospheric conditions. 20 mL of a 0.1 M $NaClO_4$ (Merck) solution were added to 500 mg of the rock material (63 to 200 µm fraction) in 50 mL polypropylene centrifuge tubes (Cellstar). Then, the samples were aged for 24 h. After that, additional 18 mL of 0.1 M $NaClO_4$ solution were added. The desired pH was adjusted by addition of dilute $HClO_4$ (Merck) or NaOH (Merck). For studies at pH values higher than 7, a calculated amount of $NaHCO_3$ was added to accelerate the equilibration process with atmospheric CO_2. In the following days the pH was readjusted until the pH was stable. Then 2 mL of a humic acid stock solution (100 mg humic acid/L, 0.1 M $NaClO_4$) was added to reach the final volume of 40 mL and a humic acid concentration of 5 mg/L. The humic acid/mineral contact time was 14 days. The pH was checked and adjusted every day. Then, the experiment was started by adding 84 µL of a $4.8 \cdot 10^{-4}$ M uranyl perchlorate stock solution, prepared in $5 \cdot 10^{-3}$ M $HClO_4$, to obtain a uranyl concentration of $1 \cdot 10^{-6}$ M. The pH was readjusted immediately after the addition of the perchlorate solution. Then, the samples were rotated end-over-end at room temperature for about 60 hours. After this time, the final pH values were determined. Subsequently, the samples were centrifuged at 10000 rpm for 30 minutes. The supernatant was filtered using Minisart N membranes (Sartorius) with a pore size of 450 nm. To avoid contamination caused by conservation agents in the filter membranes the membranes were washed five times with 20 mL of Milli-Q water (Milli-RO/Milli-Q-System, Millipore).

The supernatant (non-filtered solution) and the 450 nm filtrate were analyzed for the final uranium and humic acid concentration. It could be shown that there was no significant difference between the concentrations determined for the supernatant and the 450 nm filtrate. The uranium concentration was determined by ICP-MS (Inductive Coupled Plasma-Mass

Spectrometry, Mod. ELAN 5000, Perkin Elmer). The concentration of the natural humic acid was determined by UV/Vis spectrophotometry (Mod. 8452A, Hewlett Packard) at 254 nm. The concentration of the ^{14}C-labelled synthetic humic acid was determined both by UV/Vis spectrophotometry and by Liquid Scintillation Counting (LSC, Beckman Instruments) after combustion of the material with a sample oxidizer (Mod. P 307, Canberra-Packard).

In addition, the uranium sorption onto the wall of the centrifuge tubes was determined. The effect was about 2-3 % at pH 5 to 7.7. In the acid and alkaline pH range, the vial wall sorption was 0.2-1 %.

The amount of uranium adsorbed to the mineral surface was calculated as the difference between the initial U(VI) concentration ($1 \cdot 10^{-6}$ M) and the sum of the final uranium concentration in the 450 nm filtrates and the amount of uranium adsorbed onto the wall of the experimental vials.

The difference between the initial humic acid concentration (5 mg/L) and the sum of the corresponding final concentration in the 450 nm filtrates and the amount of humic acid sorbed onto the centrifuge tube walls was attributed to humic acid sorption onto the mineral. In case of the ^{14}C-labelled synthetic humic acid the amount of humic acid sorbed onto the phyllite was additionally determined by LSC.

14.2 Results and discussion

In Fig. 14.1 and 14.2 the results of the uranium sorption experiments carried out in the presence of 5 mg/L humic acid are depicted. For the ^{14}C-labelled synthetic humic acid (^{14}C-M1) the humic acid uptake was determined by UV/Vis spectrophotometry of the solution and by LSC measurements both of the solution and of the phyllite. The results of both methods agree well (relative standard deviation: 5 % (2σ)).

Fig. 14.1 shows the humic acid uptake by phyllite for Kranichsee humic acid and for ^{14}C-M1 as a function of pH. Both humic acids are strongly taken up over the entire pH range. From pH 3.6 to 7.7: 86 to 94 % of the Kranichsee humic acid are adsorbed. Above pH 8, the humic acid sorption decreases to 78 % at pH 9.4. The sorption of the synthetic ^{14}C-M1 is in the pH range from 3.6 to 7.7 somewhat lower (4 to 6 %) than the sorption of the Kranichsee humic acid and above pH 8 higher (2 to 5 %) than the sorption of the Kranichsee humic acid.

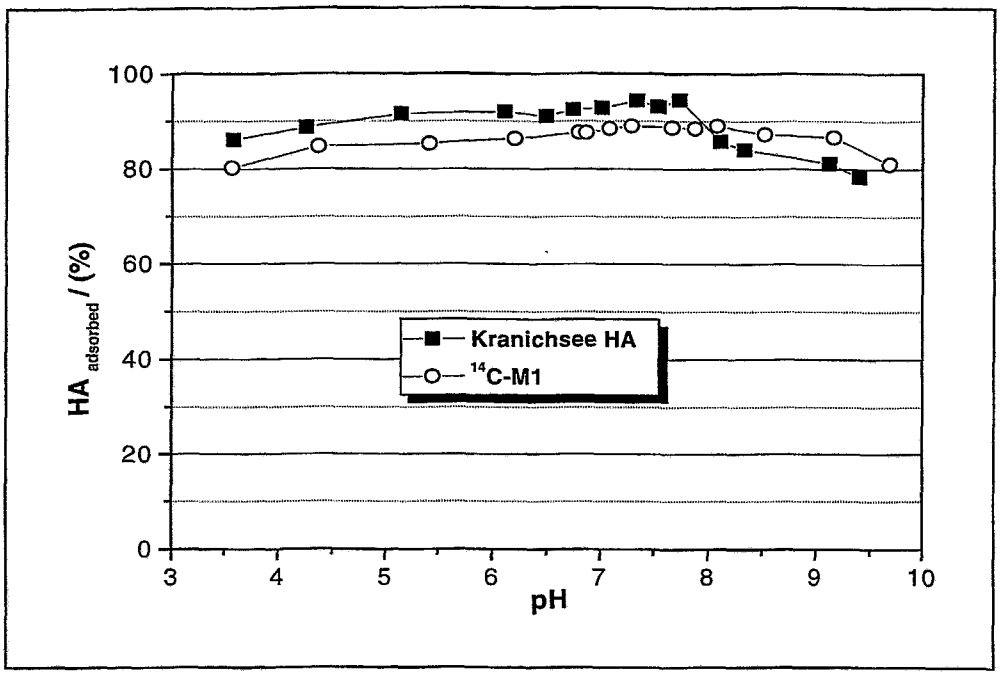

Figure 14.1: Humic acid uptake by phyllite in experiments conducted in the presence of 5 mg HA/L.(Kranichsee humic acid: determined by UV/Vis spectrophotometry; ^{14}C-M1: determined by LSC).

This high humic acid sorption onto phyllite cannot only be attributed to the specific surface area of phyllite of 4.0 m^2/g which was determined by the BET method. Instead of that, we believe that ferrihydrite is responsible for the high humic acid adsorption onto phyllite. Ferrihydrite ($Fe_2O_3 \cdot 1.8\ H_2O$) as secondary mineral phase is formed in the course of the sorption experiments (proved by Arnold et al. [57]) and is visible as precipitate with a slight reddish-brownish color. It has a high specific surface area of 600 m^2/g and thus, it is expected to offer a significant sorption potential both to uranium and to humic acid. This assumption is supported by results found by Payne et al. [53] who investigated the uranium adsorption on ferrihydrite in the presence of humic acid. They found that the humic acid uptake by ferrihydrite as a function of pH was generally strong (approx. 82 to 90 % between pH 3.5 to 9) and decreased only at pH values higher than pH 9.

When discussing the results of the sorption experiments further, it has to be taken into account that the rock material had already been contacted with humic acid for 14 days before uranium(VI) was added. That means, the mineral surfaces are likely to be coated with humic acid at the beginning of the sorption experiments. Thus, sorption sites of the solids may either be blocked by adsorbed humic acid from other aqueous species or the humic acid may provide additional sorption sites due to its complexing ability.

The uranyl sorption onto phyllite in the presence of humic acid was compared to the uranyl sorption found by previously conducted experiments where the sorption of U(VI) onto phyllite was studied in the absence of humic material [57]. The experimental conditions of these experiments were the same as described in paragraph 14.1.2. Fig. 14.2 shows the pH-dependent U(VI) uptake onto phyllite in the absence and in the presence of the natural and the synthetic humic acid.

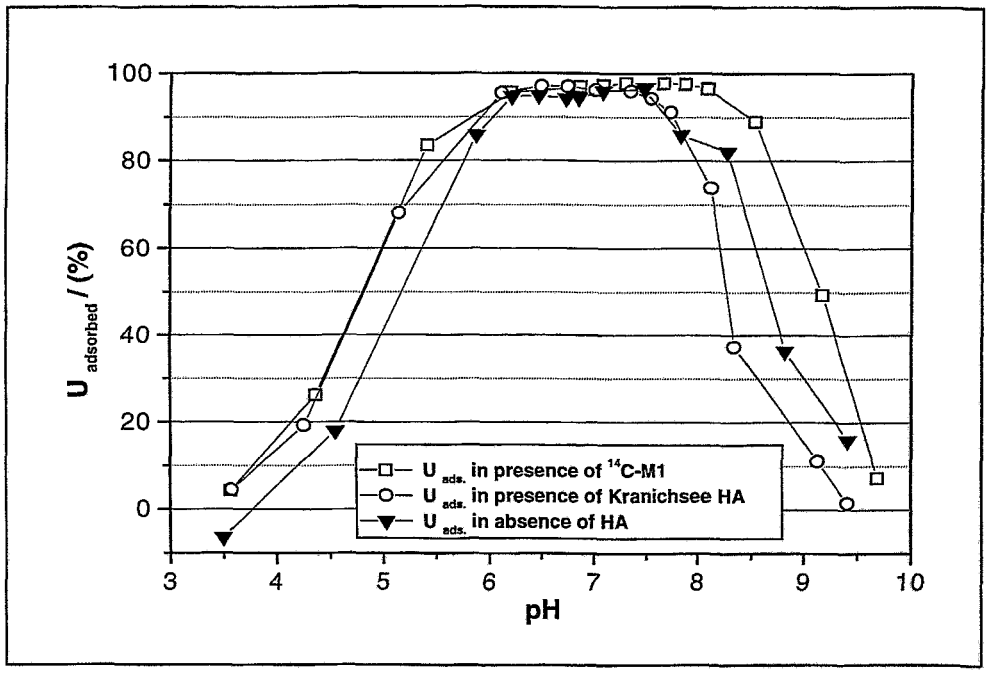

Figure 14.2: Uranium uptake by phyllite in experiments conducted in the presence of 5 mg HA/L. Data for uranium uptake in the absence of humic acid [57] are also shown.

The pH-dependent uranium adsorption on phyllite in the presence of the natural and the synthetic humic acid is similar to the uranium adsorption on phyllite in experiments conducted in the absence of humic acid. The strong uranyl sorption on phyllite (95 - 97 % in the absence of humic acid) is not significantly changed by humic acid in the pH range from 6 to 7.5. This very strong uranium adsorption on phyllite can also be attributed to the component ferrihydrite. Oxidic iron present in solution is known to form coatings on the surface of other minerals and to adsorb uranium well in composite minerals [58]. The small amount of dissolved humic acid (6-7 % of the total humic acid content) is not able to decrease the uranyl uptake on the solid by forming aqueous uranyl humate complexes. Consequently, the maximum of the uranium sorption on phyllite is not shifted to lower pH values, as known for the mineralogical constituents of the phyllite (muscovite, albite and quartz) [59], but remains unchanged in the pH range from 6 to 7.5 when humic acid is present at 5 mg/L. On

the other hand, the large amount of humic acid sorbed onto the mineral surface can only induce a very small enhancement of the uranium sorption. That means, the influence of humic acid on the uranium sorption is suppressed in the near neutral pH range.

In the pH range from 3.6 to 6, the uranium uptake on phyllite is somewhat higher when humic acid is present. This may be attributed to the fact that humic acid is sorbed on the mineral surface thereby providing additional sorption sites due to their complexing ability and/or due to adsorption of uranyl humate complexes on the mineral surface. The enhancement of the uranium uptake is almost the same for Kranichsee humic acid and for ^{14}C-M1. However, above pH 7.5, the influence of the two humic acids on the uranyl uptake by phyllite is different. The Kranichsee humic acid slightly reduces the uranyl sorption on phyllite whereas the synthetic humic acid, ^{14}C-M1, increases the uranyl sorption on phyllite compared to experiments carried out in the absence of humic acid. According to the speciation calculation considerable amounts of HCO_3^- are available to form complexes with uranyl ions ($UO_2(CO_3)_3^{4-}$, $UO_2(CO_3)_2^{2-}$). The inorganic carbonates have a higher complexing ability towards uranyl ions than humic acid. Nevertheless, the weakly sorbing uranyl carbonate complexes [60,61] are not able to predominate the influence of humic acid. Although the uptake of ^{14}C-M1 on phyllite at alkaline pH values is somewhat higher than the uptake of Kranichsee humic acid, there should be additional reasons for their different influence on the uranium sorption.

We conclude that the influence of humic acid on the uranium sorption depends on the pH of the solutions and on the humic acid in question. We conclude further that the ^{14}C-labelled synthetic humic acid (^{14}C-M1) is suitable for future experiments studying the kinetics and reversibility of the uranium and humic acid sorption onto minerals.

15 Conclusions

Within this project four different humic acid model substances with different functionality were developed according the melanoidin concept: a synthetic humic acid with a high content of aromatic structural elements and a low number of carboxylic groups (type M1), a synthetic humic acid type M1 of high purity, a synthetic humic acid with a carboxylic group content comparable to most natural occurring humic acids (type M42), and a nitrogen-free synthetic humic acid.

All synthesized humic acid model substances were characterized for their functional and structural properties and compared to purified commercially available natural humic acid from Aldrich. A radiometric method for determination of functional groups was applied beside conventionally direct and indirect potentiometric titration methods.

The synthetic model substances show structural and functional properties which are comparable to natural humic acids. The functional and structural properties of the synthetic humic acids can be varied by varying the precursor substances. One great advantage of the humic acid model substances represents their low up to not detectable content of inorganic impurities, especially iron, compared to natural humic acids. Furthermore, the synthetic humic acids show a more homogenous distribution of their charge-to-size ratios indicating a higher homogeneity.

Modified humic acids with blocked phenolic hydroxyl groups were also synthesized. They can be used to study the influence of phenolic hydroxyl groups on the complexation behavior of humic acids.

^{14}C-labelled humic acids were synthesized according to the melanoidin concept. They show a stable isotopic labelling in their molecular structure. Applying this synthetic pathway, it is possible to obtain humic acid model substances with specific activity levels, that enables their use in migration and sorption experiments under environmentally relevant conditions.

Synthetic humic acid type M1 and synthetic humic acid type M1 with blocked phenolic hydroxyl groups were distributed to the project partners for comparative studies.

Comparative studies for the interaction of synthetic and natural humic acids with uranium(VI) at pH $\leq$4 were performed by extended X-ray absorption fine structure spectroscopy (EXAFS), laser-induced fluorescence spectroscopy, and FTIR spectroscopy.

The analysis of U L_{III}-edge EXAFS data of different uranyl humates using Fluka humic acid and synthetic humic acid type M1 yielded axial U-O distances of 1.77 – 1.78 Å and five

equatorial oxygen atoms at distances of 2.37 – 2.39 Å. The equatorial U-O distances for the uranyl humates indicate predominately monodentate coordination of the humic acid carboxylic groups with the uranium. Assuming charge neutralization for the complexation of uranyl ions with humic acid, neutral ligands contribute to the coordination number of five. Similar structural parameters were determined for synthetic humic acid type M1 and Fluka humic acid which indicate a similar complexation behavior. In addition, FTIR spectroscopy showed a comparable coordination of UO_2^{2+} ions with Aldrich humic acid and the synthetic humic acids type M1 and type M42.

Applying laser-induced fluorescence spectroscopy, we determined a similar complexation behavior for synthetic humic acid type M42 and Aldrich humic acid. We determined corresponding loading capacities and complexation constants for the complexation with UO_2^{2+} ions at pH 4.

The spectroscopic methods showed that the synthetic humic acid model substances simulate very well the functionality of natural humic acids. This allows their application in model investigations to improve the knowledge about the complexation process between humic acids and metal ions.

For the first time, we investigated the influence of phenolic hydroxyl groups on the complexation behavior of humic acids with UO_2^{2+} ions. We used the modified humic acid type M1 with blocked phenolic hydroxyl groups as well as the unmodified synthetic humic acid type M1. Applying the charge neutralization model, both humic acids showed comparable complexation constants. However, significant differences exist in their loading capacities with uranyl ions at pH 4. From this we conclude that the blocking of the phenolic hydroxyl groups changes the humic acid complexation behavior with UO_2^{2+} ions.

First laserspectroscopic studies were performed to investigate the complexation behavior of uranium(VI) with humic acid in the absence of CO_2 at pH 7. The complexation experiments showed that uranium(VI) reacts with humic acids under formation of a ternary uranyl hydroxo humate complex. We assumed that $UO_2(OH)_2$ reacts under ligand exchange with the humic acid. For the total complexation reaction, we determined a complexation constant of $\log \beta_{0.1M} = 6.35$. For the charge neutralization reaction of UO_2OH^+ with humic acid at pH 7 in 0.1 M $NaClO_4$, we determined a loading capacity for the humic acid with UO_2OH^+ of 0.91 ± 0.28 and a complexation constant of $\log \beta_{0.1M} = 5.83 \pm 0.14$. However, to verify these first results additional measurements are recommended.

The migration behavior of uranium in a sandy aquifer system rich in humic substances (Pleistocene quartz sand, groundwater GoHy-532 from Gorleben site, Germany) was studied in laboratory column experiments. A part of the injected uranium migrates non-retarded, slightly faster than the groundwater. This migration behavior can be attributed to the association of uranium with humic colloids, which move faster due to size exclusion processes. The migration behavior of uranium is strongly influenced by the kinetically-controlled interaction processes of uranium with humic colloids. The recovery of non-retarded uranium increases with increasing uranium/groundwater contact time before injection into the column. Furthermore, the recovery of humic colloid-borne uranium decreases with decreasing groundwater flow velocity and increasing column length which corresponds to an increasing residence time of uranium in the column.

Batch experiment were performed to investigate the influence of humic acids on the sorption behavior of uranium onto phyllite, a rock material from the uranium mine 'Schlema-Alberoda' in Western Saxony (Germany). The batch experiments were conducted applying a natural site-specific humic acid (Kranichsee humic acid) as well as a ^{14}C-labelled synthetic humic acid type M1. The natural humic acid and the synthetic humic acid have a similar sorption behavior on phyllite. Their influence on the uranyl sorption is also comparable, especially in the acidic and neutral pH range. In the pH range from 3.6 to 6, the uranium uptake on phyllite is somewhat increased when humic acid is present. In the neutral pH range, the uranium adsorption on phyllite in the presence of humic acids is similar to the uranium adsorption in the absence of humic acids. In the pH range between 7.7 and 9.7, the synthetic humic acid increases the uranyl sorption whereas the natural humic acid decrease the uranyl sorption compared to experiments conducted in the absence of humic acid.
We conclude from the batch experiments that the influence of humic acids on the uranium sorption mainly depends on the pH of the solutions. Furthermore, we conclude that it is useful to use ^{14}C-labelled synthetic humic acid model substances for sorption experiments.

The results of these studies improve the knowledge of the complexation behavior of humic acids with uranium(VI) under aerobic conditions. Nevertheless, in future it will be necessary to investigate the complexation behavior of uranium and other actinides, e.g., thorium and neptunium with humic acids under anaerobic, i.e., reducing conditions. This includes studying the complexation behavior of these actinides in the tetravalent oxidation state with humic materials as well as studying their sorption and migration behavior in the presence of humic

materials. Furthermore, the knowledge about the redox properties of humic substances requires improvement.

Our study also showed the necessity to study kinetic processes controlling the migration behavior of uranium and other actinides in the presence of humic substances. Furthermore, it is necessary to include complexation models of humic acids with actinides in existing modeling codes for geochemical transport. A more detailed knowledge is needed of the interaction of humic acids with actinide ions other than uranium. This knowledge can be obtained using unmodified and modified synthetic and natural humic acids, for instance humic acid with blocked phenolic hydroxyl groups.

This increased knowledge will lead to a better modeling of the geochemical interaction of actinides and to an significantly improved risk assessment for the long-term storage of nuclear waste in underground repositories.

16 References

[1] Choppin, G.R.: The Role of Natural Organics in Radionuclide Migration in Natural Aquifer Systems. Radiochim. Acta **58/59**, 113 (1992).

[2] Jensen, B.S., Halken, T., Jestin, I., Jorgensen, D.: *The role of colloids in the migration of radioelements.* Final report, EUR 16763 EN, 1996, p. 36.

[3] Pompe, S.: *Entwicklung huminsäureähnlicher Melanoidine als Funktionalitätsmodelle für Huminsäuren und ihr Vergleich mit Fluka-Huminsäure hinsichtlich ihres Komplexbildungsverhaltens gegenüber Uran(VI).* Doctoral thesis, TU Dresden, 1997.

[4] Hänninen, K.I., Klöcking, R., Helbig, B.: Synthesis and Characterization of Humic Acid-Like Polymers. Sci. Tot. Environm. **62**, 201 (1987).

[5] Maillard, L.C.: Synthèse des Matières Humique par Action des Acides Aminès sur les Sucres Réducteurs. Ann. Chim. (Paris) **5**, 258 (1916).

[6] Enders, C., Theis, K.: Die Melanoidine und ihre Beziehung zu den Huminstoffen. Brennstoff Chemie **19**, 360 (1938).

[7] Angrick, M., Rewicki, D.: Die Maillard-Reaktion. Chemie in unserer Zeit **14**, 149 (1980).

[8] Hodge, J.E.: Chemistry of Browning Reactions in Model Systems. J. Agric. Food Chem. **1**, 928 (1953).

[9] Stevenson, F.J.: *Humus Chemistry.* John Wiley & Sons, New York, 1994.

[10] Pompe, S., Bubner, M., Denecke, M.A., Reich, T., Brachmann, A., Geipel, G., Nicolai, R., Heise, K.H., Nitsche, H.: A comparison of natural humic acids with synthetic humic acid model substances: characterization and interaction with uranium(VI). Radiochim. Acta **74**, 135 (1996).

[11] Kim, J.I., Buckau, G.: *Characterization of reference and site specific humic acids.* RCM-Report 02188, TU München, 1988.

[12] Bubner, M., Heise, K.H.: Characterization of Humic Acids. II. Characterization by Radioreagent-Derivatization with [^{14}C]Diazomethane. Forschungszentrum Rossendorf, Institute of Radiochemistry Annual Report 1993, **FZR-43**, 22 (1994).

[13] Stevenson, F.J.: *Humus Chemistry.* John Wiley&Sons, New York, 1982.

[14] Grauer, R.: *Zur Koordinationschemie der Huminstoffe*, Paul Scherrer Institut, Switzerland, Bericht Nr. 24, 1989, p. 7.

[15] Pompe, S., Heise, K.H., Nitsche, H.: Capillary electrophoresis for a "finger-print" characterization of fulvic and humic acids. J. Chromatogr. A **723**, 215 (1996).

[16] MacCarthy, P., Rice, J.A.: Spectroscopic Methods (Other Than NMR) for Determining Functionality in Humic Substances. In: *Humic Substances in Soil, Sediment, and Water*. G.R. Aiken, D.M. McKnight, R.L. Wershaw and P. MacCarthy (eds.). Wiley&Sons, New York, 1985, ch. 21.

[17] Bayer, E., Albert, K., Bergmann, W., Jahns, K., Eisener, W., Peters, K.: Aliphatische Polyether, Grundbausteine von natürlichen Huminstoffen: Nachweis durch Festkörper-^{13}C-NMR-Spektroskopie. Angew. Chem. **96**, 151 (1984).

[18] Ikan, R., Rubinsztain, Y., Ioselis, P., Aizenshtat, Z., Pugmire, R., Anderson, L.L., Woolfenden, W.R.: Carbon-13 cross polarized magic-angle samples spinning nuclear magnetic resonance of melanoidins. Org. Geochem. **9**, 199 (1986).

[19] Ishiwatari, R., Morinaga, S., Yamamoto, S., Machihara, T., Rubinsztain, Y., Ioselis, P., Aizenshtat, Y., Ikan, R.: A Study of the formation mechanism of sedimentary humic substances. – I. Characterization of synthetic humic substances (melanoidins) by alkaline potassium permanganate oxidation. Org. Geochem. **9**, 11 (1986).

[20] Carlsen. L., Lassen, P., Warwick, P., Randall, A.: Radio-Labelled Humic and Fulvic Acids: A New Approach to Studies on Environmental Fate of Pollutants. In: *Humic Substances in the Global Environment and Implications on Human Health.* (N. Senesi, T.M. Miano, eds.), Elsevier Science, 1994, p. 1107.

[21] Warwick, P., Carlsen, L., Randall, A., Zhao, R., Lassen, P.: ^{14}C and ^{125}I Labelling of Humic Materials for Use in Environmental Studies. Chemistry and Ecology **8**, 65 (1993).

[22] Carlsen, L., Lassen, P., Christiansen, J.V., Warwick, P., Hall, A., Randall, A.: Radiochim. Acta **58/59**, 371 (1992).

[23] Bubner, M., Pompe, S., Meyer, M., Heise, K.H., Nitsche, H.: Synthesis of Isotopically Labeled Synthetic Humic Acids. Forschungszentrum Rossendorf, Institute of Radiochemistry Annual Report 1998, **FZR-247**, 25 (1999).

[24] Denecke, M.A., Pompe, S., Reich, T., Moll, H., Bubner, M., Heise, K.H., Nicolai, R., Nitsche, H.: Measurement of the Structural Parameters for the Interaction of Uranium(VI) with Natural and Synthetic Humic Acids using EXAFS. Radiochim. Acta **79**, 151 (1997).

[25] Koningsberger, D.C., Prins, R. (eds.): *X-Ray Absorption: Principles, Applications, Techniques of EXAFS, SEXAFS and XANES*. John Wiley and Sons, New York, 1988.

[26] George, G.N., Pickering, I.J.: *EXAFSPAK: A suite of Computer Programs for Analysis of X-ray Absorption Spectra.* Stanford Synchrotron Radiation Laboratory, Stanford, CA, USA, 1995.

[27] Rehr, J.J., Albers, R.C., Zabinsky, S.I.: High-Order Multiple-Scattering Calculations of X-ray-Absorption Fine Structure. Phys. Rev. Lett. **69**, 3397 (1992).

[28] Hudson, E.A., Allen, P.G., Terminello, L.J., Denecke, M.A., Reich, T.: Polarized X-Ray-Absorption Spectroscopy of the Uranyl Ion: Comparison of Experiment and Theory. Phys. Rev. B **54**, 156 (1996).

[29] Denecke, M.A., Reich, T., Pompe, S., Bubner, M., Heise, K.H., Nitsche, H., Allen, P.G., Bucher, J.J., Edelstein, N.;., Shuh, D.K.: Differentiating between Monodentate and Bidentate Carboxylate Ligands Coordinated to Uranyl Ions Using EXAFS. J. Physique IV 7, C2-637-8 (1997).

[30] Koglin, E., Schenk, H.J., Schwochau, K.: Spectroscopic Studies on the Binding of Uranium by Brown Coal. Appl. Spectrosc. **32**, 486 (1978).

[31] Wolery, T.J.: *EQ3/6, A Software Package for the Geochemical Modeling of Aqueous Systems.* UCRL-MA-110662 Part 1, Lawrence Livermore National Laboratory, 1992.

[32] Grenthe, I., Fuger, J., Konings, R.J.M., Lemire, R.J., Muller, A.B., Nguyen-Trung, Cregu, C., Wanner, H.: *Chemical Thermodynamics of Uranium*, 1st ed., Elsevier Science, Amsterdam, 1992.

[33] Brachmann, A.: *Zeitaufgelöste laser-induzierte Fluoreszenzspektroskopie zur Charakterisierung der Wechselwirkung des Uranylions mit Huminsäuren und Carboxylatliganden.* Doctoral thesis, TU Dresden, 1997.

[34] Kim, J.I., Czerwinski, K.R.: Complexation of Metal Ions with Humic Acids: Metal Ion Charge Neutralization Model. Radiochim. Acta **73**, 5 (1996).

[35] Czerwinski, K.R., Buckau, G., Scherbaum, F., Kim, J.I.: Complexation of the Uranyl Ion with Aquatic Humic Acid. Radiochim. Acta **65**, 111 (1994).

[36] Pompe, S., Brachmann, A., Bubner, M., Geipel, G., Heise, K.H., Bernhard, G., Nitsche, H.: Determination and Comparison of Uranyl Complexation Constants with Natural and Synthetic Humic Acids. Radiochim. Acta **82**, 89 (1998).

[37] Heise, K.H., Nicolai, R., Pompe, S., Bubner, M., Nitsche, H.: FTIR-Untersuchungen zur Komplexierung von Uran(VI) durch huminsäureähnliche Melanoidine. GDCh-Tagung, FG Nuklearchemie, Dresden, 07.-09.09.1998.

[38] Choppin, G.R., Allard, B.: Complexes of Actinides with Naturally Occurring Organic Compounds. In: *Handbook on the Physics and Chemistry of the Actinides.* Vol. 3, (A.J. Freeman and C. Keller, eds.), Elsevier Sci. Publ., Amsterdam, 1985, p. 407.

[39] Zeh, P., Czerwinski, K.R., Kim, J.I.: Speciation of Uranium in Gorleben Groundwaters. Radiochim. Acta **76**, 37 (1997).

[40] Glaus, M.A., Hummel, W., Van Loon, L.R.: Stability of Mixed-Ligand Complexes of Metal Ions with Humic Substances and Low Molecular Weight Ligands. Environ. Sci. Technol. **29**, 2150 (1995).

[41] Davies, C.W.: Ion Association: Butterworths, London, 1962.

[42] Artinger, R., Kienzler, B., Schüßler, W., Kim, J.I.: Effects of humic substances on the ^{241}Am migration in a sandy aquifer: column experiments with Gorleben groundwater/sediment systems. J. Contam. Hydrol. **35**, 261 (1998).

[43] Kim, J.I., Delakowitz, B., Zeh, P., Klotz, D., Lazik, D.: A Column Experiment for the Study of Colloidal Radionuclide Migration in Gorleben Aquifer Systems. Radiochim. Acta **66/6**7, 165 (1994).

[44] Kim, J.I., Zeh, P., Runde, W., Mauser, C., Paskalidis, B., Kornprobst, B., Stöwer, C.: *Nuklidmigration (99Tc, 237Np, 238Pu, 241Am) im Deckgebirge und Salzstsock des geplanten Endlagers Gorleben.* RCM-Report 01495, TU München, 1995.

[45] Kim, J.I., Delakowitz, B., Zeh, P.: *Migration behaviour of radionuclides. In: Colloid migration in groundwaters: geochemical interactions of radionuclides with natural colloids.* Final report, EUR 16754EN, 1996, p. 63.

[46] Artinger, R., Kienzler, B., Schüßler, W., Kim, J.I.: Sampling and Characterization of Gorleben Groundwater/Sediment Systems for Actinide Migration Experiments. In: *Effects of Humic Substances on the Migration of Radionuclides: Complexation and Transport of Actinides.* First Technical Progress Report of the EC Project No. FI4W-CT96-0027 (G. Buckau, ed.). Forschungszentrum Karlsruhe, Wissenschaftliche Berichte, FZKA 6124, Karlsruhe, 1998, p. 23.

[47] Artinger, R., Seibert, A., unpublished.

[48] Rao, L., Choppin, G. R., Clark, S. B.: A study of metal-humate interactions using cation exchange. Radiochim. Acta **66/67**, 141 (1994).

[49] Schmeide, K., Zänker, H., Heise, K.H. and Nitsche, H.: Isolation and Characterization of Aquatic Humic Substances from the Bog "Kleiner Kranichsee". In: *Effects of Humic Substances on the Migration of Radionuclides: Complexation and Transport of Actinides.* First Technical Progress Report of the EC Project No. FI4W-CT96-0027

(G. Buckau, ed.). Forschungszentrum Karlsruhe, Wissenschaftliche Berichte, FZKA 6124, Karlsruhe, 1998, p. 161.

[50] Beneš, P., Kratzer, K., Vlcková, Š. and Šebestová, E.: Adsorption of Uranium on Clay and the Effect of Humic Substances. Radiochim. Acta **82**, 367 (1998).

[51] Ho, C.H. and Miller, N.G. (1985) Effect of Humic Acid on Uranium Uptake by Hematite Particles. J. Colloid Interf. Sci. **106**, 281 (1985).

[52] Labonne-Wall, N., Moulin, V. and Vilarem, J.-P.: Retention Properties of Humic Substances onto Amorphous Silica: Consequences for the Sorption of Cations. Radiochim. Acta **79**, 37 (1997).

[53] Payne, T.E., Davis, J.A. and Waite, T.D.: Uranium Adsorption on Ferrihydrite - Effects of Phosphate and Humic Acid. Radiochim. Acta **74**, 239 (1996).

[54] Payne, T.E., Shinners, S. and Twining, J.R.: Uranium Sorption on Tropical Wetland Sediments. In: *Uranium Mining and Hydrogeology II. Proceedings of the International Conference and Workshop. Freiberg, Germany, September 1998*, (ed. B. Merkel, C. Helling and St. Hurst), von Loga, Köln, 1998, pp. 298.

[55] Ticknor, K.V., Vilks, P. and Vandergraaf, T.T.: The effect of fulvic acid on the sorption of actinides and fission products on granite and selected minerals. Appl. Geochem. **11**, 555 (1996).

[56] Arnold, T., Zorn, T., Bernhard, G. and Nitsche, H.: Characterization of Phyllite with SEM/EDS, PIXE, and Thin Section Microscopy. Forschungszentrum Rossendorf, Institute of Radiochemistry Annual Report 1997, **FZR-218**, 1 (1998).

[57] Arnold, T., Zorn, T., Bernhard, G. and Nitsche, H.: Sorption of Uranium(VI) onto Phyllite. Chem. Geol. **151**, 129 (1998).

[58] Payne, T.E., Davis, J.A. and Waite, T.D.: Uranium Retention by Weathered Schists - The Role of Iron Minerals. Radiochim. Acta **66/67**, 297 (1994).

[59] Schmeide, K., Jander, R., Heise, K.H. and Bernhard, G.: Effect of Humic Acid on the Uranium(VI) Sorption onto Phyllite and its Mineralogical Constituents. In: *Effects of Humic Substances on the Migration of Radionuclides: Complexation and Transport of Actinides.* Second Technical Progress Report of the EC Project No. FI4W-CT96-0027 (G. Buckau, ed.). Forschungszentrum Karlsruhe, Wissenschaftliche Berichte, FZKA 6324, Karlsruhe, 1999, p. 199.

[60] Ticknor, K.V.: Uranium Sorption on Geological Materials. Radiochim. Acta **64**, 229 (1994).

[61] Waite, T.D., Davis, J.A., Payne, T.E., Waychunas, G.A. and Xu, N.: Uranium(VI) Adsorption to Ferrihydrite: Application of a Surface Complexation Model. Geochim. Cosmochim. Acta **58**, 5465 (1994).

[62] Schnitzer, M., Khan, S.U.: *Humic substances in the environment.* A.D. McLaren, (Hrsg.), Marcel Dekker, Inc., New York, 1972.

17 Acknowledgment

The authors would like to thank Monika Meyer, Rosemarie Ruske, Renate Jander and Andrea Schubert for their valuable help in synthesizing, purification and characterization of the humic acids, Dr. Gerhard Schuster for thermoanalytical investigations, Dr. Waltraud Wiesener for ICP-MS analyses as well as Roswita Nicolai and Heidemarie Görner from the Institute of Bioinorganic and Radiopharmaceutical Chemistry for FTIR spectroscopic measurements and elemental analyses, respectively.

Thanks are given to Dr. Gerhard Geipel for the very good cooperation and his support during the performance and evaluation of laserspectroscopic investigations.

We thank Dr. Melissa Denecke and Dr. Tobias Reich for the very good collaboration in the performance and evaluation of the EXAFS measurements. We would also like to thank HASYLAB for the allotment of measurement time.

Dr. Vinzenz Brendler we thank for speciation calculations.

We would like to thank Dr. Klaus Albert and Matthias Pursch from the Institute of Organic Chemistry of the University Tübingen for recording of ^{13}C-CP/MAS-NMR spectra and for their support in the interpretation of these spectra.

The authors thank Prof. Dr. J.I. Kim for giving us the possibility to perform column experiments at the Institute of Nuclear Waste Management in Karlsruhe. In particular we thank Dr. Robert Artinger for the very good cooperation in performing and evaluating the column experiments.

At this place we would like to thank all colleagues who contributed to the success of this work.

A Appendix - Analytical methods used for the characterization of humic acids

A.1 Elemental analysis

The determination of the carbon, hydrogen and nitrogen content of the humic acids was performed with an elemental analyzer (model CHNS-932, Leco, St. Joseph, MI, USA).
Ash and moisture contents of the humic acids were determined thermoanalytically with the CH-analyzer RC 412 (Leco, St. Joseph, MI, USA) and the thermoanalyzer STA 92 (Setaram, Lyon, France). The samples were heated in a stream of oxygen. The amount of water, which was released up to about 150 °C, was measured for the estimation of the moisture content. The ash content corresponds to the ignition residue after heating the sample to 700 °C.
The inorganic constituents of the humic acids were determined by ICP-MS analyses after digestion of the humic acids with HNO_3 in a microwave.

A.2 Functional groups

A.2.1 Radiometric determination of functional groups [12]

[^{14}C]diazomethane with a known specific activity was used for the radiometric determination of humic acid carboxylic and phenolic OH groups. It was produced from diazald-N-methyl-[^{14}C] with a specific activity of 1.9 GBq/mmol (Sigma, Aldrich) that was diluted with inactive Diazald® (Aldrich). The methylation of the humic acid was carried out under reduced pressure at –10 to 0 °C in a vacuum apparatus. The specific activity of the humic acids after methylation was determined by liquid scintillation counting (Beckman Instruments, Fullerton, CA, USA) after combustion of the substances with a sample oxidizer (model P307, Canberra-Packard, Warrenville, IL, USA).
The saponification of the permethylated humic acids was done by stirring the humic acid with methanolic NaOH at 70 °C for 4 hours. The activity of the methanol which was released during the saponification was also determined by liquid scintillation counting.

A.2.2 Calcium acetate method

The carboxylic group content of the humic acids was determined with the calcium acetate method according the method described in [62], which allows the humic acid to react with an excess of 1 N $Ca(CH_3COO)_2$. Humic acids liberate acetic acid during the reaction with calcium acetate. The released acetic acid is then titrated with NaOH solution.

$$2R-COOH + Ca(CH_3COO)_2 \rightarrow (R-COO)_2Ca + 2CH_3COOH$$

R: Humic acid molecule

For sample preparation and preparation of the calcium acetate solution CO_2-free water was used. The samples were prepared and titrated under inert gas. For titration, we used the automatic titration system TPC 2000 (Schott, Hofheim, Germany) applying the titration software TR 600, version 5.02.

A.2.3 Barium hydroxide method

The total proton exchange capacity was determined by the barium hydroxide method described in [62], which allows humic acid to react with an excess of $Ba(OH)_2$, followed by titration of the unused base with 0.1 M HCl:

$$Ba(OH)_2 + 2HA \rightarrow BaA_2 + 2H_2O$$

HA: Humic acid

Sample preparation as well as titration were done under inert gas. CO_2-free water was used. For titration, we used the automatic titration system TPC 2000 applying the titration software TR 600, version 5.02.

The difference between the total proton exchange capacity determined by barium hydroxide method and the carboxylic group content determined by calcium acetate exchange corresponds to the number of phenolic OH groups of the humic acid.

A.2.4 Direct titration

The determination of the humic acid proton exchange capacity was performed by acid-base titration of humic acid which was previously dissolved in alkaline solution.
A stock solution of humic acid was made by dissolving humic acid in a known volume of 0.1 M NaOH and diluting this solution with 0.1 M $NaClO_4$ under inert gas conditions. An aliquot of this solution was then titrated against 0.1 M $HClO_4$ under inert gas to determine the excess of NaOH which was not used for dissolving, i.e., deprotonation of the humic acid.

A.3 Capillary electrophoresis

Capillary electrophoretic investigations were performed using the capillary electrophoresis system P/ACE 2050 (Beckman Instruments, Palo Alto, CA, USA) with a variable separation voltage of 1 to 30 kV and an UV photometer detector. Before sample loading, the capillary was conditioned for 2 min with 0.1 M NaOH and then for 2 min with buffer solution. As electrolyte system we used a potassiumdihydrogenphosphate-sodiumtetraborate buffer (3 mM KH_2PO_4, 6 mM $Na_2B_4O_7$) with pH 8.9. The sample was injected into the column by pressure injection for 15 s. The separation was carried out at 30 °C with a voltage of 30 kV. Detection was done on-line at the catodic site of the capillary at 214 nm. The humic acids were dissolved in 10^{-3} M NaOH with a concentration of 400 mg/L. The solutions were used directly for injection. No filtration or other special sample treatment was necessary.

A.4 Structural characterization

A.4.1 FTIR spectroscopy

FTIR measurements were carried out with the spectrometer model SPECTRUM 2000 (Perkin Elmer Europe B.V., Nieuwerke, NL). Spectra were recorded in the MIR range as KBr pellets and in the FIR range as polyethylene pellets with a diameter of 13 mm and optimized sample amounts.

A.4.2 ^{13}C-CP/MAS-NMR spectroscopy

^{13}C-CP/MAS-NMR measurements were performed by a Bruker MSL 200 spectrometer (Bruker, Rheinstetten, Germany). Magic-angle spinning was executed at rates of 10000 Hz. The spectra were recorded using 90° pulse length of 4.4 µs, contact time of 1 ms, and delay time of 1 s.

A.4.3 Pyrolysis-Gas chromatography/Mass spectrometry (Py-GC/MS)

The filament pyrolysis system Pyroprobe (model 2000, CDS Analytical Inc., Oxford, PA, USA) on-line coupled with a gas chromatograph (model HP 5890, Hewlett Packard, Waldbronn, Germany) with a mass selective detector (mass range 20-450 atomar mass units; model HP 5871a) was used. Pyrolysis and separation were done in a helium atmosphere as described in [3].